

**Generating Process and Economic Data Needed for Preliminary Design of PureVision
Biorefineries**

DOE Project No. DE-FG36-05GO85004
Kiran L. Kadam, PhD, Technical Director
Ed Lehrburger, Project Director

Final Nonproprietary Technical Report

PureVision Technology, Inc.
511 McKinley Ave.
Ft. Lupton, CO 80621
December 28, 2007

This non-proprietary report suitable for distribution is being submitted with STI form 241.3 in compliance with final reporting requirements under DOE Project No. DE-FG36-05GO85004. A Confidential Final Report containing proprietary data and detailed subcontractor reports is being submitted separately to the DOE Golden office.

Consortium Members

PureVision Technology, Inc. (applicant and contractor)
Hazen Research, Inc.
Harris Group
Entek Manufacturing, Inc. (Entek Extruders)
Membrane Technology and Research, Inc.
National Renewable Energy Laboratory
University of Utah
MAST (Membrane Applied Science & Technology Center, University of Colorado at Boulder)
Auburn University's PPREC
PPG Industries, Inc.
Weyerhaeuser Company
Louisiana State University
M.A. Patout & Son, Ltd.

Executive Summary

The overall objective of the project was to define a two-stage reactive fractionation process for converting corn stover into a solid cellulose stream and two liquid streams containing mostly hemicellulosic sugars and lignin, respectively. Toward this goal, biomass fractionation was conducted using a small continuous pilot unit with a nominal capacity of 100 pounds per day of dry biomass to generate performance data using primarily corn stover as feedstock.

In the course of the program, the PureVision process was optimized for efficient hemicellulose hydrolysis in the first stage employing autohydrolysis and delignification in the second stage using sodium hydroxide as a catalyst. The remaining cellulose was deemed to be an excellent substrate for producing fermentation sugars, requiring 40% less enzymes for hydrolysis than conventional pretreatment systems using dilute acid. The fractionated cellulose was also determined to have potential higher-value applications as a pulp product. The lignin coproduct was determined to be substantially lower in molecular weight (MW) compared to lignins produced in the kraft or sulfite pulping processes. This low-MW lignin can be used as a feed and concrete binder and as an intermediate for producing a range of high-value products including phenolic resins. This research adds to the understanding of the biomass conversion area in that a new process was developed in the true spirit of biorefineries. The work completed successfully demonstrated the technical effectiveness of the process at the pilot level indicating the technology is ready to advance to a 2–3 ton per day scale. No technical showstoppers are anticipated in scaling up the PureVision fractionation process to commercial scale. Also, economic feasibility of using the PureVision process in a commercial-scale biorefinery was investigated and the minimum ethanol selling price for the PureVision process was calculated to be \$0.94/gal ethanol vs. \$1.07/gal ethanol for the NREL process. Thus, the PureVision process is economically attractive.

Given its technical and economic feasibility, the project is of benefit to the public in the following ways: 1) it demonstrated a novel biomass fractionation process that can provide domestic supply of renewable transportation fuel from all three biomass components (cellulose, hemicellulose and lignin), 2) the lignin stream from the process has many higher-value applications beyond simply burning the lignin for energy as proposed by competing technologies, 3) it can be deployed in rural areas and create jobs in these areas, and 4) it can add to the nation's economy and security.

TABLE OF CONTENTS

1. PREAMBLE.....	5
PUREVISION’S FRACTIONATION TECHNOLOGY	5
PROJECT OBJECTIVE	5
PROJECT TASKS, MILESTONES AND ASSOCIATED METRICS.....	6
2. MATERIALS AND METHODS.....	6
SUBSTRATE.....	6
OPERATING CONDITIONS	8
PROTOCOL FOR SAMPLE PREPARATION	9
LIGNIN PRECIPITATION	10
DATA ANALYSIS.....	10
SEVERITY FACTORS	10
3. RESULTS AND DISCUSSION	12
PUREVISION PROCESS: ORIGINAL DESIGN VS. MODIFIED DESIGN	12
TASK 1. OPTIMIZE FRACTIONATION OF CORN STOVER AT PDU-SCALE	14
<i>First Stage Optimization</i>	14
3.1.1.1. Autohydrolysis.....	14
3.1.1.2. Acid Catalyzed Prehydrolysis.....	15
3.1.1.3. Cocurrent vs. Countercurrent Mode.....	15
Selection of Prehydrolysis Mode	17
<i>Second Stage Optimization</i>	17
<i>Mass Balance</i>	17
3.1.1.4. Sugar Degradation under Alkaline Conditions.....	18
3.1.1.5. Lignin Analysis of Liquors and Solids.....	18
3.1.1.6. Sources of Errors	18
<i>Bagasse Fractionation</i>	19
TASK 2. INVESTIGATE CORN STOVER HYDROLYZATE LIQUOR FRACTIONS FOR SEPARATION AND PURIFICATION	
TECHNIQUES AND COMMERCIAL APPLICATIONS	19
<i>Simulated Moving Bed Chromatography</i>	19
NREL.....	19
PPG Industries.....	20
University of Utah.....	20
Weyerhaeuser.....	22
MAST.....	22
MTR	22
TASK 3. CELLULOSE FRACTION EVALUATION, UTILIZATION AND MARKET ANALYSIS.....	24
<i>Enzymatic Hydrolysis</i>	24
<i>Pulp and Paper Production</i>	24
TASK 4. PERFORM ASPEN MODELING OF THE PUREVISION BIOREFINING PROCESS	25
<i>Technoeconomic Analysis</i>	25
3.1.1.7. Methodology.....	25
3.1.1.8. Analysis Results.....	27
<i>Bagasse Feedstock Assessment</i>	28
TASK 5. FINALIZE PRELIMINARY DESIGN SPECIFICATIONS, ENGINEERING, AND COSTING FOR THE PROTOTYPE	
REACTOR.....	29
4. CONCLUSION.....	29
5. PRODUCTS DEVELOPED AND TECHNOLOGY TRANSFER ACTIVITIES.....	31
PRESENTATIONS	31
PUBLICATIONS	32
6. FUTURE WORK	32

7. REFERENCES.....	33
8. APPENDICES.....	35
8.1 AUBURN UNIVERSITY REPORT	35
8.2 NREL REPORT	42
8.3 MTR REPORT	43
8.4 WEYERHAEUSER REPORT	49
8.5 PPG INDUSTRIES REPORT	57
<i>PPG Industries Attachments</i>	63
8.6 MAST REPORT.....	75

Tables

TABLE 1. MILESTONES AND ASSOCIATED METRICS	7
TABLE 2. CORN STOVER COMPOSITION.....	7
TABLE 3. SUGARCANE BAGASSE COMPOSITION	8
TABLE 4. MASS AND COMPONENT BALANCE CLOSURE.....	17
TABLE 5. KEY COSTS AND INCOMES FOR THE TWO PROCESSES.....	27
TABLE 6. SENSITIVITY ANALYSIS	27
TABLE 7. OPERATING CONDITIONS AND PROCESS PERFORMANCE	30

Figures

FIGURE 1. PHOTOGRAPH OF THE PDU.....	9
FIGURE 2. PROTOCOL FOR FIRST-STAGE SAMPLE PREPARATION.....	11
FIGURE 3. PROTOCOL FOR SECOND-STAGE SAMPLE PREPARATION.....	11
FIGURE 4. CONCEPTUAL REPRESENTATION OF THE PUREVISION PROCESS: TWO COUNTERCURRENT STAGES.....	13
FIGURE 5. REPRESENTATION OF THE MODIFIED PUREVISION PROCESS: WITH A COUNTERCURRENT FIRST STAGE AND A COCURRENT SECOND STAGE.....	13
FIGURE 6. PLUG FLOW REACTOR SCHEMATIC (COCURRENT MODE), WHERE ΔV = FINITE ELEMENT OR PLUG TRAVELING THROUGH THE REACTOR; T = TIME, T_1 = TIME WHEN THE PLUG ENTERS THE REACTOR, T = PLUG RESIDENCE TIME.	16
FIGURE 7. PUREVISION REACTOR SCHEMATIC SHOWING LIQUID AND SOLIDS PATHS (COUNTERCURRENT MODE).	16
FIGURE 8. GPC OF LIGNIN FROM FIRST AND SECOND STAGE LIQUORS.....	20
FIGURE 9. FLOW DIAGRAM OF THE ENHANCED THREE-STAGE PROCESS FOR CONVERSION OF LIGNIN TO ALKYL BENZENE GASOLINE BLENDING COMPONENTS.	21
FIGURE 10. SCHEMATIC OF ELECTRODIALYSIS SETUP.....	23
FIGURE 11. DIAGRAM OF THE TEST APPARATUS FOR SEPARATION OF SUGARS THROUGH THIN COMPOSITE MEMBRANES.	24
FIGURE 12. SCHEMATIC OF THE NREL BIOREFINERY.....	26
FIGURE 13. SCHEMATIC OF THE PUREVISION BIOREFINERY.	26
FIGURE 14. EFFECT OF SELLING PRICE OF LIGNIN ON MESP.....	28

1. Preamble

This project entitled, "Generating Process and Economic Data for Design of PureVision Biorefineries" was funded by FY05 and FY06 Congressional earmarks to PureVision Technology, Inc. (PureVision). This effort initiated research and development on advancing Pure Vision's new biorefining process (Wingerson 2002; Wingerson 2003), which converts different biomass feedstocks into fiber, fuel and other industrial chemicals. This continuous process relies on a conveyor apparatus that accomplishes biomass fractionation in a relatively short time compared to traditional biomass pretreatment or pulping processes. This approach dissolves and separates hemicellulose and lignin from biomass leaving relatively pure cellulose. Enzymatic hydrolysis of this cellulose stream requires significantly lower enzyme loadings, offering concomitant reduction in production costs. The hemicellulose sugars captured in the hydrolyzate liquor and the cellulose-derived glucose may then be fermented to ethanol. The non-sulfur lignin is highly reactive and may be used for many value-added products including binders, adhesives and resins or converted to liquid fuels. The reactive fractionation technology is being advanced to economically convert diverse domestic biomass into fiber, ethanol and other industrial fuels and chemicals, specifically in rural areas where agricultural-based biorefineries of the future will be located. Biorefining of agricultural residues and energy crops will create added income for farmers and furnish a technology platform for innovative biomass utilization. This project has laid the foundation for commercial collaborations for advancing rural biorefineries.

PureVision's Fractionation Technology

The following summarizes distinguishing features of the PureVision fractionation technology:

1. Ability to fractionate biomass into its three major components.
2. Continuous countercurrent pretreatment of biomass.
3. Production of low-lignin cellulose (2-4% Klason lignin on dry weight basis) that requires about 60% less enzyme, resulting in decreased cost of fermentation sugars and ethanol.
4. Production of a purified, sulfur-free, low-molecular weight lignin, which can be used as a biobased raw material for manufacturing a myriad of industrial and consumer products.
5. Process versatility to gear the cellulose stream toward glucose or pulp/cellulose derivatives.
6. Flexible biorefineries that are capable of producing a wide range of petroleum-substitute products— not limited to biofuels—and shown to be economically feasible based on preliminary analysis.

Project Objective

The overall objective of the project is to define a two-stage reactive fractionation process for converting targeted biomass including corn stover and bagasse into a solid cellulose stream and two liquid streams containing mostly hemicellulosic sugars and lignin, respectively. Toward this goal, research was performed at the process development unit (PDU)-scale to generate performance data for process modeling and technoeconomic analysis (preliminary mass and heat balances, capital and operating costs) to convert biomass into product streams.

Project Tasks, Milestones and Associated Metrics

The project tasks and subtasks presented in the Statement of Work (SOW) are listed below, and milestones and associated metrics are enumerated in Table 1.

- Task 1. Optimize fractionation of corn stover at PDU-scale.
 - Subtask 1.1. Optimize corn stover fractionation and begin bagasse fractionation.
 - Subtask 1.2. Conduct characterization of biomass fractions.
- Task 2. Investigate corn stover hydrolyzate liquor fractions for separation and purification techniques and commercial applications.
 - Subtask 2.1. Conditioning and separation of xylose fraction.
 - Subtask 2.2. Fermentation of xylose into xylitol, ethanol or other industrial chemicals.
 - Subtask 2.3. Conditioning, separation and utilization of the lignin fraction.
 - Subtask 2.4. Enzymatic hydrolysis of cellulose fraction.
 - Subtask 2.5. Production of ethanol from cellulose fraction.
- Task 3. Cellulose fraction evaluation, utilization and market analysis.
- Task 4: Perform Aspen modeling of the PureVision biorefining process.
 - Subtask 4.1. Process and economic modeling.
 - Subtask 4.2. Life cycle analysis.
 - Subtask 4.3. Bagasse feedstock assessment by LSU.
 - Subtask 4.4. Bagasse feedstock assessment by M. A. Patout.
- Task 5: Finalize preliminary design specifications, engineering, and costing for the prototype reactor.
 - Subtask 5.1. Develop design for prototype.

2. Materials and Methods

The general operating information is summarized below.

Substrate

Corn stover of Colorado stock was hammer milled through 1/2" screen at the Hazen Research, Inc. (Hazen) facility and used as substrate. The substrate moisture was in the range of 4–7 wt% and determined regularly during operation. Composition of corn stover is tabulated in Table 2; this is based on PureVision's in-house analysis and NIR compositional data provided by NREL (National Renewable Energy Laboratory, Golden, Colorado).

Initial processing was conducted using sugarcane bagasse from Louisiana during the last few months of the program. Bagasse was acquired from M.A. Patout & Son Ltd. (Patout), delivered to Hazen and hammer milled. While the process was not optimized for bagasse, the PureVision team performed fractionation studies on bagasse, demonstrating the ability to obtain three streams (cellulose, hemicellulose and lignin) and gained experience with handling a second feedstock during the program. Bagasse composition (done by Prof. YY Lee of Auburn University) is listed in Table 3.

Table 1. Milestones and associated metrics

	Milestone	Metric
1	Optimized fractionation process using corn stover as feedstock: ethanol product target	1) 75–80% yield of hemicellulosic sugars in the first stage 2) 80–85% lignin hydrolysis in the two stages combined 3) 75–80% of theoretical yield of cellulosic sugars enzymatic hydrolysis with 7 FPU/g cellulose loading
2	Optimized fractionation process using corn stover as feedstock: pulp product target	1) 50% yield of hemicellulosic sugars in the first stage 2) 85–90% lignin hydrolysis in the two stages combined 3) Suitable for blending with wood-based pulp at ≤30% level
3	Interim Stage Gate Review (ISGR)	Pass Interim Stage Gate Review #2
3	Begin processing and work toward optimizing the fractionation using bagasse as feedstock: ethanol product target	1) 75–80% yield of hemicellulosic sugars in the first stage 2) 80–85% lignin hydrolysis in the two stages combined 3) 75–80% yield of cellulosic sugars enzymatic hydrolysis with 7 FPU/g cellulose loading
4	Develop process for sugar/lignin separation from first-stage liquor (corn stover as feedstock)	1) Removal of 85% of xylose with minimal lignin carryover 2) 75–80% of theoretical conversion of xylose to xylitol/ethanol
5	Develop process for controlled precipitation of lignin (corn stover as feedstock)	Recovery of 80–85% of lignin from the second-stage hydrolyzate liquor stream
6	Conduct Aspen modeling of the PureVision biorefining process	1) Economic data and ethanol/pulp MESP (minimum ethanol selling price)—core technology 2) Preliminary economic data on integrated biorefinery
7	Complete preliminary design specifications, engineering and costing for the prototype reactor	Design and engineering data to prepare for procurement and fabrication of prototype reactor

Table 2. Corn stover composition

Component	Wt%
Glucan	35.2
Xylan	19.8
Galactan	1.3
Arabinan	2.5
Mannan	0.6
Lignin	16.9
Protein	5.4
Acetyl	2.4
Uronic acid	3.2
Extractives	4.9
Ash	4.7
Total	100.0

Table 3. Sugarcane bagasse composition

Component	Wt%
Glucan	41.5
Xylan	22.1
Galactan	1.1
Arabinan	1.1
Mannan	0.8
Lignin	23.2
Acetyl	4.5
Other	1.7
Ash	4.0
Total	100.0

Operating Conditions

PureVision has been developing its fractionation technology since 1999. In 2003, development efforts began to utilize a continuous reactor capable of handling approximately 100 pounds of biomass per day. A process development unit (PDU) was built that utilizes a modified 27 mm twin-screw extruder from Entek. The PDU originally was constructed to demonstrate three streams (cellulose, hemicellulose and lignin) can be extracted from biomass using the countercurrent process, whereby the solids move through the reactor by the rotating screws and the liquid moves in countercurrently. Since demonstrating the countercurrent process, the PDU has been employed to optimize the process, undertake feedstock evaluations and to generate solid and liquid samples for assays and evaluations. A photograph of the PDU is shown in Figure 1.

Experimental conditions for the first-stage countercurrent operation were as follows:

- Equipment: PDU that includes a 27 mm twin-screw extruder (Entek Extruders, Lebanon, OR)
- Extruder speed: 14-50 rpm
- Liquid discharge screw speed: 15 rpm
- Moyno pump: automatic operation based on pressure setting for the reactor chamber
- Solids feed rate: variable using the Acrison feeder in volumetric or gravimetric mode
- Liquid flow rate: water and reagent solutions at variable feed rates, countercurrent mode
- Temperature: variable

While the second stage was initially planned to be in countercurrent mode, PureVision proposed to DOE to modify the original plan and to instead use cocurrent mode in the second stage. Experimental conditions for the second stage cocurrent operation were as follows:

- Equipment: single-screw extruder
- Extruder speed: 2–4 rpm
- Liquid flow rate: water and reagent solutions at variable feed rates, cocurrent mode
- Temperature: variable

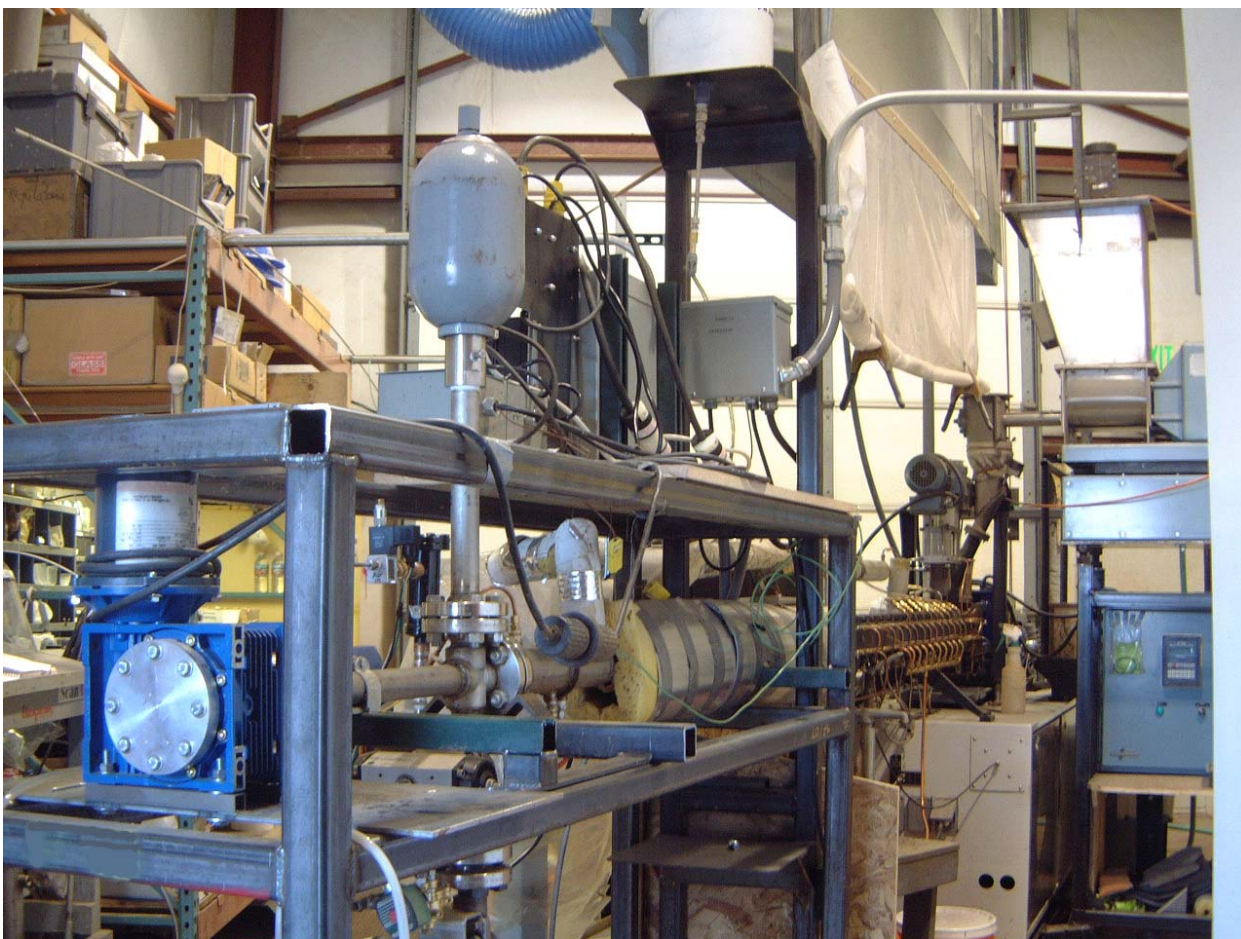


Figure 1. Photograph of the PDU.

Protocol for Sample Preparation

Both liquid and solid phase samples were collected for each design point. Protocols for sample preparation are shown in Figure 2 and Figure 3. Sugar concentrations of the liquid stream were determined by HPLC. Additional hydrolysis was necessary to detect oligomeric sugars, which constituted about 85–95% of total sugars for autohydrolysis. Liquid phase lignin (acid soluble lignin) was determined by UV absorbance of the liquor samples measured at 320 nm.

The solids were subjected to carbohydrate and Klason lignin analyses. Precipitate from the second stage liquor was also analyzed for sugars and Klason lignin.

Lignin Precipitation

A process described by Lora et al. (1988) deals with lignin from black liquor produced by pulping wood with ethanol at high temperatures and pressures. Lignin is precipitated by diluting the black liquor with water and acid to achieve pH of 3 or less at a temperature of $<75^{\circ}\text{C}$. When subsequently dried, the recovered lignin is in powder form, which can be easily converted into a fine uniform size suitable for use without further significant processing.

In precipitating lignin, the method of diluting the residual black liquor with the water and acid is not critical, as long as there is rapid and intimate mixing. Although a conventional static dispersion mixer can be used, and the black liquor can also be preferentially diluted by means of a venturi-type device that creates finely divided streams to enhance mixing. Lignin rapidly precipitates from the resulting diluted residual black liquor in the form of fine solids, which can be collected and concentrated by centrifugation. The process described by Lora et al. (1988) was adapted in this project. The special characteristics of PureVision lignin and its potential uses are discussed later.

Data Analysis

Averages of two (Phase I) or three (Phase II) experimental values for all design points were used to generate the graphs that follow. Design Expert™ software's statistical package and multivariate linear regression were used for data analysis.

Severity Factors

The standard severity factor (combination of temperature and residence time) and the combined severity factor (combination of acid catalyst concentration, temperature, and residence time) can be used to present the data more cohesively. The two severity factors are defined below.

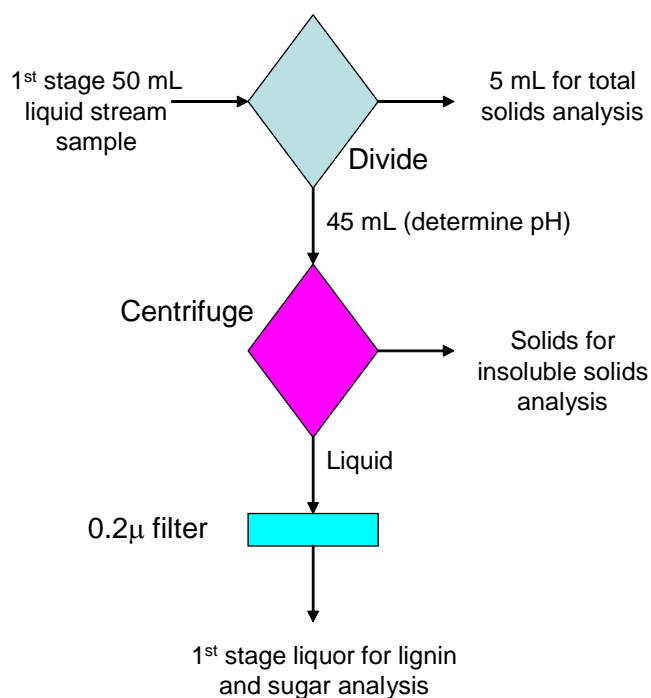


Figure 2. Protocol for first-stage sample preparation.

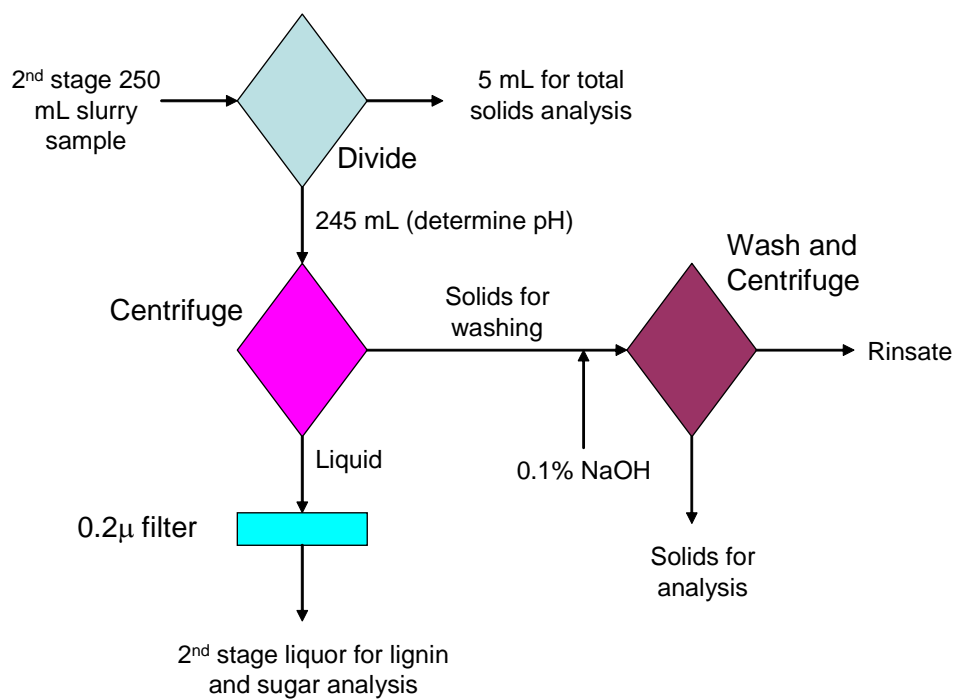


Figure 3. Protocol for second-stage sample preparation.

reaction ordinate (severity) factor $R_o = \int e^{(T_{\text{exp}} - T_b / 14.75)} dt$,

where, T_{exp} = experimental temperature in °C

T_b = base temperature of 100°C

t = reaction time

combined severity factor $R_c = \log R_o - pH$

where, pH refers to the liquid phase pH.

Using an assumed one-minute residence time in the extruder, severity factors can be calculated. A new combined severity factor, heretofore not reported in the literature, was also defined for the alkaline hydrolysis of lignin:

alkaline severity factor $R_a = \log R_o + pH$

where, pH refers to the liquid phase pH.

3. Results and Discussion

PureVision Process: Original Design vs. Modified Design

The basic process schematic of the original design is shown in Figure 4. Pretreatment is accomplished via autohydrolysis or with the aid of weak acids. The countercurrent flow of the two streams results in a temperature gradient in the reactor. The liquid stream encounters lower temperatures as it travels toward the exit, and degradation reactions are impeded as a result. Furthermore, solid/liquid (S/L) separation is *in situ* and at operating temperature.

No heat loss occurs because the hot dewatered pretreated solids (~50%) proceed to the second stage without flashing (as is the case when the S/L separation is decoupled from the hydrolyzer). The objective for the first stage is to conduct efficient hemicellulose hydrolysis, plus hot separation of the liquid. Countercurrent delignification was originally envisioned to be carried out in the second stage, yielding a liquid stream—containing mostly lignin—and a solid cellulose product that has been dewatered to ~50% solids.

However, in the modified design (Figure 5), cocurrent delignification is carried out in the second stage, yielding a slurry (see section “Second Stage Design and Cost Considerations” for justification for this design change). After S/L separation, a liquid stream rich in lignin and a solid cellulose product are obtained. The objective for the second stage is to maximize lignin hydrolysis without cellulose loss.

For the second stage of the PureVision process, a simple mixing/transport screw is used; the cost of such a screw will be an order of magnitude lower than that of an equivalent Entek twin-screw extruder. Also, the benefits of the countercurrent mode are less evident for the second stage, and the cocurrent mode has its own advantages including compatibility with any feedstock suitable for first-stage processing, and an estimated hardware cost an order of magnitude lower than that of an extruder-based countercurrent-flow system. Conceptual representation of the revised PureVision process, with a countercurrent first stage and a cocurrent second stage, is provided in Figure 5. PureVision petitioned DOE for this design change, which was approved.

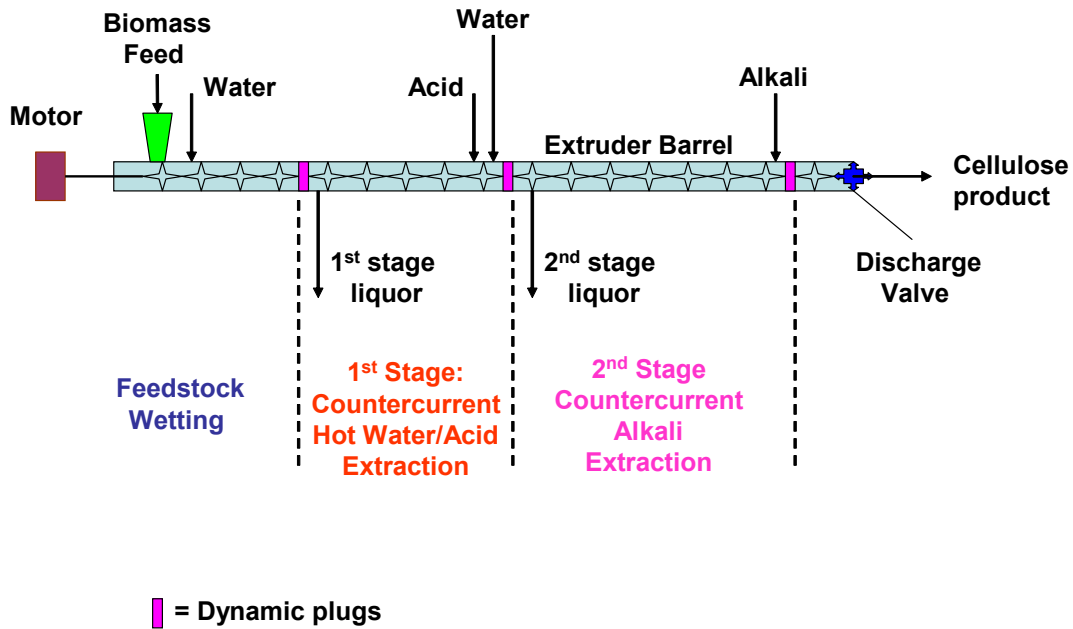


Figure 4. Conceptual representation of the PureVision process: two countercurrent stages.

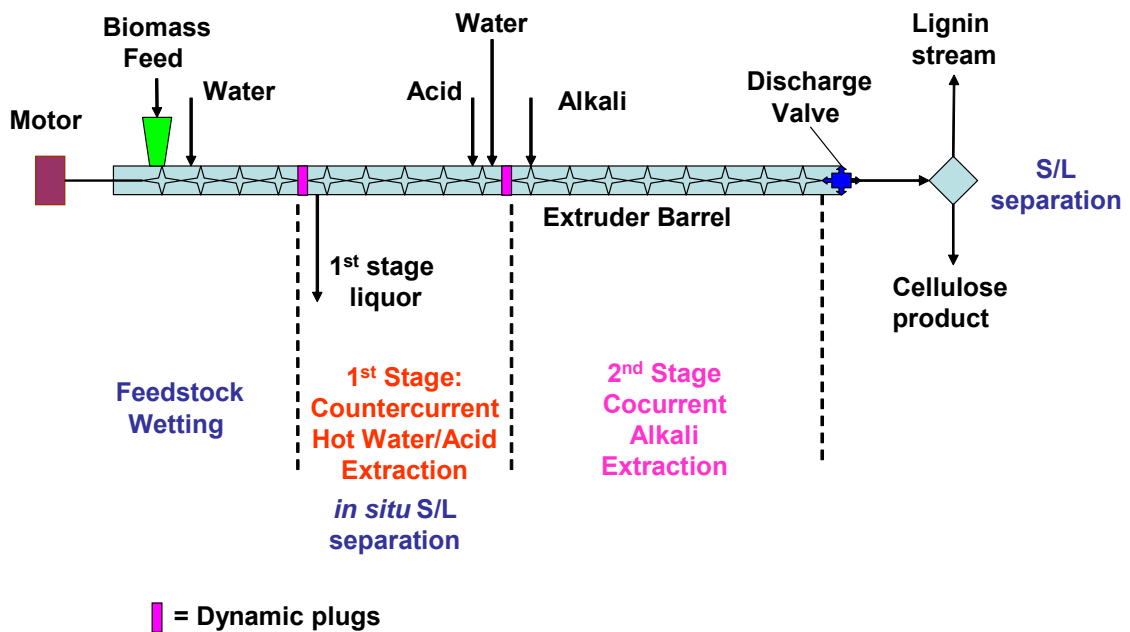


Figure 5. Representation of the modified PureVision process: with a countercurrent first stage and a cocurrent second stage.

The revised second stage is a simple heated tube mated directly to the solid discharge port of the first stage to preserve critical temperatures and pressures. The reaction barrel contains an auger turning at low speed to provide needed mixing to preclude settling of solids. The single-screw auger facilitates material transport in a plug-flow manner and provides mixing action, which enhances chemical reaction rates. Separate drive motors are provided for the first and second stages. A pressure controlled discharge valve releases second-stage reaction products for filtration and rinsing to complete the fractionation process. Requisite reaction times are easily provided by selecting appropriate length and diameter for the tube.. Given that *in situ* solid/liquid separation is not inherent in a cocurrent, plug-flow system, adjunct processes for filtering and washing the discharged slurry are necessary in order to achieve separate liquid and solid product streams.

Task 1. Optimize Fractionation of Corn Stover at PDU-Scale

First Stage Optimization

The objective of this effort was to generate performance data for the first stage. Prehydrolysis with and without acid addition was evaluated.

3.1.1.1. Autohydrolysis

Autohydrolysis was conducted at various extruder speeds, temperatures and liquid flow rates. The range of conditions was as follows: extruder RPM 14–28, temperature 190–220°C, and liquid flow rate 30–110 mL/min. Extruder rpm also determines solids feed rates because the extruder is operated within a narrow range of torque, which is affected by solids feed rate. A key observation is that xylan recovery is mostly in oligomeric form, which is highly desirable because it prevents any degradation reactions that can potentially occur with the monomeric form. This is a result of using endogenous weak acid and a short residence time during pretreatment.

A general trend toward higher xylan solubilization with increasing liquid flow rates was observed. This led us to believe that the liquid residence time was as important as the solids residence time. Viscous drag between the solids and the liquid flowing countercurrently tends to compress the solids and increase their density. Higher liquid flows may compress the solids and retard their progress. This will increase severity and contribute to higher xylan solubilization. The interaction between liquid and solids is critical to extruder performance. Hence, L/S ratio was used as a parameter that combines both solids and liquid flow rates. Data from 55 experimental conditions were analyzed using multivariate linear regression.

A maximum xylose recovery was discerned with respect to temperature for a given L/S ratio. Higher xylan solubilization was achieved with increasing L/S ratio. This is interpreted to mean that at higher L/S ratios, the solubilized sugars are rapidly washed away in the first stage liquor thereby minimizing their loss to secondary reactions. Conversely, at lower L/S ratio, the sugars linger in the reactor longer allowing parasitic

reactions to degrade them into byproducts. At temperatures beyond the maximum, the rates of reaction increase for secondary pathways toward degradation products.

Although higher L/S ratios yield higher xylose recoveries, there is a practical limitation on L/S ratio. At L/S ratio of 6, about 60% xylose recovery is achieved, and although higher L/S ratios yield incrementally higher xylose recoveries, the dilution of the first stage liquor is too great. Hence, L/S ratio of 6 is considered to be a good compromise with about 16% effective solids concentration in the reactor. For L/S ratio of 6, 210°C was the optimum temperature of operation.

Glucose recovery was <10% indicating that not much cellulose is being degraded. The behavior of glucose recovery is qualitatively similar to that of xylose recovery, which is not unexpected since this glucose is being released mostly from hemicellulose. Plots of lignin recovery as a function of L/S ratio and temperature indicated that both higher L/S ratio and temperature increased lignin recovered in the first stage liquor.

We have observed previously that during autohydrolysis lignin recovery concomitantly increases with xylose recovery and that acid addition during pretreatment retards lignin solubilization. It should also be noted that these lignin recoveries are based on UV absorbance of the liquor samples measured at 320 nm and extinction coefficient published by NREL. As non-lignin entities can contribute to the UV absorbance, these data should be used with some caution.

3.1.1.2. Acid Catalyzed Prehydrolysis

The NREL process uses an acid concentration of about 0.03 g/g biomass, and in this work the maximum sulfuric acid concentration was 0.01 g/g biomass. This because stable extruder operation was impossible under more severe conditions, i.e., the second plug was too weak and the pressure could not be maintained. Data from 19 experimental conditions resulting in stable extruder operation were analyzed using multivariate linear regression. At higher L/S ratios, acid addition at 200°C can lead to xylose recoveries of 70% or slightly higher. However, at lower L/S ratios, acid addition does not significantly affect xylose recovery. This may be due to a lower combined severity because low L/S ratios do not compress the solids enough to retard their progress. This will decrease severity and a much higher acid concentration would be needed to achieve higher xylan solubilization.

3.1.1.3. Cocurrent vs. Countercurrent Mode

The Sunds reactor used by NREL and others is a cocurrent plug flow reactor (PFR). In a PFR, fluid is perfectly mixed in radial direction but not in axial direction. So when dealing with slurries, solids and liquid have the same residence time, τ (Figure 6). Conversely, the PureVision reactor is not like a PFR, with liquid and solids paths being countercurrent to each other as shown in Figure 7. The liquid follows a tortuous path, and residence times of solids and liquid are not the same.

Cocurrent systems such as the Sunds reactor can achieve 85% hemicellulose hydrolysis using acid concentration of about 0.03 g/g biomass, the liquor pH being around ≤ 2 . We

cannot, for reasons elaborated above, use such high acid loadings. Hence, ~70% xylose recovery seems to be the limit for corn stover using our countercurrent system even with acid addition. The liquor pH values are much higher than those used by cocurrent modes of operation such as the NREL process. We have also observed that under same operating conditions, we achieve pH that is one unit lower in cocurrent mode vs. that in countercurrent mode. The fundamental distinctions elaborated above may explain why these two systems behave differently in terms of hemicellulose hydrolysis.

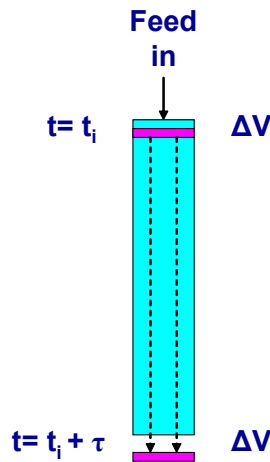


Figure 6. Plug flow reactor schematic (cocurrent mode), where ΔV = finite element or plug traveling through the reactor; t = time, t_i = time when the plug enters the reactor, τ = plug residence time.

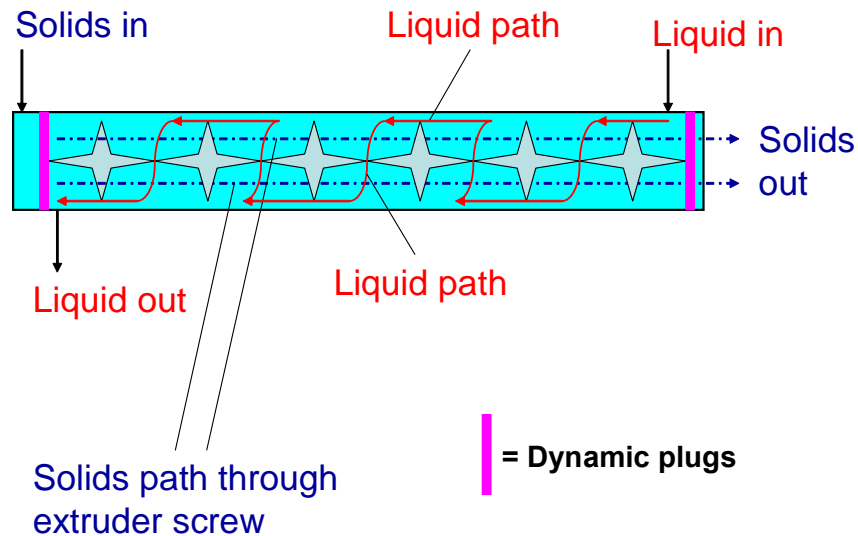


Figure 7. PureVision reactor schematic showing liquid and solids paths (countercurrent mode).

Selection of Prehydrolysis Mode

As acid addition does not seem to be significantly beneficial, autohydrolysis was selected as the preferred mode. Although this can reduce ethanol yields, the benefits of autohydrolysis are: 1) no cost of acid, 2) less expensive materials of construction, 3) no gypsum formation and related disposal and handling costs, and 4) no need for S/L separation after liquor conditioning.

Second Stage Optimization

The system was operated with the two stages running in tandem to conduct experiments using statistical designs. The first stage conditions were held constant at $T=210^{\circ}\text{C}$, 28 rpm, and 72 mL/min ($L/S = \sim 6$). The goal of second stage optimization was to achieve $\leq 5\%$ residual lignin in the solids stream with minimum NaOH charge and cellulose degradation. NaOH charge of 0.12 g/g biomass, corresponding to the kraft process, was used the upper limit.

Design-Expert software was used to analyze the entire dataset results and develop predictive statistical models. Statistical analysis of residual lignin data led to the conclusion that a residence time of ca. 11 min was optimal and that NaOH charge of >0.1 g/g biomass did not offer additional benefit. As we wish to minimize NaOH consumption, the effect of NaOH charge on residual lignin was further analyzed and led to the conclusion that NaOH charge of 0.06 g/g biomass can be used to produce a solids stream with $\sim 5\%$ residual lignin. These experiments proved our ability to conduct the two stages of the PureVision process in tandem with countercurrent autohydrolysis in the first stage and cocurrent lignin hydrolysis in the second stage with NaOH addition.

The residual lignin data were also analyzed with help of the alkaline severity factor. There was observed a good linear relationship between lignin removal efficiency and the alkaline severity factor. Hence this new severity factor may also be used in pulping applications and alkaline pretreatments.

Mass Balance

Preliminary mass and component balances were conducted around the process. Total mass and glucan balances were within ca. 10% (Table 4). Xylan is degraded to its acid form under alkaline conditions, and hence xylan balance closure was off significantly. Lignin balance did not close with good tolerance; however, as explained above, lignin analysis is also fraught with problems leading to poor mass balance closure.

Table 4. Mass and component balance closure

	Production run 1	Production run 2	Production run 3
Total solids	98.9	89.3	89.8
Glucan	94.0	90.1	97.0
Xylan	75.6	75.8	71.7
Lignin	97.0	87.8	86.1

3.1.1.4. Sugar Degradation under Alkaline Conditions

The reason for not detecting xylose or glucose in the second stage liquor is that sugars readily undergo degradation reactions in alkaline solution including the formation of multiple sugar acids from an individual sugar: for example, lactic, glyceric and ribonic acid from ribose. Rate of sugar degradation is much greater under alkaline pH conditions, compared with that at neutral pH (Benjakul et al. 2005).

Other researchers have shown that when spruce hydrolyzate from dilute-acid pretreatment was treated at pH 9 and 80°C for 1 h, >25% of the glucose was lost (Nilvebrant et al. 2003). Among the monosaccharides, xylose was degraded faster under alkaline conditions than the hexoses (glucose, mannose, and galactose), which were degraded more rapidly than arabinose. Their results suggested that hydrolyzates can be treated using alkali at temperatures below 30°C at any pH between 9.0 and 12.0 without encountering sugar degradation or formation of inhibitory aliphatic acids. The choice of alkali was also important because treatment with $\text{Ca}(\text{OH})_2$ instead of NaOH resulted in more substantial degradation of sugars.

3.1.1.5. Lignin Analysis of Liquors and Solids

Corn stover feedstock and second stage solids were analyzed for Klason lignin, and first and second stage liquors were analyzed for lignin using UV absorbance. The same method with the same extinction coefficient as that used for acid-soluble lignin was used for second stage liquors as no published method for alkaline conditions was available.

Determination of lignin is a problem faced by all researchers in the biomass field. Hatfield et al. (2005) report a similar difficulty in measuring lignin content in forages. Most frequently used lignin assays are the acid detergent, Klason, permanganate, and acetyl bromide lignin methods. Each of these methods gave different lignin values, the variance depending on the type of forage sample. For example, acid detergent, Klason, permanganate, and acetyl bromide lignin methods gave the following values for alfalfa stems: 93, 145, 158, and 135 g lignin/kg cell wall, respectively. These differences were greater for grasses: 25, 77, 45, and 92 g lignin/kg cell wall from corn (*Zea mays L.*) stalks analyzed by acid detergent, Klason, permanganate, and acetyl bromide lignin methods, respectively. This highlights how different lignin determination methods can yield widely varying lignin contents. This is further exacerbated for hydrolyzed/solubilized lignin because lignin fragments of varying molecular weights are present, and all these entities have different absorbances at a given wavelength and hence, different extinction coefficients. Total lignin removal based on solids analysis, however, is reliable because both were subjected to the same Klason lignin assay.

3.1.1.6. Sources of Errors

Sources of errors in mass and component balances are listed below:

Total mass:	calculation of solids feed rate from Acrison output, sampling errors.
Glucan:	glucose degraded to its acid form in the second stage.
Xylan:	xylose degraded to its acid form in the second stage.

Lignin: soluble lignin based on UV absorbance at 320 nm and extinction coefficient may not be accurate, some “pseudo-lignins” survive acid hydrolysis step and end up contributing to Klason lignin values.

Bagasse Fractionation

Once a DOE Interim Stage Gate Review determined that the fractionation process for corn stover had been optimized, PureVision was given approval to begin processing bagasse in February, 2007. At a first stage temperature of 195°C about 57% was achieved, and at a second stage temperature of 200°C to produce with <5% Klason lignin. Hence, bagasse fractionation needed slightly less severe conditions compared to those for corn stover. This conceptually proves that bagasse fractionation is feasible, but a more detail investigation with bagasse is needed to compile a database comparable to that provided above utilizing corn stover.

Task 2. Investigate Corn Stover Hydrolyzate Liquor Fractions for Separation and Purification Techniques and Commercial Applications

Simulated Moving Bed Chromatography

Both autohydrolysis and acid-catalyzed prehydrolysis of biomass to sugars can generate byproducts (e.g., acetic acid) and sugar degradation products (furfural and HMF). Lignin and other components in the biomass will also degrade to a variety of phenolic compounds. These compounds can act as inhibitors to downstream fermentation. This subtask investigated the potential use of simulated moving bed (SMB) chromatography process for the separation of sugars, lignin, and fermentation inhibitors from the first stage hydrolyzate of the PureVision process.

Standard post-hydrolysis steps include overliming with CaOH to neutralize sulfuric acid and to remove some of the inhibitors before fermentation. Wooley et al. (1998) showed that chromatography processes could be used instead to isolate the sugars leading to better fermentation than the overlimed hydrolyzate. Xie et al. (2005) designed and tested SMB processes for sugars isolation using NREL corn stover acid-hydrolyzate. The published work resulted from a project report from Wang and coworkers in a DOE funded project (Wang et al. 2003)

The low concentration of known inhibitors (HMF, furfural and acetic acid) have recently been shown to have negligible effects at concentrations below 5 g/L for the LNH-ST 424 engineered yeast (Mosier et al. 2006). Our first stage liquor has low levels of these inhibitors, and we surmised, at this point, that SMB may not be an economical avenue. We may revisit the use of SMB for improving hydrolyzate fermentability when further results are available from ongoing and planned fermentability studies.

NREL

Gel permeation chromatography (GPC) of first and second stage liquors was conducted by NREL. The average molecular weight is 900 for first stage lignin and 1,800 for second stage lignin, latter still being an order of magnitude smaller than kraft lignin with a MW

of ~50,000. Using an average phenylpropane unit molecular weight of 180-200, we see peaks for monomers, dimmers, trimers and tetramers for first stage lignin only. The peak at around 900 Dalton seen can be interpreted as a pentamer. A lower MW may signify more reactivity thereby facilitating further conversion to value-added products.

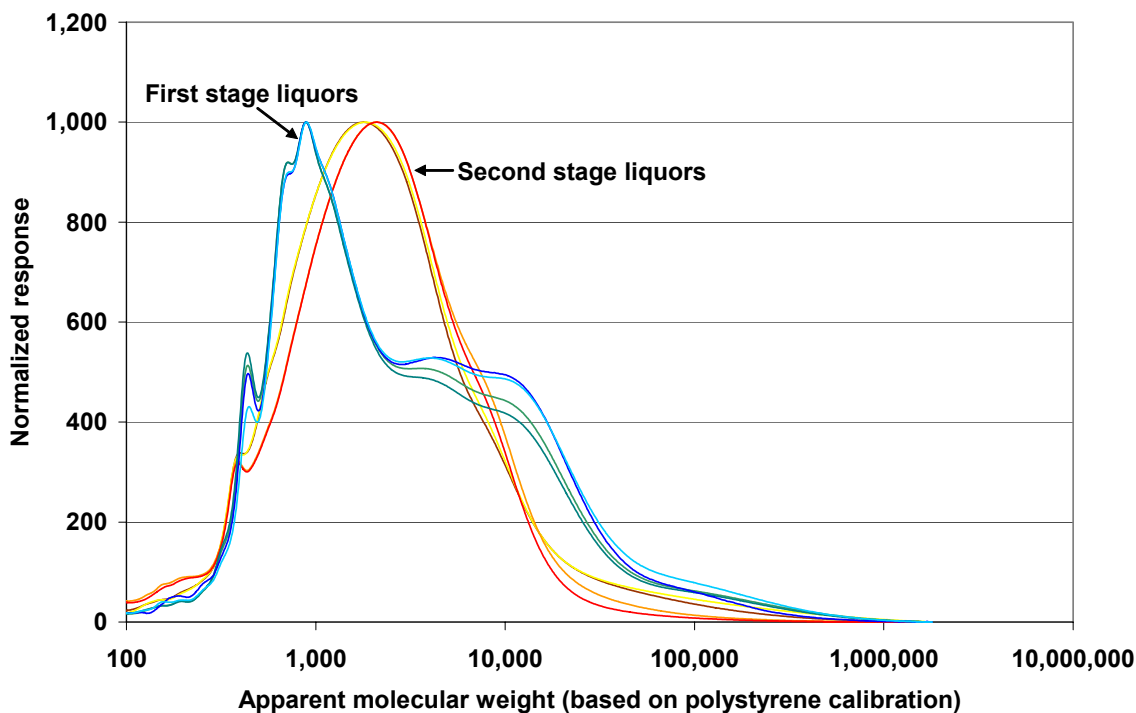


Figure 8. GPC of lignin from first and second stage liquors.

PPG Industries

Because of problems with traditional wet lab titration methods for the determination of phenolic content with lignin materials, alternative methods were evaluated by PP&G. After review of the literature, they identified a P-31 NMR method developed for the analysis of lignin materials that are first derivatized with 2-chloro-4,4,5,5-tetramethyl-1,3,2-dioxaphospholane (Argyropoulos et al. 1993; Granata and Argyropoulos 1995). The literature reports results that can be used to quantify not only total phenolic content, but the amount of aliphatic hydroxyl, Syringyl, Guaiacyl/Dimethoxy phenols, and carboxylic acids. This information is important because the amount of phenol along with the types of phenolic groups present will determine the reactivity of a given lignin material. Based on this analysis, PureVision lignin is suitable for PPG Industries' goal of using it in coating applications, and hence, it is being evaluated for the same.

University of Utah

This research program evaluated catalytic conversion of PureVision lignin samples to hydrocarbon products. Figure 9 depicts a flow diagram of the enhanced three-stage process for conversion of lignin to alkylbenzene gasoline blending components.

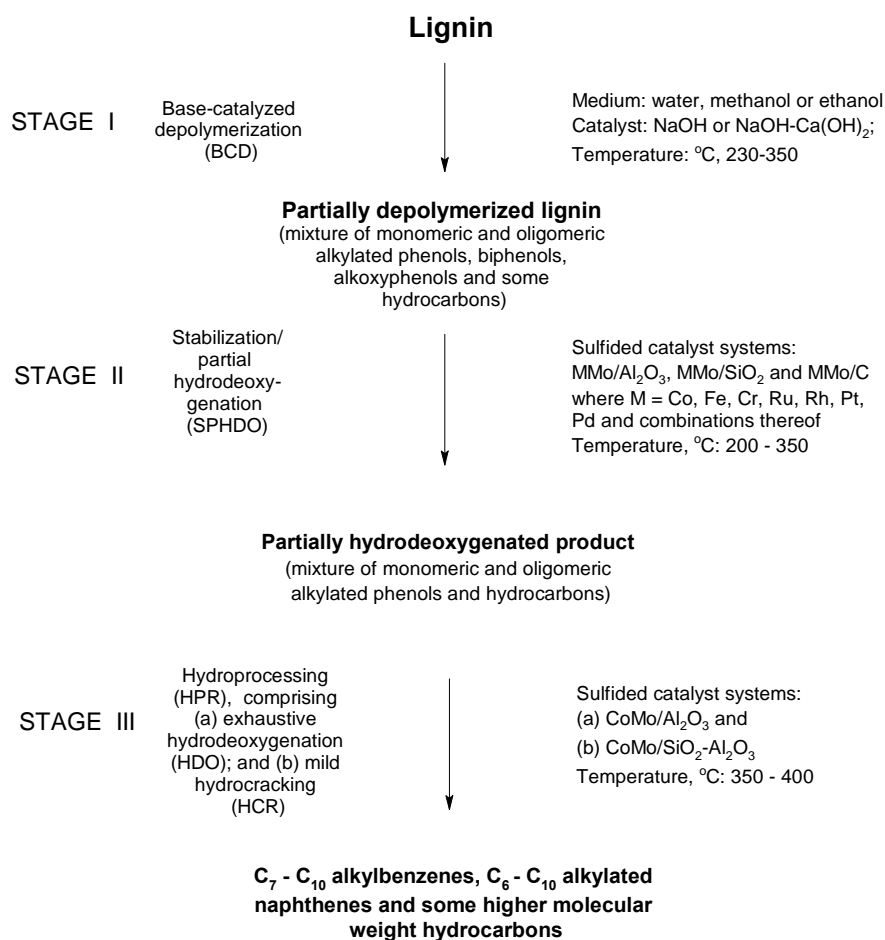


Figure 9. Flow diagram of the enhanced three-stage process for conversion of lignin to alkylbenzene gasoline blending components.

Key conclusions were as follows:

- Catalytic conversion of PureVision lignin, with the use of water as reaction medium, leads to products similar to those obtained from other types of lignin; however, its rate is distinctly higher.
- Consequently, higher BCD conversion to ether-soluble product provides higher yields of final products.
- Development of BCD-SPHDO-HPR (base-catalyst depolymerization-stabilization/partial hydrodeoxygenation-catalytic hydroprocessing) process of PureVision lignin leads to a flexible multi-product technology.
- The catalytic conversion of PureVision lignin can provide at least four overlapping fuel products, including a high-octane alkylbenzene gasoline additive, jet fuel aromatic components, a paraffinic diesel or jet fuel component, and jet/rocket naphthenic fuel (naphthenic kerosene).

Weyerhaeuser

Key points in the Weyerhaeuser report are as follows:

- The liquor fraction contains some sugars at low concentrations (5% total). They exist in oligomeric form.
- The lignin fractions, by contrast, are 95% pure. Heating values are consistent with typical lignin heating values. The IR spectra are comparable to hardwood lignins. The melting point/rheology of the lignin was not yet shown to be compatible with the needs of phenol-formaldehyde resin substitute.
- The fiber fraction has a moderate lignin content (10.7%) but is mechanically comminuted to an extreme that would make it well suited to enzymatic hydrolysis or further chemical processing.

MAST

The MAST (Membrane Applied Science & Technology Center at the University of Colorado, Boulder, CO) subtask focused on evaluation and development of membrane-based processes for fractionation and recovery of lignin, sugar, and electrolytes (including alkaline and acidic species) from aqueous solutions in biomass processing. Specifically they studied the separation of lignin and sodium hydroxide from the alkaline second stage liquor using the electrodialysis setup shown in Figure 10. Key results were as follows:

- Greater than 78% of the Na^+ ions contained in the raw hydrolysis liquor, ends up in the ED concentrate stream. This latter stream is what can be recycled back to the hydrolysis reactor. Approximately 80.6% of the lignin fed to the UF was in the retentate. The final ED diluate contained ~15% of the recovered lignin with the remaining ~4.4% being in the ED concentrate (to be recycled to the hydrolysis reactor), the solid precipitate, and lost in the material balance uncertainties. Thus, >95% of the Klason lignin was recovered in two separate product streams.

The basic conclusion is that it is technically feasible to separate lignin and Na from the second stage liquor; however, more work is needed.

MTR

The scope of work required from MTR (Membrane Technology and Research, Inc., Menlo Park CA) included the following specific objectives:

1. To permeate the xylose (and glucose) and reject the lignin from the first-stage liquor streams using MTR's non-porous ultrafiltration membrane.
2. To separate and purify the mixed sugars, the lignin and potentially the caustic contained within the second-stage liquor streams using MTR's non-porous ultrafiltration membrane, with the aim of rejecting the lignin from the other stream components.

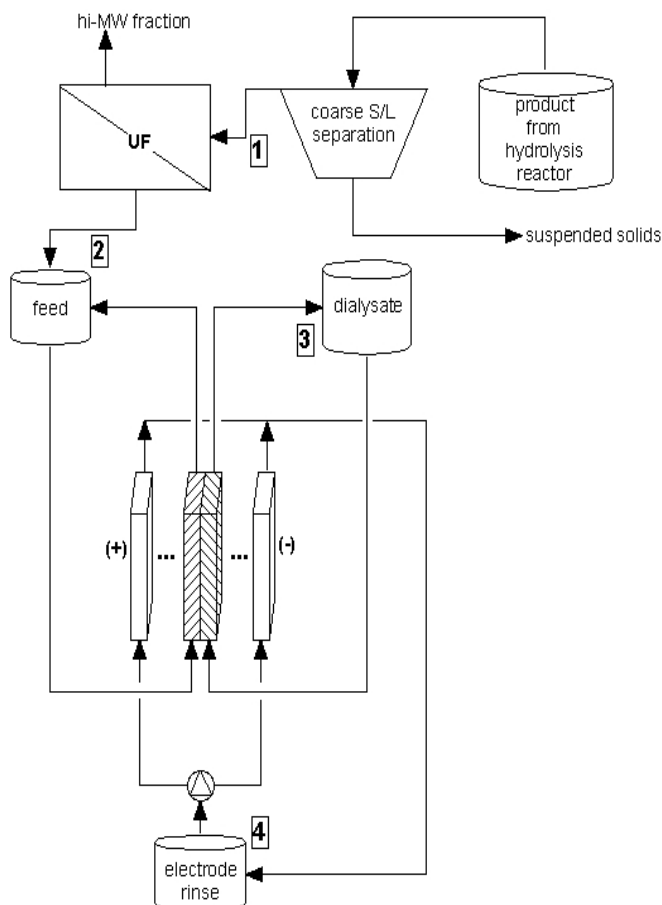


Figure 10. Schematic of electro dialysis setup.

Diagram of the test apparatus is shown in Figure 11. Key results were as follows:

The two ultrafiltration membranes identified by MTR for lignin/sugar separations did not perform well based on PureVision's permeate analysis. This is mainly because the molecular weight (MW) of the lignin is about 1,000, which is not that much different from the MW of sugars. Ultrafiltration membranes generally have a MW cutoff of 10,000 and may work for high MW lignins such as kraft lignin and liginosulfonates. Literature research did not find other appropriate ultrafiltration membranes for such applications. The basic conclusion was that ultrafiltration membranes are too porous and tighter membranes are needed to separate lignin and sugars from the first stage liquor; this will require more work.

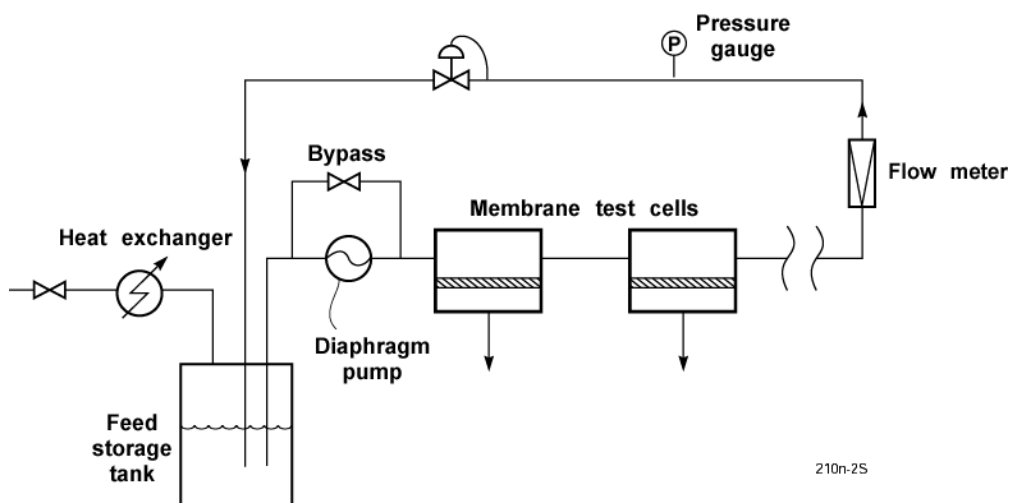


Figure 11. Diagram of the test apparatus for separation of sugars through thin composite membranes.

Task 3. Cellulose Fraction Evaluation, Utilization and Market Analysis

Enzymatic Hydrolysis

The NREL base case assumes an enzyme loading of 12 FPU/g cellulose (Aden et al. 2002); an enzyme loading of 5 FPU/g cellulose was used for hydrolyzing the PureVision corn stover solid substrate. At this low enzyme loading almost complete cellulose hydrolysis of “as is” corn stover solids was achieved in 7 days even at 10% solids. This is in comparison to 80% hydrolysis obtained by Kadam et al. (2004) in 7 days with 12 FPU/g cellulose (from pretreated corn stover).

As the solids substrate from PureVision’s fractionation process is very high in cellulose (~85–90%), 10% solids release enough sugars to yield about 5% ethanol during SSF/HHF, which is considered a minimum ethanol concentration in terms of reasonable distillation energy (HHF: hybrid hydrolysis and fermentation). Obviously, increasing solids loadings achieved through a fed-batch mode will yield higher sugar and hence, higher ethanol concentration thereby reducing distillation energy. The PureVision substrate, besides needing less enzyme, can achieve 50% higher ethanol concentration compared to a typically pretreated substrate.

Pulp and Paper Production

Fiber testing was performed at Auburn University’s Pulp and Paper Research Education Center (Auburn, AL). Corn stover pulp was blended with other pulps to test it as a substitute for some of the hardwood pulp. Unbleached pine and Southern hardwood pulps were utilized in conjunction with corn stover pulp. The corn stover pulp substitutes for various amounts of the hardwood pulp in the blends, with pine pulp remaining at 50%. The standard composition is equal parts of pine and hardwood, i.e., 50% each for the top ply of a linerboard, which is a target application.

Corn stover pulp substituted hardwood pulp at 10 and 30% levels, the hardwood pulp portion was reduced accordingly with softwood pulp staying constant at 50%. TAPPI (Technical Association of the Pulp and Paper Industry, Norcross, Georgia, USA) standard handsheets of the pure corn stover pulp and pulp blends were made for physical testing. Tests showed that corn stover pulp may be blended at 10-20% level without too much degradation of pulp properties. Corn stover pulp reduced the strength of the sheet as the proportion was increased. Bulk, porosity and Taber stiffness showed slight increase showing that the substitution of corn pulp produced open structure sheet than the standard softwood/hardwood blend. Caliper and porosity increased indicating that the corn pulp produced a more bulky, open sheet than the standard hardwood. A 10% substitution of hardwood pulp by the corn stover pulps do not show much change in most of the properties investigated.

Task 4. Perform Aspen modeling of the PureVision Biorefining Process

Technoeconomic Analysis

Preliminary economic analysis was conducted on the PureVision process for ethanol production from corn stover in comparison to the NREL process. Both the NREL plant (Figure 12) and the PureVision plant (Figure 13) produce ethanol and electricity, whereas the latter also generates lignin as a sellable output. The lignin is to be sold on the outside market as concrete binder or feed binder. An Aspen-based process model was developed by Harris Group.

3.1.1.7. Methodology

The NREL process as modeled in Aspen (Aden et al. 2002) was used as a baseline and the NREL pretreatment section was replaced with PureVision's pretreatment or fractionation scheme. The lignin produced is sold instead of burning as in the NREL process. To satisfy thermal needs of the PureVision biorefinery, additional corn stover (ca. 23%) is burned as fuel to generate LP and HP steam; hence, the front-end of the PureVision plant needs to be commensurately larger.

The Aspen model was used to generate mass and energy flows, and the equipment was resized accordingly. The scaling factors in the NREL design report were used to estimate resized equipment costs. Table 5 shows the capital and operating costs for the two processes, PureVision's capital costs being about 10% higher. However, it should be noted that the turbogenerator is not fully optimized, and its further optimization will reduce capital costs for the PureVision plant.

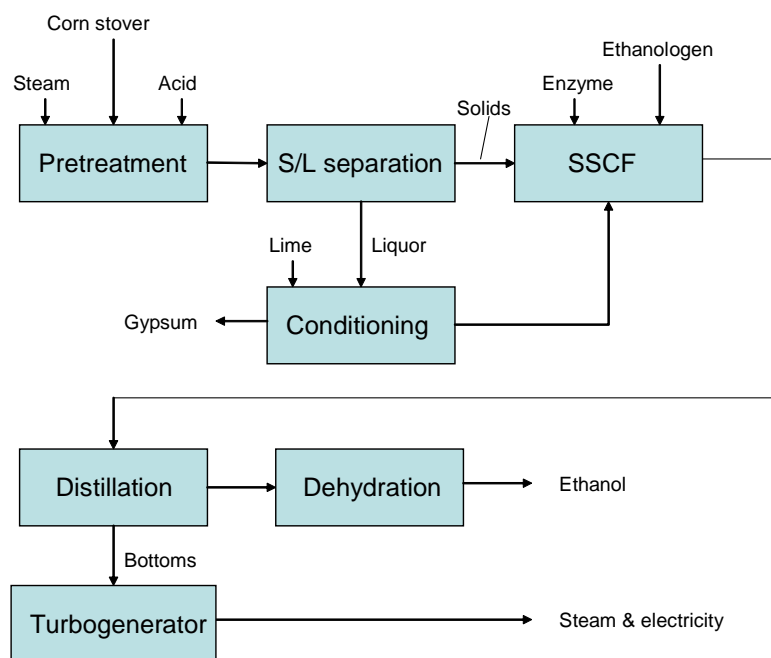


Figure 12. Schematic of the NREL biorefinery.

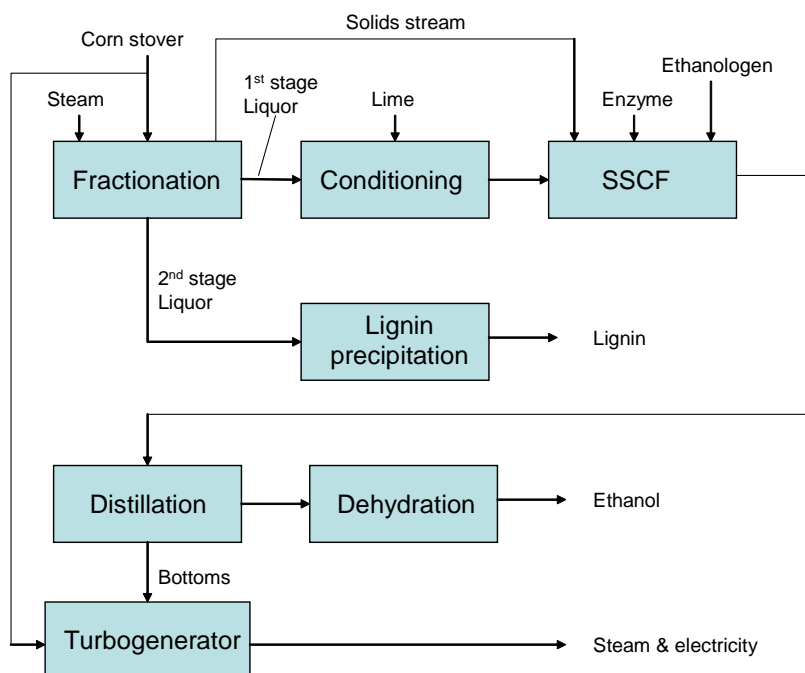


Figure 13. Schematic of the PureVision biorefinery.

The main differences are that the PureVision process uses extra corn stover as fuel and needs NaOH. Conversely, since autohydrolysis mode is used it also uses less H₂SO₄, which is used only in lignin precipitation. The selling price of electricity is the same for both scenarios, whereas PureVision process enjoys additional sales from lignin modeled at \$300/short ton. This price is based on the lower end of lignin applications such as concrete binder (\$250/short ton) and as feed binder (\$350–425/short ton). Hence, a \$300/short ton or \$330/mt selling price is a reasonable assumption.

3.1.1.8. *Analysis Results*

Following the NREL protocol of assuming 100% equity and a 10% discounted cash flow rate of return (ROR), the minimum ethanol selling price (MESP) was calculated for both scenarios. The baseline MESP is \$1.07/gal ethanol for the NREL process vs. \$0.94/gal ethanol for the PureVision process. Thus, the PureVision process offers a significant economic advantage. The major economic drivers for the PureVision process are selling price of lignin and cost of NaOH. Figure 14 shows the effect of lignin selling price on MESP. It is thus essential to accurately value the lignin product. The NaOH usage can be reduced by further optimizing the second stage parameters of residence time and temperature. When NaOH consumption is reduced to 0.04 g/g biomass, the MESP drops to \$0.84/gal ethanol, a substantial decrease (Table 6). Also, as the turbogenerator is not fully optimized yet, the corn stover consumption for fuel can be lower than the current additional 23% requirement. If corn stover usage as fuel is reduced by half and NaOH consumption is 0.04 g/g biomass, the MESP drops to \$0.80/gal ethanol (Table 6). Alternatives to NaOH are also being investigated which can lower base costs. As these changes are quite feasible, the PureVision process presents a considerable economic upside compared to the NREL process and is worthy of scale-up to commercial scale.

Table 5. Key costs and incomes for the two processes

	NREL	PVT
Total installed equipment cost, \$MM/yr	113.8	122.6
Variable operating costs, \$MM/yr	37.9	51.4
Income from lignin	0.0	35.0
Income from electricity	6.5	4.0

Table 6. Sensitivity analysis

Scenario	Minimum ethanol selling price, \$/gal
NREL—base case	1.07
PureVision—base case	0.94
PureVision—NaOH reduced to 0.04 g/g biomass	0.84
PureVision—NaOH reduced to 0.04 g/g biomass and corn stover as fuel reduced by half	0.80

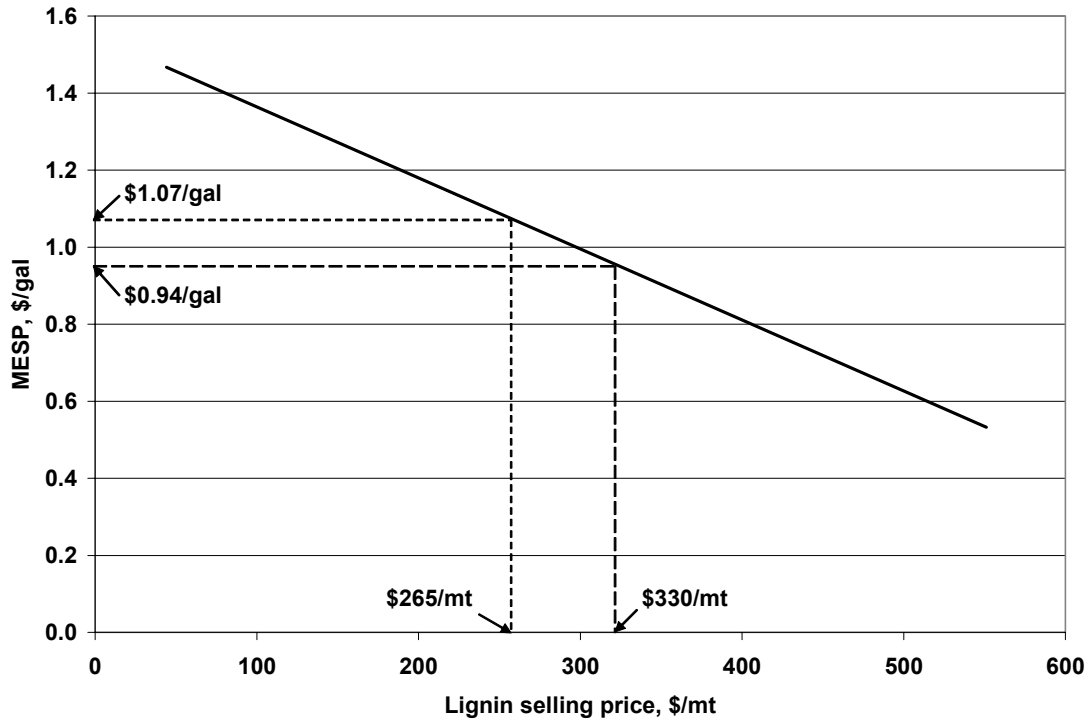


Figure 14. Effect of selling price of lignin on MESP.

Bagasse Feedstock Assessment

PureVision engaged two subcontractors to undertake feedstock availability assessments for bagasse in Louisiana and adjoining states: Subtask 4.1 Bagasse Assessment by Louisiana State University (LSU) and Subtask 4.2 Feedstock Assessments by M.A. Patout (Patout). The objective of these assessments was to determine the availability of bagasse for siting a commercial bagasse recovery operation using the PureVision technology and to seek a go/no-go decision by M.A. Patout on their interest in pursuing such a program.

In compliance with the award, each subcontractor submitted a formal report to PureVision. Professor Sun Joseph Chang of the School of Renewable Natural Resources of the Louisiana State University (LSU) Agricultural Center completed a report. M.A. Patout and Son (owner of Raceland Raw Sugar Corporation) provided an investigation regarding the present cane biomass capabilities of its three sugar cane factory operations. The bulk of the information in this report was incorporated into the LSU report.

Based on the data provided in the two reports presented by PureVision subcontractors, there is an adequate supply of biomass to site up to five 75-ton per day bagasse-to-mills in Louisiana. The availability of bagasse for only part of the year as a result of only one harvest presents a difficult situation, which could be offset by applying wet storage techniques to preserve the bagasse as a year-round feedstock and by using woody biomass when bagasse is unavailable.

Future efforts toward developing the PureVision technology for bagasse pulping applications in Louisiana need to address the following market entry barriers:

1. Identify end user pulping mills that would be interested in bagasse pulp either in the form of market pulp or in a co-location scenario to produce pulp for on-site paper manufacturing. Louisiana has 13 pulp mills.
2. Undertake process optimization and scaleup studies aimed at meeting desired pulp specifications.
3. Complete simulated bagasse storage techniques employing “wet storage” to determine if year-round operations are feasible and how effective wet storage is at mitigating fiber degradation.
4. Undertake economic evaluations inclusive of harvest, storage, transportation, processing.

M.A. Patout, the largest sugarcane processor in the U.S., made the corporate decision to move ahead with a gasification process to extract energy from bagasse. Accordingly, PureVision did not submit any follow-on proposals to Patout to advance a formal commercialization initiative and a no-go decision was made regarding immediate opportunities to pursue a PureVision bagasse project with Patout.

Task 5. Finalize Preliminary Design Specifications, Engineering, and Costing for the Prototype Reactor

Entek Extruders estimated capital cost of a 250 mm future twin-screw extruder with 72 L/D to be \$2.08 million (plastics industry design). The capacity was estimated to be 80 mtpd of dry biomass. This cost reduces to \$0.83 million for a commercial-scale extruder using biorefinery design. The cost of a single-screw extruder for the second stage is to be estimated to be \$83,000. Hence, a 2,000 mtpd (dry basis) plant will require \$23 million in extruder capital. This is based on the current design of a twin-screw extruder for the first stage and a single-screw extruder for the second stage. A new design is being developed by PureVision in collaboration with Buhler (Uzwil, Switzerland) that will substantially reduce the extruder capital costs.

4. Conclusion

The overall objective of the project was to define a two-stage reactive fractionation process for converting corn stover into a solid cellulose stream and two liquid streams containing mostly hemicellulosic sugars and lignin, respectively. Toward this goal, biomass fractionation was conducted using a pilot unit with a nominal capacity of 100 pounds per day of dry biomass to generate performance data for the first and second stage using primarily corn stover as feedstock.

One of the most significant features of the PureVision technology documented in this program is the ability to separate cellulosic biomass into its three primary constituents, hemicellulose, lignin and cellulose. The actual process occurs rapidly in approximately 15 min. Documentation of the accomplishment of the primary milestone of separating biomass into three separate streams was presented during our first DOE-Stage Gage

Review in 2006. Subsequently, the PureVision process was optimized for efficient hemicellulose hydrolysis in the first stage and delignification in the second stage. The level of process performance achieved in this program is summarized in Table 7. These process performance targets satisfy the goals set forth in the project's statement of work SOW. The commercial potential of the process is further borne out by comparative economic analysis, which demonstrated that PureVision's process is economically superior to the NREL process.

Table 7. Operating conditions and process performance

	Operating conditions	Process performance
First stage	T = 210°C, L/S ratio = 6	60-65% xylose recovery in first stage liquor
Second stage	T = 220°C, NaOH charge = 0.06 g/g biomass, residence time = 11 min	30–35% solids yield (mostly cellulose), 2-3 wt% residual lignin in solids
Enzymatic hydrolysis	T = 50°C, as-is solids, cellulase loading of 5 FPU/g cellulose	60% and 80% theoretical glucose yield in 48 h for first and second generation cellulase, respectively

Of many exciting results from this program, there are four advancements worthy of mention. The first involves producing the hemicellulose-rich hydrolyzate in the first stage via autohydrolysis. Several major pretreatment technologies require the addition of acid during pretreatment step to facilitate subsequent enzymatic hydrolysis. The most popular technology that has been advanced by NREL during the last decade is an acid-based pretreatment. Using corn stover as the feedstock, the PureVision has demonstrated pretreatment with no addition of acid or any other reagent. The benefits of autohydrolysis are:

1. There are no costs associated with both purchasing and storing the acid.
2. Less caustic reagent additive is needed to neutralize the hydrolyzate since only endogenous acetic acid needs to be neutralized.
3. There is no formation of gypsum and there are no disposal costs associated with getting rid of the gypsum.
4. The pretreatment reactor costs can be lower since less expensive materials of construction can be used.

Another highlight of the program was the ability to produce a relatively pure cellulose substrate. Enzymatic hydrolysis experiments documented an enzyme loading of 5 FPU/g cellulose using the PureVision substrate compared to 12 FPU/g cellulose used in the NREL process.

A third noteworthy program result involves the general use of the PureVision lignin. While most cellulosic biorefining technologies are planning to burn the lignin for process steam and electricity, PureVision and our industrial collaborators have learned that the unique low-MW lignin is too valuable to burn for electricity and steam. PureVision worked with Weyerhaeuser and PPG Industries to demonstrate higher-value applications of the lignin. Weyerhaeuser had and continues to be interested in using the unique

PureVision lignin as a raw material to manufacture wood glues and adhesives. Currently their glues and adhesives are made with oil-based raw materials. PPG continues to be interested in using the PureVision lignin as a raw material to manufacture resins and coatings and has committed to participating in future PureVision programs. In both cases, the lignin as a bio-based raw material is worth over \$300/ton versus approximately \$45/ton to burn for electricity and steam.

The fourth significant result concerns a novel application of the PureVision lignin. PureVision tasked the University of Utah (UoU) to investigate using the unique PureVision lignin to produce a high-octane bio-gasoline. This lignin-to-biofuel work was a continuation of work previously under investigation by NREL and the UoU during the 1990s. The findings of the UoU work show that the PureVision lignin can be used to produce biodiesel, bio-jet fuel and bio-rocket fuel. This advancement not only identifies a pathway and markets for high-value lignin applications but also demonstrates that nearly all constituents of lignocellulosic biomass can be used to produce biofuels in the PureVision process.

The work completed successfully demonstrated the technical effectiveness of the process at the pilot level indicating the technology is ready to advance to a 2–3 ton per day scale. No technical showstoppers are anticipated in scaling up the process to commercial scale. Also, economic feasibility of the proposed biorefinery was investigated and the minimum ethanol-selling price for the PureVision process was calculated to be \$0.94/gal ethanol vs. \$1.07/gal ethanol for the NREL process. Thus, the PureVision process is economically attractive. Given its technical and economic feasibility, the project is being scaled up with world-class collaborators as listed in “Future Work.”

5. Products Developed and Technology Transfer Activities

Presentations

1. Kiran L. Kadam, Chim Y. Chin, and Lawrence W. Brown. *A Biomass Fractionation Process for the Production of Ethanol and Low-Molecular Weight Lignin*. Presented at International Symposium on Clean Energy Technology, Shanghai, China, November 21-23, 2007.
2. Kiran L. Kadam, Chim Y. Chin, and Lawrence W. Brown. *Optimization of a Biomass Fractionation Process and Evaluation of Its Economic Feasibility*. Presented at American Institute of Chemical Engineers (AIChE) Annual Meeting, Salt Lake City, UT, November 4-9, 2007.
3. Kadam, K.L., R.C. Wingerson, C.Y. Chin and L.W. Brown. *Biorefinery for producing ethanol, wood adhesives and specialty pulp products*. Presented at World Congress on Industrial Biotechnology and Bioprocessing, Orlando, Florida, March 2007.
4. Kadam, K.L., R.C. Wingerson, L.W. Brown and E. Lehrburger. *Flexible biorefinery for producing value-added streams: evaluation of the cellulose stream as a source of sugars and pulp*. Presented at AIChE National Meeting, San Francisco, California, November 2006.
5. Kadam, K.L. *Flexible biorefinery for generating value-added products from agricultural residues*. Presented at Biorefineries Asia, Bangkok, Thailand, June 2006 (invited presentation).

6. Kadam, K.L. *A green process for producing fermentable sugars and pulp from biomass*. Presented at *PacifiChem 2005*, Honolulu, HI, December 2005.
7. Kadam, K.L., R.C. Wingerson, and E. Lehrburger. *A process for refining biomass into value-added products*. Presented at *AIChE National Meeting*, Cincinnati, OH, November 2005.
8. Kiran L. Kadam, Ed Lehrburger, and Carl Lehrburger. *Greenhouse Gas Reduction Opportunities via Processing Agricultural Residues in Rural Biorefineries*. Presented at *3rd USDA Symposium on Greenhouse Gases & Carbon Sequestration in Agriculture & Forestry*, Baltimore, MD, March 21-24, 2005.

Publications

1. K. L. Kadam, C. Y. Chin and L. W. Brown. Flexible biorefinery for producing fermentation sugars, lignin and pulp from corn stover. *J. Industrial Microbiology & Biotechnology's Special Issue on BioEnergy* (**invited paper** accepted for publication).
2. Kiran L. Kadam, Chim Y. Chin, and Lawrence W. Brown. *Continuous Biomass Fractionation Process for Producing Ethanol and Low-Molecular Weight Lignin*. Submitted to *Bioresource Technology*.
3. Kendra R. Colyar, John Pellegrino and Kiran Kadam. *Fractionation of pre-hydrolysis products from lignocellulosic biomass by an ultrafiltration ceramic tubular membrane*. *Separation Science & Technology* (accepted for publication).

6. Future Work

The work so far has successfully demonstrated the PureVision process at the PDU level. Hence, it is ready to advance to a 2–3 tpd level. Toward this goal the following tasks/activities are proposed:

1. Finalize detailed engineering and design specifications for the prototype reactor system.
2. Build and operate 2–3 dry tpd prototype-scale system (currently underway) and develop process performance data at prototype scale.
3. Revise Aspen model for the core process and update economic feasibility of the overall process.

Concurrent with these activities, PureVision is also engaged in the following:

1. Working with Buhler and others to design/develop lower-cost extruder configurations.
2. Based on data generated at the 2-3 tpd prototype, development of 75 tpd is being planned to be co-located at an existing ethanol plant.
3. Additional feedstock testing programs are underway and planned.
4. Lignin application programs with PPG, Weyerhaeuser and the University of Utah are expected to continue and additional lignin programs are planned.
5. Pulp applications only peripherally addressed in this program will be undertaken to demonstrate higher-value applications of the fractionated cellulose.

7. References

- Aden A, Ruth M, Ibsen K, Jechura J, Neeves K, Sheehan J, Wallace R, Montague L, Slayton A, Lukas J. 2002. Lignocellulosic Biomass to Ethanol Process Design and Economics Utilizing Co-Current Dilute Acid Prehydrolysis and Enzymatic Hydrolysis for Corn Stover. NREL, Golden, CO. Report nr NREL/TP-510-32438.
- Argyropoulos D, Bolker H, Heitner C, Archipov Y. 1993. ^{31}P NMR spectroscopy in wood chemistry. Part V: Qualitative analysis of lignin functional groups. *J. Wood Chem Tech.* 13(2):187-212.
- Benjakul S, Visessanguan W, Phongkanpai V, Tanaka M. 2005. Antioxidative activity of caramelisation products and their preventive effect on lipid oxidation in fish mince. *Food Chemistry* 90:231-239.
- CARB. 1998. Comparison of the Effects of a Fully-Complying Gasoline Blend and a High RVP Ethanol Gasoline Blend on Exhaust and Evaporative Emissions. California Air Resources Board, Sacramento, CA.
- Chen R, Lee Y, Torget R. 1996. Kinetic and modeling investigation on two-stage reverse-flow reactor as applied to dilute-acid pretreatment of agricultural residues. *Applied Biochemistry Biotechnology* 57/58:133-146.
- Chin C, Wang NH. 2004. Simulated Moving Bed Equipment Designs. *Separation and Purification Reviews* 33(2):77-155
- Chum HL, Johnson DK, Black SK, Overend RP. 1990. Pretreatment catalysis effects and the combined severity parameter. *Ind. Eng. Chem. Res.* 29(2):156-162.
- CRFA. 1999. Emissions Impact of Ethanol. Canadian Renewable Fuels Association, Guelph, Ontario, Canada.
- Esteghlalian AR, Srivastava V, Gilkes N, Gregg D, J., Saddler JN. 2000. An overview of factors influencing the enzymatic hydrolysis of lignocellulosic feedstocks. *ACS Symp. Ser.* 769:100-111.
- Granata A, Argyropoulos D. 1995. 2-Chloro-4, 4, 5, 5-tetramethyl-1, 3, 2-dioxaphospholane, a Reagent for the Accurate Determination of the Uncondensed and Condensed Phenolic Moieties in Lignins. *J. Agric. Food Chem* 43:6.
- Harvey CA, Adler J. Effects of gasoline-oxygenate blends on motor vehicle emissions; 1988; Tokyo, Japan. Sanbi Insatsu Co. Ltd., Japan.
- Hatfield R, Fukushima RS. 2005. Can Lignin Be Accurately Measured? *Crop Sci.* 45:832-839.
- Kadam KL, Rydholm EC, McMillan JD. 2004. Development and validation of a kinetic model for enzymatic hydrolysis of lignocellulosic biomass. *Biotechnology Progress* 20(3):698-705.
- Katz M, Rosen H. 1991. *Microeconomics*. Sydney: Irwin Inc.
- Leftwich R, Eckert R. 1985. *The Price System and Resource Allocation*. Sydney: The Dryden Press.
- Lora JH, Katzen R, Cronlund M, Wu CF; 1988. Recovery of lignin. United States patent 4,764,596.
- McTaggart D, Findlay C, Parkin M. 1992. *Economics*. Sydney: Addison Wesley Publishers Ltd.
- Mosier N, Warner R, Sedlak M, Ho N, Hedrickson R, Ladisch M. 2006. Effect of Fermentation Inhibitors on the Cofermentation of Glucose and Xylose from

- Pretreated Lignocellulosic Biomass by Recombinant Yeast. AIChE Annual Meeting. San Francisco, CA.
- Mun S, Chin C, Xie Y, Wang N. 2006. Standing Wave Design of Carousel Ion-exchange Processes for the Removal of Zinc Ions from a Protein Mixture using Chelex 100. *Ind. Eng. Chem. Res.* 45:316-329.
- Nilvebrant NO, Persson P, Reimann A, De Sousa F, Gorton L, Jönsson LJ. 2003. Limits for alkaline detoxification of dilute-acid lignocellulose hydrolysates. *Applied Biochemistry and Biotechnology* 107(1-3):615-628(14).
- Overend RP, Chornet E. 1987. Fractionation of lignocellulosics by steam-aqueous pretreatments. *Phil. Trans. R. Soc. Lond.*:523-536.
- Schell DJ, Farmer J, Newman M, McMillan JD. 2003. Dilute-sulfuric acid pretreatment of corn stover in pilot-scale reactor investigation of yields, kinetics, and enzymatic digestibilities of solids. *Applied Biochemistry Biotechnology* 105-108:69-85.
- Taylor AB, Bell AJ, Moran DP, Hodgson NG, Myburgh IS, Botha JJ. Gasoline/alcohol blends: Exhaust emissions, performance and burn-rate in a multi-valve production engine; 1997; San Antonio, TX.
- Tucker MP, Kim KH, Newman MM, Nguyen QA. Effects of temperature and moisture on dilute-acid steam-explosion pretreatment of corn stover and cellulase enzyme digestibility; 2004; Chattanooga, TN.
- Wang NH, Xie Y, Ho N. 2003. Novel Simulated Moving Bed Technologies for Isolation of Sugars from Biomass Hydrolyzate: Final Report. DOE Project No: DE-FC36-01GO11071, A000.
- Wingerson RC; 2002. Method of treating lignocellulosic biomass to produce cellulose patent United States Patent 6,419,788.
- Wingerson RC; 2003. Cellulose production from lignocellulosic biomass patent United States Patent 6,620,292.
- Wooley R, Ma Z, Wang NH. 1998. A Nine-Zone Simulating Moving Bed for the Recovery of Glucose and Xylose from Biomass Hydrolyzate. *Ind. Eng. Chem. Res.* 37:3699-3709.
- World-Bank. 1996. Pollution Prevention and Abatement: Pulp and Paper Mills. World Bank, Environment Department, Technical Background Document.
- Wright J, d'Agincourt C. 1984. Evaluation of Sulfuric Acid Hydrolysis Processes for Alcohol Fuel Production. Golden, CO: Solar Energy Research Institute. Report nr SERI/TR-231-2074.
- Xie Y, Chin C, Phelps D, Lee C, Lee K, Mun S, Wang N. 2005. A Five-zone Simulated Moving Bed for Isolation of Sugars from Biomass Hydrolyzate. *Ind. Eng. Chem. Res.* 45:9904-9920.

8. Appendices

8.1 Auburn University Report

Pulp Treatment

Three corn stover pulp samples from second stage were received on 3/19/07 from PureVision Technology. We received unbleached Pine and Southern Hardwood pulps from a local mill with the intention of testing the suitability of the corn stover solids as a replacement for hardwood pulp in linerboard. The mill pulps were washed and dewatered. The freeness and consistency of all three corn stover pulps were then measured. The mill pulps were refined in a laboratory valley beater. Table 1 shows the pulp freeness of all the samples and the blends used. TAPPI standard handsheets of blends of pulps were made for physical testing. The blends substitute the PureVision pulp for 10 and 30% of the amounts of the hardwood pulp.

Table 1. Description of blends used.

Sample ID	Sample Composition (%)				
	Softwood Pulp (390ml CSF)	Hardwood Pulp (360ml CSF)	Corn Stover Pulp		
			Condition-1 (565ml CSF)	Condition-2 (490ml CSF)	Condition-3 (425ml CSF)
Control	50	50	-	-	-
C1-10	50	40	10	-	-
C1-30	50	20	30	-	-
C2-10	50	40	-	10	-
C2-30	50	20	-	30	-
C3-10	50	40	-	-	10
C3-30	50	20	-	-	30

Results and Conclusions

Standard tests performed on the handsheets were grammage, caliper, tensile strength, stretch, tensile energy absorption (T.E.A.), Burst (Mullen), Tear, folds, stiffness and Porosity (Gurley). The table 2 and 3 show the average and standard deviation for each set of tests. Table 4 shows the calculated values of strength properties of the blends. The results are also shown in Figures 1 through 8. The corn stover pulp reduced

the strength of the sheet as the proportion was increased. Bulk, porosity and Taber stiffness showed slight increase showing that the substitution of corn pulp produced open structure sheet than the standard softwood/hardwood blend. A 10% substitution of hardwood pulp by the corn stover pulps do not show much change in most of the properties investigated.

Table 2. Test results of Tappi standard handsheets of blends.

Sample ID		Handsheet Test Results								
		Basis Wt. (g/m ²)	Caliper (mm)	Tensile (kg)	Elongation (%)	TEA (J/m ²)	Burst (kPa)	Tear		Air Resistance (sec.)
								g	mN	
Control	Mean	63.19	0.12	7.34	2.46	7.47	272.19	52.52	515.01	27.18
	SD	4.29	0.01	0.89	0.35	1.83	23.45	2.57	25.18	4.64
C1-10	Mean	60.69	0.12	6.33	2.60	7.12	241.06	47.34	464.22	24.78
	SD	3.27	0.01	0.40	0.34	1.33	26.73	2.09	20.48	4.64
C1-30	Mean	61.44	0.12	4.72	1.98	3.87	159.88	49.92	489.52	8.52
	SD	1.37	0.01	0.21	0.17	0.46	14.50	3.37	33.03	0.79
C2-10	Mean	62.88	0.12	6.35	2.30	6.14	238.44	56.56	554.63	24.78
	SD	0.95	0.02	0.38	0.31	1.24	16.90	2.80	27.46	2.46
C2-30	Mean	60.50	0.12	4.63	2.10	4.14	157.07	47.82	468.92	11.14
	SD	0.80	0.01	0.24	0.31	0.77	18.59	1.98	19.38	2.00
C3-10	Mean	62.13	0.12	6.41	2.64	7.23	230.94	53.32	522.86	18.50
	SD	3.36	0.01	0.43	0.14	0.70	32.98	1.34	13.13	1.86
C3-30	Mean	57.81	0.12	4.27	2.27	4.23	157.00	44.24	433.82	8.04
	SD	1.69	0.01	0.19	0.19	0.50	10.11	2.03	19.95	0.51

Table 3. Folding endurance and Taber stiffness of Tappi standard handsheets of blends.

	Folding Endurance		Taber Stiffness	
	Mean	SD	Mean	SD
Control	215.50	78.13	1.58	0.25
C1-10	170.75	39.107	1.72	0.18
C1-30	44.875	15.87	1.76	0.20
C2-10	115.50	39.86	1.84	0.29
C2-30	43.75	13.90	1.49	0.12
C3-10	128.88	22.64	1.77	0.45
C3-30	44.88	15.27	1.47	0.05

Table 4. Calculated strength properties of handsheets of blends.

Sample ID	Calculated Results						
	Bulk (cm ³ /g)	Apparent Density (g/cm ³)	Tensile Strength (kN/m)	Burst Index (kPa·m ² /g)	Tear Index (mN·m ² /g)	Tensile Index (N·m/g)	Breaking Length (km)
Control	1.87	0.54	4.80	4.31	8.15	75.80	5.05
C1-10	1.90	0.53	4.14	3.97	7.65	68.26	4.55
C1-30	1.97	0.51	3.09	2.60	7.97	50.26	3.35
C2-10	1.90	0.53	4.15	3.79	8.82	66.07	4.40
C2-30	1.99	0.50	3.03	2.59	7.75	50.10	3.34
C3-10	1.96	0.51	4.19	3.71	8.42	67.46	4.50
C3-30	2.03	0.49	2.79	2.71	7.50	48.33	3.22

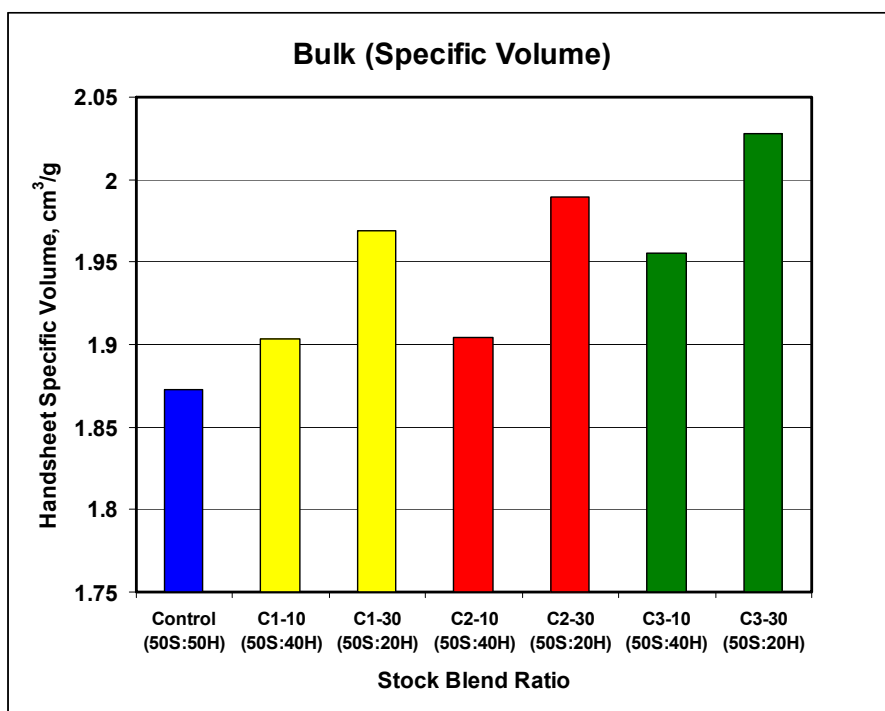


Figure 1. Bulk values of blends.

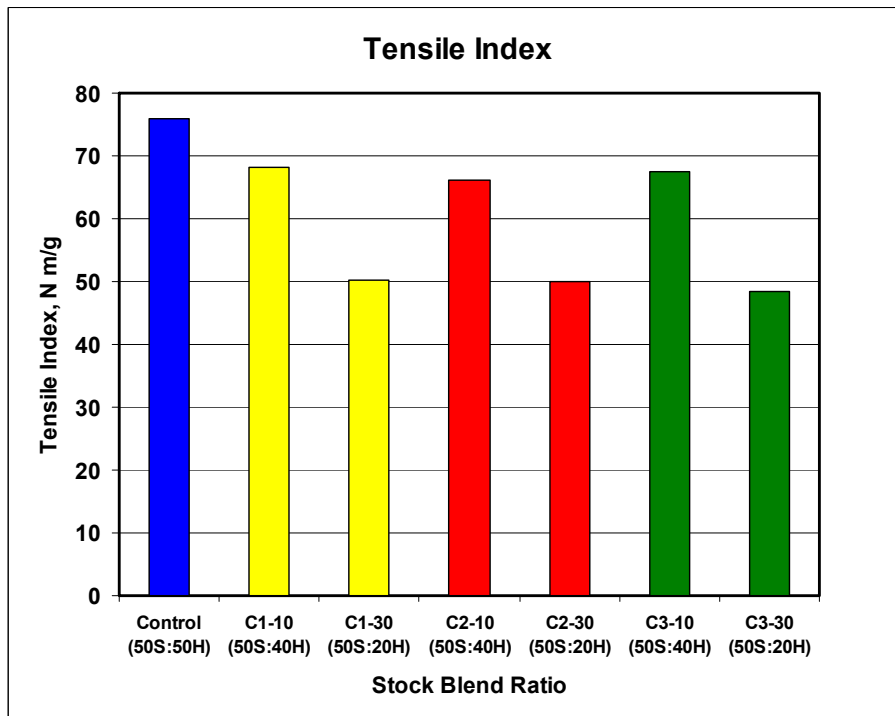


Figure 2. Tensile Index values of blends

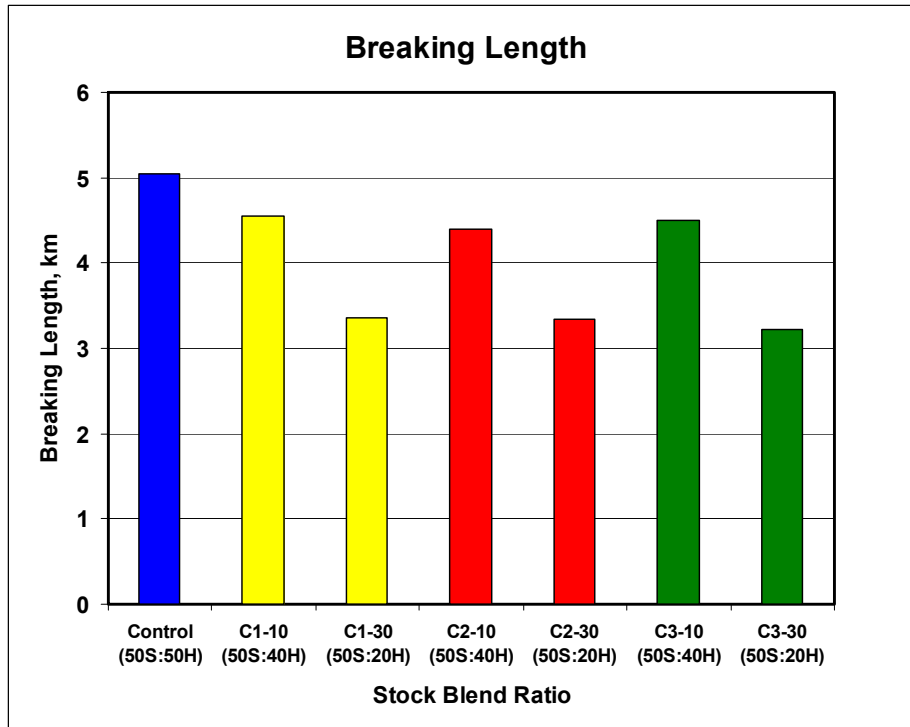


Figure 3. Breaking length values of blends

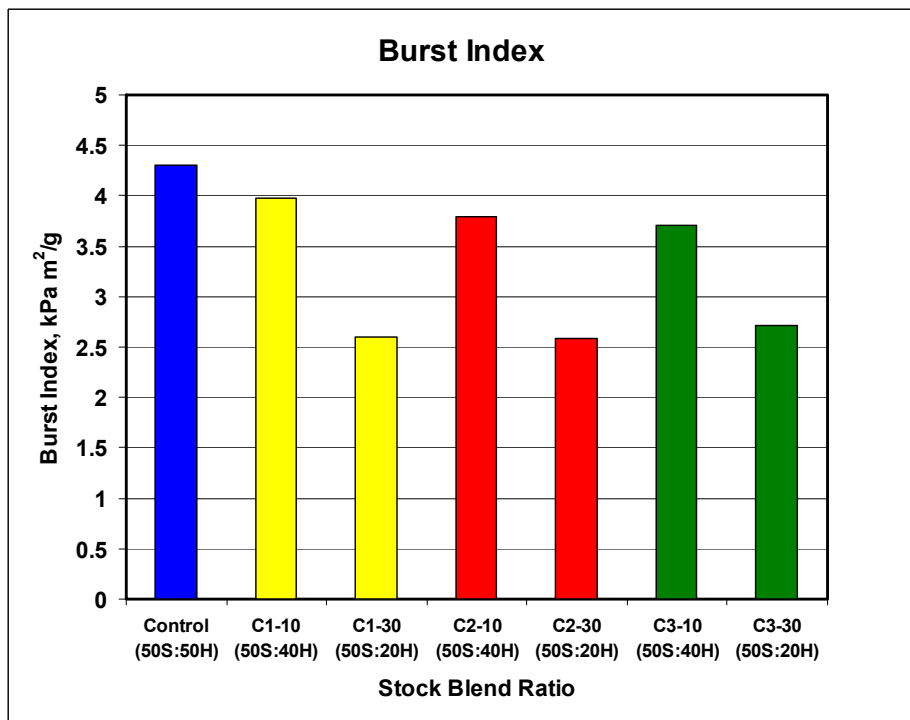


Figure 4. Burst index values of blends

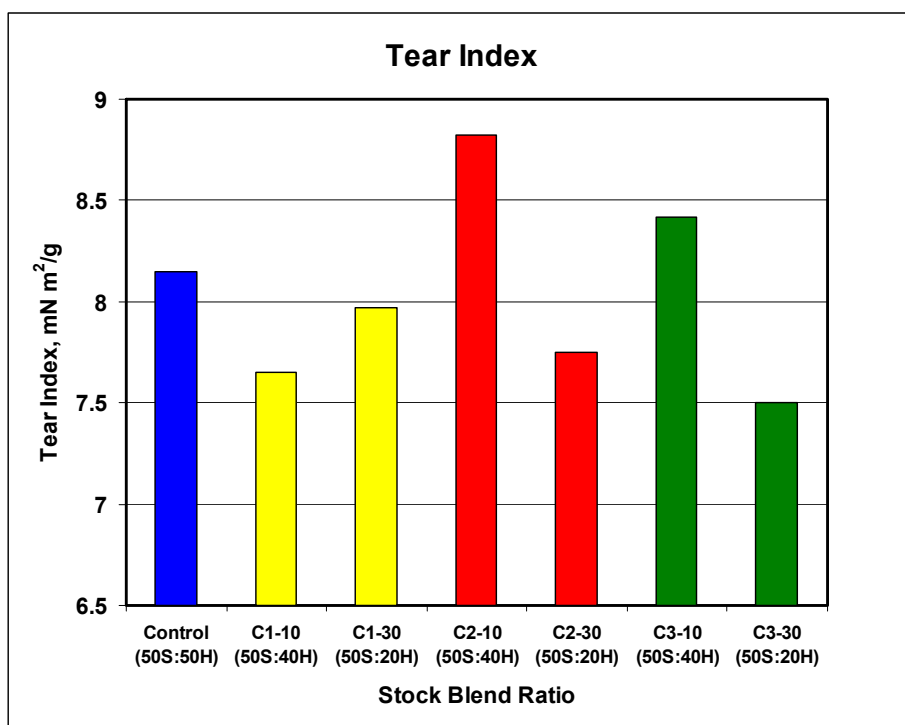


Figure 5. Tear index values of blends

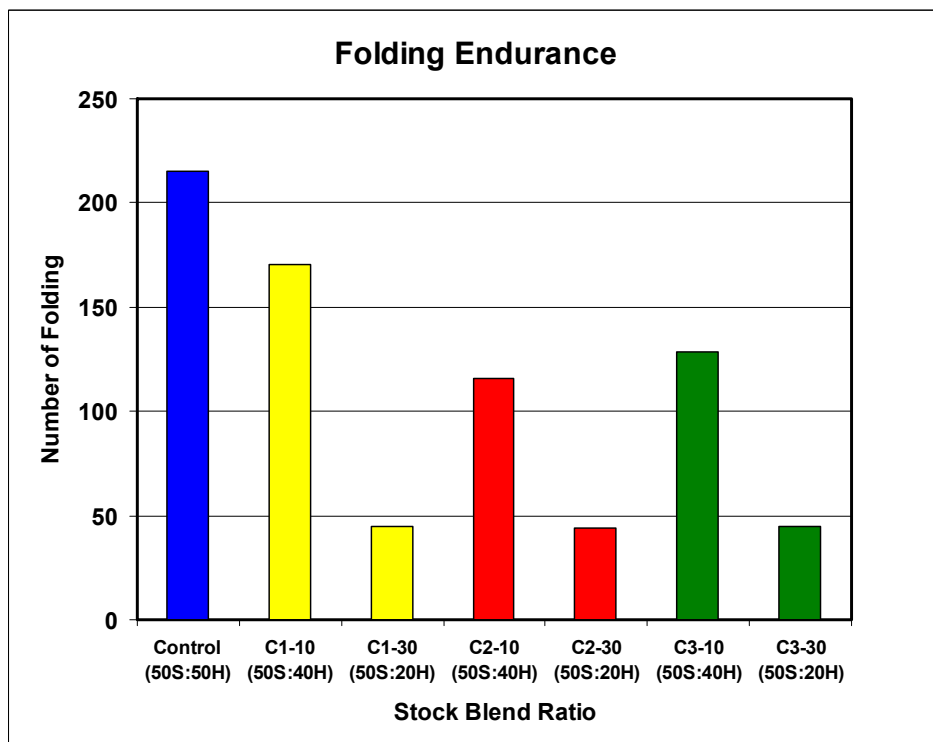


Figure 6. Folding endurance values of blends

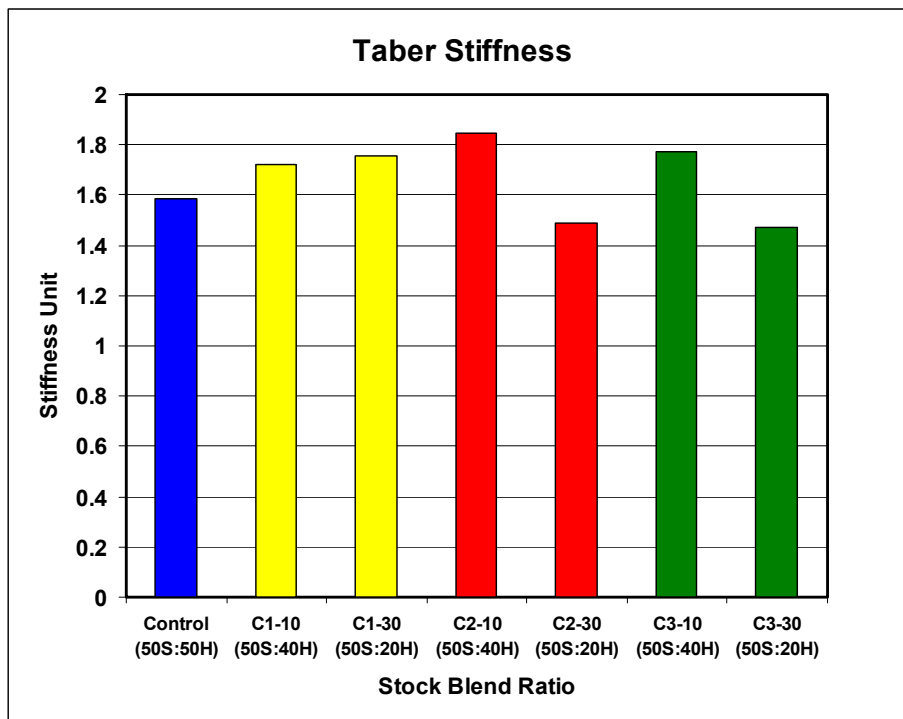


Figure 7. Taber stiffness values of blends

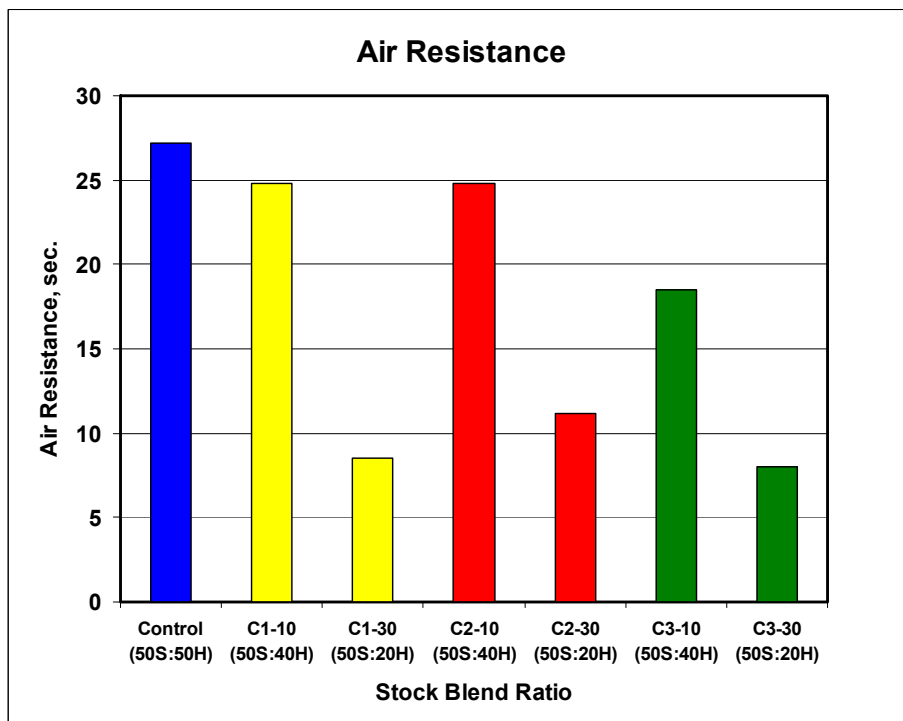


Figure 8. Air resistance values of blends

8.2 NREL Report



NREL National Renewable Energy Laboratory

*A national laboratory of the U.S. Department of Energy
Office of Energy Efficiency & Renewable Energy*

Innovation for Our Energy Future

October 31, 2007

Ed Lehrburger, President
PureVision Technology, Inc.
511 McKinley Ave.
Ft. Lupton, CO 80621

Dear Mr. Lehrburger:

Below I have summarized the work conducted by NREL in the analysis of samples provided by PureVision during the past approximately two years under the CRADA No. CRD-05-165.

On 12/14/05 four samples of first and second stage liquors were received. A report on the analyses of these samples was sent to PureVision on 1/6/2006. The report included data on pH, titration, lignin content, lignin molecular weight distribution, and hydrolyzate components, including monosaccharides, oligosaccharides, carboxylic acids, and furfurals, for each of the four samples.

Six additional samples were received from PureVision on 3/6/07. The samples were two wet second stage solids, two first stage liquors and two second stage liquors. The wet solids were analyzed and the anhydrosugar composition of the solids was provided to PureVision on 7/2/07. The liquor samples were also analyzed and a report including pH, lignin content, lignin molecular weight distribution, and hydrolyzate components, including monosaccharides, and oligosaccharides for each of the four samples was provided to PureVision on 9/13/07.

With completion of these analyses work to be performed for this CRADA was completed.

Yours Sincerely,

David K. Johnson, PhD
Senior Chemist
Chemical and Biosciences Center
National Renewable Energy Laboratory
1617 Cole Blvd
Golden, CO 80401
303-384-6263



PureVision Biorefineries

Phase I

Grant Number DE-FG36-05GO85004
Final Sub-Contract Report

Report Period: March 2006 to July 2006

by

Membrane Technology and Research, Inc.
1360 Willow Road
Menlo Park, CA 94025

August 9, 2006

prepared for

PUREVISION TECHNOLOGY, INC
Attn: Dr. Ed Lehrburger and Dr. Kiran Kadam
511 McKinley Avenue
Fort Lupton, Colorado 80621

Contributors:

Yu (Ivy) Huang (P.I.)
Tiem Aldajani
Ingo Pinnau
Alvin Ng

1. PROJECT OBJECTIVES AND GOALS

The overall objective of this project was to generate process and economic data for preliminary designs of PureVision Biorefineries. In the process being designed, two stages of hydrolyzate liquor streams were produced from three feedstocks: corn stover, loblolly pine and bagasse. The major components of the first-stage liquor streams are xylose (and glucose) and lignin; the major components of the second-stage liquor streams are sugars, lignin and caustic. The scope of work required from MTR included the following specific objectives:

- (1). To permeate the xylose (and glucose) and reject the lignin from the first-stage liquor streams using MTR's non-porous ultrafiltration membrane.
- (2). To separate and purify the mixed sugars, the lignin and potentially the caustic contained within the second-stage liquor streams using MTR's non-porous ultrafiltration membrane, with the aim of rejecting the lignin from the other stream components.

To meet these objectives, we proposed the tasks as follows:

- Task 1. Develop membranes for optimum separation
- Task 2. Perform laboratory tests with the selected membranes
- Task 3. Conduct preliminary analysis of the permeate and send samples to
PureVision for further analysis.

2. RESULTS

The following section describes our progress in completing each of the project tasks.

Task 1. Membrane development for optimum separation

The non-porous ultrafiltration membranes we used in this work are composite membranes of the type shown in Figure 1. These membranes are prepared by a multi-step procedure. First, a microporous support layer is cast onto a fabric web. The support layer is then coated with a gutter layer and a selective polymer layer.

A number of different ultrafiltration polymer membranes were prepared for this application. These membranes were tested with pure xylose and glucose model solutions, aiming at 100 wt% permeation of these sugars. Since no commercial low-molecular-weight lignin (MW \leq 1,000) is currently available, we could not test the membranes with a pure lignin solution. Most of the membranes showed 100% sugar permeation. These membranes were then further evaluated with the stream liquors; two composite membranes were selected based on the membrane flux. Membranes with extremely high

flux and membranes with extremely low flux were screened out. Higher flux membranes gave permeate with darker color indicating the excess permeation of lignin, while lower flux membranes implied potential practical application problems.

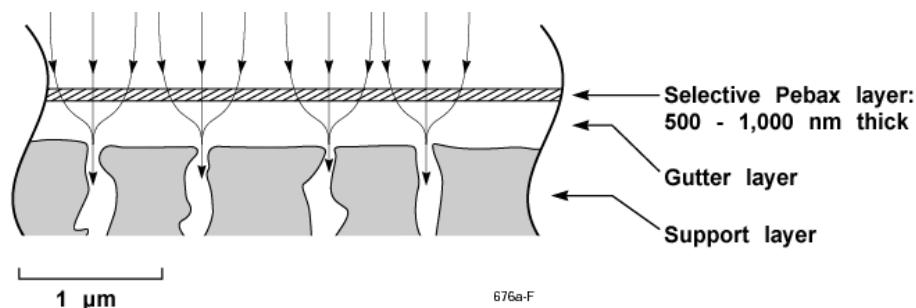


Figure 1. Cross-section (approximately to scale) of the multilayer composite membranes prepared for this project.

Task 2. Perform laboratory tests with the selected membranes

Figure 2 shows the experimental set-up for the ultrafiltration membrane performance test; the experiment was conducted under different feed pressures at room temperature. To prevent the feed from being heated during the operation of the feed pump, a heat exchanger was installed before the pump to maintain the stable feed composition. Both hydrostatic and continuous flow operation modes were studied with the samples. The results showed that continuous flow mode provided higher flux than hydrostatic mode. This finding could be related to membrane fouling issues, which often arise during hydrostatic operation. Therefore, continuous operation mode was preferred and used during the project.

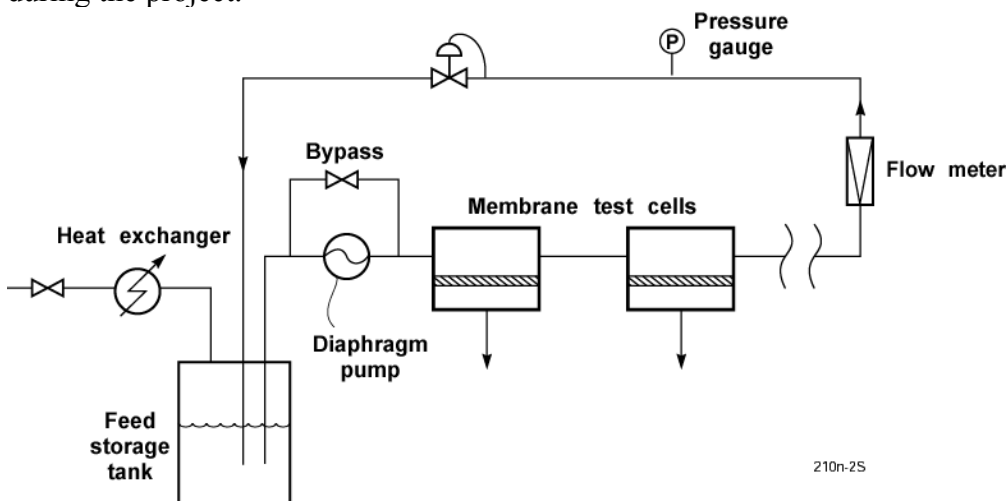


Figure 2. Diagram of the test apparatus for separation of sugars through thin composite membranes.

For each test, the pressure was gradually increased from 50 psi to 130 psi. The lower end of the pressure range was selected based on the osmotic pressure of the feed solution, which was about 45 psi.

Task 3. Preliminary analysis of permeate samples

Based on the assumption that the lignin in the feed is the source of the sample color, the color comparison method was used to conduct the preliminary analysis of permeate samples. Reference samples were made by diluting the feed to provide samples containing 50, 40, 30, 20, 10 and 5% of the lignin content of the original feed. These samples corresponded to results that would be obtained for 50, 60, 70, 80, 90 and 95% rejection of lignin, respectively. The color of each permeate sample was then compared with the color of these reference samples to obtain an estimation of the lignin rejection percentage. Tables 1 and 2 show the results using such color comparison method. Tests on the rejection rates for sugars were not performed due to the lack of proper instrumentation (such as HPLC, UV absorption) at MTR.

Table 1. Lignin Rejection Rate via Color Comparison Method for Stage 1 Hydrolyzates Using Ultrafiltration Membranes at Different Pressures

Membrane	Feed Pressure (psi)	Membrane Flux (kg/m ² ·h)	Lignin Rejection Rate (%) via Color Comparison
MTR-1	50	10.45	80
	70	10.12	80
	90	9.35	80
	130	8.69	80
MTR-2	50	3.09	90
	70	4.34	90
	90	5.33	95
	130	7.01	92.5

Table 2. Lignin Rejection Rate via Color Comparison Method for Stage 2 Hydrolyzates Using Ultrafiltration Membranes at Different Pressures

Membrane	Feed Pressure (psi)	Membrane Flux (kg/m ² ·h)	Lignin Rejection Rate(%) via Color Comparison
MTR-1	50	6.49	70
	70	6.92	70
	90	5.16	75
	130	4.77	70
MTR-2	50	1.81	85
	70	1.68	80
	90	1.59	85
	130	2.49	87.5

These results are consistent with our expectations that the MTR-2 membrane would perform better than the MTR-1 membrane. For the MTR-1 membrane, the higher the feed pressure, the lower the permeate flux, which indicates that the membrane fouled at higher pressures. For the MTR-2 membrane, the highest feed pressure provided the greatest permeate flux, which indicated that the membrane was not fouled and that higher feed pressure provided higher driving force, resulting in higher permeate flux. For all experiments, the lignin rejection rates are greater than 70%. The good lignin rejection was visually proven by the very light color and transparent clarity of the permeate samples. The permeate samples were refrigerated and sent to PureVision via overnight delivery.

Tables 3 and 4 show the analytical results obtained by PureVision.

Table 3. PureVision's Analysis of Permeates from Stage 1 Hydrolyzates Provided by MTR.

Membrane	Pressure (psi)	Major Components Concentration in Permeate (g/L)			Membrane Rejection Rate (%)	
		Glucose	Xylose	Lignin	Sugar	Lignin
MTR-1	50	0.7	4.4	5.8	73.3	65.2
	70	1.5	9.5	13.4	42.3	19.5
	90	0.7	4.3	16.8	74.0	-1.3
	130	1.4	8.8	8.5	46.7	48.9
MTR-2	50	0.5	3.6	13.6	78.1	18.3
	70	1.2	7.9	14.1	52.6	14.8
	90	0.5	3.3	17.5	80.1	-5.3
	130	1.0	6.6	16.8	60.0	-0.9

Feed composition comparison: 4.1 15.0 16.6

Table 4. PureVision's Analysis of Permeates from Stage 2 Hydrolyzates Provided by MTR.

Membrane	Pressure (psi)	Major Components Concentration in Permeate (g/L)			Membrane Rejection Rate (%)	
		Glucose	Xylose	Lignin	Sugar	Lignin
MTR-1	50	0.5	2.7	18.5	76.6	-10.8
	70	1.0	4.7	14.1	57.8	15.6
	90	0.5	2.3	13.6	79.0	18.8
	130	1.0	4.5	16.6	60.0	0.4
MTR-2	50	0.6	2.2	18.4	79.4	-10.2
	70	1.4	5.4	14.1	50.5	15.8
	90	0.7	2.5	13.5	77.0	19.0
	130	1.3	4.8	16.6	55.3	0.5

Feed composition comparison: 3.8 9.9 16.7

The PureVision results are inconsistent with the MTR results. In general, the PureVision results show sugars with higher membrane rejection rates than lignin, even though sugars are smaller in molecular size. In the case of the Stage 2 hydrolyzates, some analyses show 100% of the feed lignin permeated through the membrane while sugars were rejected up to 80%. In five of the sixteen permeate samples, the lignin solids concentration reported by PureVision exceeded the value of lignin measured in the original feed composition. Possible explanations of these inconsistencies may be:

- some process other than ultrafiltration is occurring (including possible formation of very-low-molecular-weight lignin fragments in the hydrolyzate),
- the UV absorption equipment is not suitable for measuring concentrations in the particular solutions being analyzed, or
- errors in the permeate concentration data analysis.

3. SUMMARY

The two ultrafiltration membranes identified by MTR for lignin/sugar separations did not perform well based on PureVision's permeate analysis. The MTR and PureVision results are nearly diametrically opposed. If the molecular weight of the lignin remains in the range of at least 1,000, while the sugars are in the range of less than 200, MTR believes that membrane rejection rates would necessarily be larger for lignin than for sugars when a feed containing both is fed to the ultrafiltration membranes used in the test cells. Literature research did not find other appropriate ultrafiltration membranes for such applications.

8.4 Weyerhaeuser Report

Weyerhaeuser Report on Fraction Characterization

Dwight Anderson, Oct. 14, 2007

Scope of Collaboration

Weyerhaeuser and PureVision's collaboration consisted of PureVision conveying a description of the technology, Weyerhaeuser discussing potential scale-up alternatives with PureVision, and Weyerhaeuser's characterization of product fractions from the PureVision process, with a view towards identifying potential commercial applications. The total matching funds tracked by Weyerhaeuser are listed in Attachment 1. They amount to \$52,370. This is lower than the original estimate because the original estimate anticipated contingencies that did not emerge. This report focuses on the characterization of product fractions, with comments on the suitability of these fractions for commercial products. The two feedstocks processed by PureVision are loblolly pine chips and corn stover. A lignin sample was analyzed by Weyerhaeuser for the pine chips, and all fractions produced by PureVision were analyzed for the corn stover work.

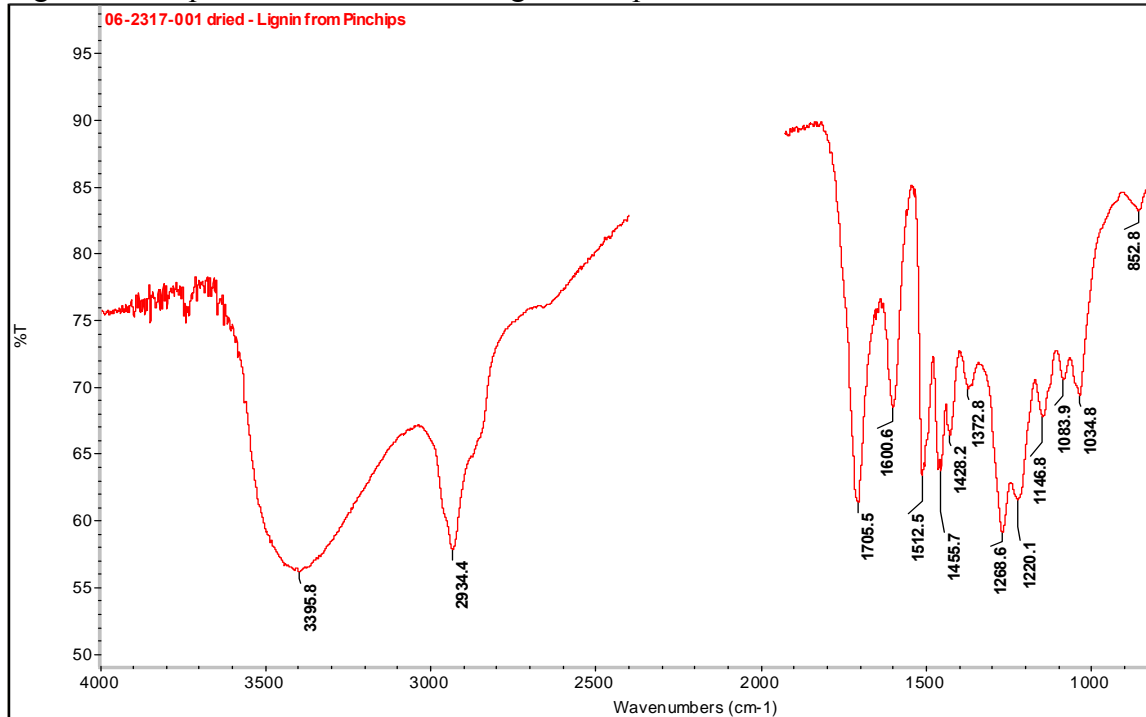
Analysis of Pine Lignin

PureVision had procured a sample of loblolly pine chips from a non-Weyerhaeuser source. Although chip size classification data is not available, their appearance was much like what would generally be considered pin chips: typically 1- 4 mm in thickness, up to a few centimeters long with many shorter pieces. These were processed to produce a pine lignin sample. This sample was of specific interest to Weyerhaeuser because pine is the most common furnish used, and the possibility exists to produce new products from it.

Most potential products, including the possibility of using lignin as a phenol source in a phenol-formaldehyde resin, require the lignin having the ability to flow at reasonable temperatures. The melting point of this dried sample was evaluated on a Mettler FP2 hot stage. No melting point was identified up to a maximum testing temperature of 300 °C. Workable temperatures would be below this temperature, ideally closer to 100 °C.

Infrared spectroscopy was used to determine the ultimate composition of the lignin material. The lignin had been received in an aqueous, acidic state at 12.2% solids. The initial scan on the as-received sample showed mostly water, so the sample was dried in an oven at 105°C and IR was re-run on the dried sample. The spectrum is shown in Figure 1. It corresponds to a composition of 66.0% carbon, 6.2% hydrogen, and 0.32% nitrogen.

Figure 1: IR Spectrum of Dried Pine Lignin Sample



Differential scanning calorimetry was sub-contracted to Ciba Testing Services to identify glass transition temperatures. Ciba's comments:

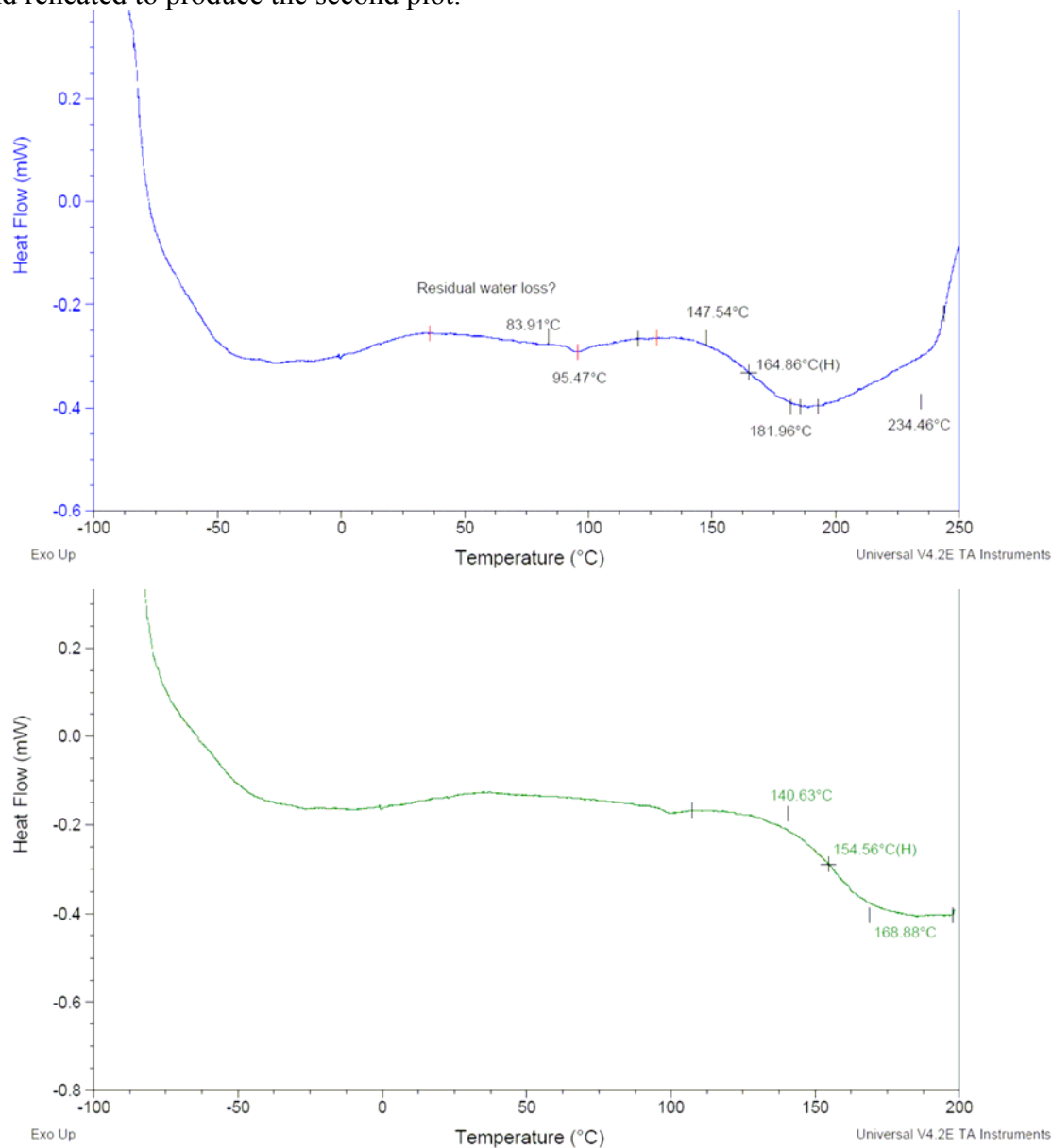
Upon drying at 150°C, the soft, wet sample becomes a brittle solid, indicating the glass transition temperature is greater than 20°C. The dried sample exhibits a change in heat capacity (baseline shift) from 140°C to 170°C, tentatively attributed to the glass transition of the lignin at approx. 155°C. During the first heating cycle, this appears as an endothermic peak, probably due to the loss of additional volatiles upon softening. After drying at 200°C, the transition appears as a ΔC_p baseline shift (T_g) in the second and third heating cycles.

There is also evidence for a transition near -70° to -80°C, which may be the T_g of another domain in the sample. This transition is too close to the starting temperature for reliable analysis. Another cooling system, such as Liq N₂, may be required to get a good scan at this temperature.

Continued heating beyond 200°C produces an exothermic event, starting at about 230°C, tentatively attributed to decomposition.

The DSC data are shown in Figure 2.

Figure 2: Differential Scanning Calorimetry data for dried lignin samples. First plot is the initial heating stage. Note that residual water may be evolved. The sample is then cooled and reheated to produce the second plot.



In summary, the pine lignin has a transition temperature characteristic of lignin, but we did not find a melting point or sufficient softening to be useful as a resin supplement. In fact, it became brittle. A more ideal lignin would have softening around 120°C. This might be achieved by reducing the amount of crosslinking within the lignin.

Analysis of Corn Stover Fractions

Corn stover was processed under conditions described elsewhere in the PureVision report to produce four fractions:

- 2nd Stage Lignin, Condition 2 Dry
- 2nd Stage Lignin Condition 2 Acetic Acid
- 2nd Stage Solids, Condition 1
- 1st Stage Liquor, Condition 3

The percent solids, ash, and heating value are listed in Figure 3. The first and second samples' heating values are consistent with what is typical for lignin, and the others are consistent with hemicelluloses and cellulose, which is what the primary constituents of those fractions are intended to be.

Figure 3: Sample Description

Client ID	Date Sampled	Lab ID	105° C	TAPPI	600° C	HHV
			Solids	Solids	Ash	
			%	%	%	BTU/lb
			As-Rec'd	As-Rec'd	O.D.	O.D.
			Basis	Basis	Basis	Basis
Corn Stover 2nd Stage Lignin-Cond 2 Dry		001	96.4	-	7.14	10960
"		001D	-	-	7.24	-
Corn Stover 2nd Stage Cond 2 Acetic Acid		002	7.96	-	14.7	10040
Corn Stover 2nd Stage Solids Cond 1		003	27.2	-	10.3	6680
Corn Stover 1st Stage Liquor Cond 3		004	9.34	9.59	11.2	7740
"		004D	-	9.52	-	-

Analysis of sugars in the liquor fraction

One commercially useful constituent expected to be in the liquor fraction would be sugars. Since the ability to retain oligomeric structure of hemicellulose is suspected to be an attribute of the PureVision process, we tested for sugars with chromatography before and after hydrolysis. Figure 4 shows the results for the 1st stage liquor condition 3. (Kraft Grande Prairie is a control pulp routinely used for this analysis.) Figure 5 shows the same results calculated as polymers. Arabinose and xylose are calculated from the monomer data by multiplying by 0.88, and galactose, glucose, and mannose use a multiplier of 0.90. The conclusion is that the great majority of the arabinose, galactose, and xylose are in polymeric form when taken from the PureVision process. The results for glucose and mannose are not conclusive because the standard deviations are too large.

Figure 4: Sugar Analysis, reported as monomers (on OD basis)

Client ID:	Lab ID:	PERCENT ARABINOSE	PERCENT GALACTOSE	PERCENT GLUCOSE	PERCENT XYLOSE	PERCENT MANNOSE
Corn Stover 1st Stage Liquor Cond 3	07-1319-004 Not Hydrolyzed	<0.07	<0.07	<5.05	<0.68	<0.59
Corn Stover 1st Stage Liquor Cond 3	07-1319-004 Hydrolyzed	0.35	0.17	0.79	2.85	0.03
Kraft Grande Prairie Control		0.72	0.39	91.74	8.45	6.92
Quantitation limit		0.07	0.07	5.05	0.68	0.59
Average		0.74	0.34	89.62	8.42	6.84
3*Standard Deviation		0.07	0.07	6.18	0.59	0.40

Figure 5: Sugar Analysis, reported as polymers (on OD basis)

Client ID:	Lab ID:	PERCENT ARABINAN	PERCENT GALACTOSE	PERCENT GLUCAN	PERCENT XYLAN	PERCENT MANNAN	TOTAL SOLIDS	TOTAL PERCENT
Corn Stover 1st Stage Liquor Cond 3	07-1319-004 Not Hydrolyzed	<0.07	<0.06	<4.55	<0.60	<0.53	6.81	6.81
Corn Stover 1st Stage Liquor Cond 3	07-1319-004 Hydrolyzed	0.31	0.15	0.72	2.51	<0.53	1.29	4.98
Kraft Grande Prairie Control		0.63	0.35	82.57	7.43	6.23	97.21	
Quantitation limit		0.07	0.06	4.55	0.60	0.53		

These five sugars analyzed for comprise 5% of the total solids in the 1st stage liquor fraction, condition 3. From Figure 3, another 11% is comprised of ash. The majority is likely lignocellulosic material that was not readily hydrolyzed by the acid treatment used to depolymerize the sugars for analysis.

Lignin Analysis

The heating values of Figure 3 suggested that these fractions may indeed be high in lignin. Chemical analysis confirmed a high lignin content. Figure 6 shows the lignin content of each sample is approximately 95%. This is primarily (~89%) acid-insoluble lignin with some acid-soluble lignin. These tests differed from the Klason lignin test on pulp in that alcohol-benzene and hot water extractions were not run beforehand.

Figure 6: Lignin Measurement

Sample Designation	Analytical Lab Code	Acid-Insoluble Residue (Wt %)	Acid-Soluble Residue (Wt %)
Corn Stover 2nd Stage Lignin - Cond 2 Dry	001	87.6	7.0
Corn Stover 2nd Stage Cond 2 Acetic Acid	002	89.0 ; 89.4	6.4 ; 5.9
Date Analyzed:		7/17/2007	7/18/2007
Analyst:		KH	KH
Method Used:		AM -T222M	AM W-1301-5 and LAP 004

Infrared spectra confirm the identify of the lignin samples. They are very similar to hardwood lignin, as expected for lignin from agricultural biomass.

Figure 7: Infrared spectrum for “2nd stage lignin, condition 2 dry” compares well with hardwood lignin (from files)

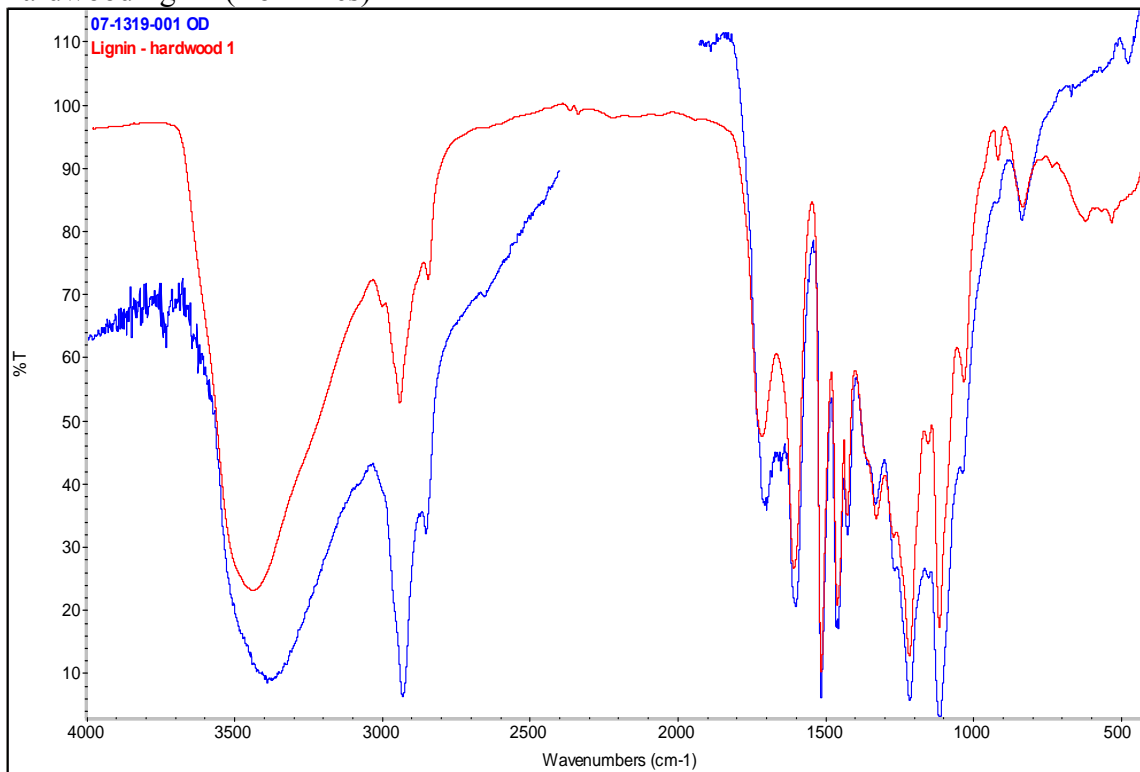
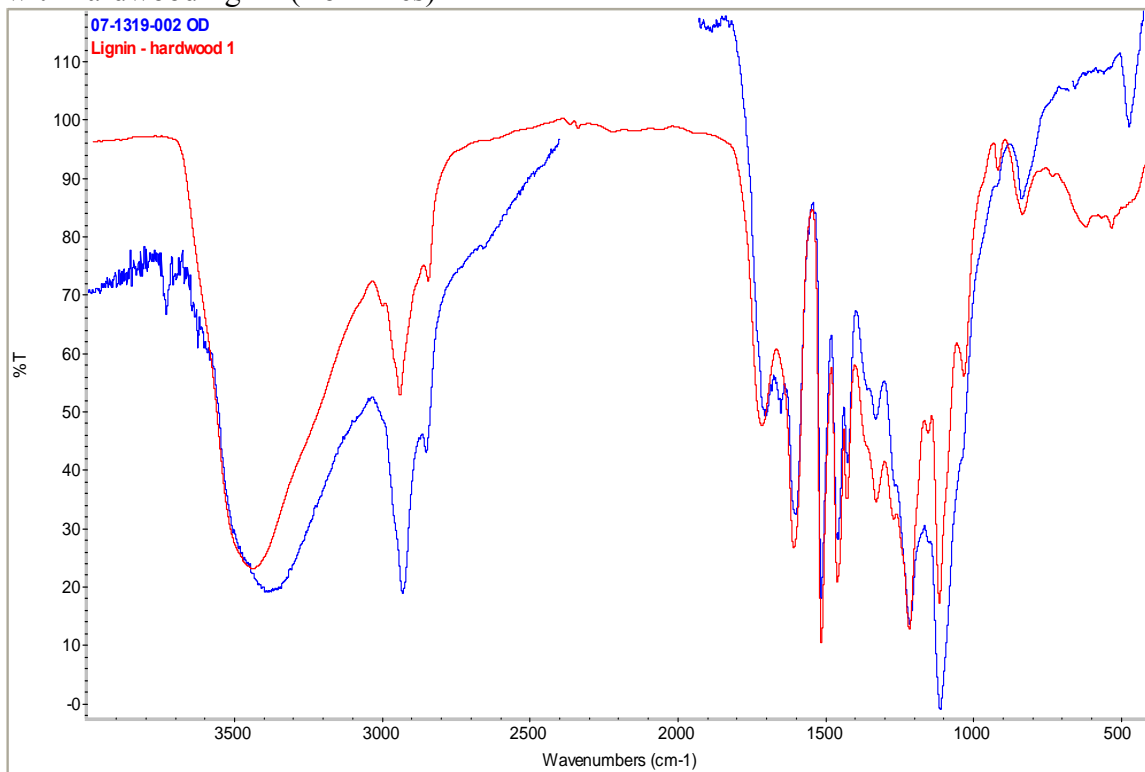


Figure 8: Infrared spectrum for “2nd stage lignin, condition 2 acetic acid” compares well with hardwood lignin (from files)



Fiber Solids Analysis

The non-lignin solids fraction, 2nd stage solids condition 1, had the appearance and feel of pulped mixed waste, suggesting a short fiber length. Solids content was 27%, ash 10% (refer again to Figure 3). The Klason lignin content was 10.7% with 0.25% acid-soluble lignin. Fiber morphology was quantified with a Fiber Quality Analyzer, which measures fiber length and shape. Figure 9 shows the results.

Figure 9: FQA results from 2nd stage solids condition 1

Fiber Properties Report

Method(s) :WM W-FQA

Customer ID	LIMS ID	n	Mean	Std Dev	Cov	Min	Max	Range
NAFL, mm								
Corn Stover 2nd Stage Solids Cond 1	07-1319-003	3	0.13	0.00	1.5	0.13	0.14	0.00
LWAFL, mm								
Corn Stover 2nd Stage Solids Cond 1	07-1319-003	3	0.18	0.00	2.7	0.18	0.19	0.01
WWAFL, mm								
Corn Stover 2nd Stage Solids Cond 1	07-1319-003	3	0.30	0.02	6.8	0.28	0.31	0.04
LW Fines, %								
Corn Stover 2nd Stage Solids Cond 1	07-1319-003	3	77.3	1.8	2.3	75.9	79.3	3.5
Curl Index,								
Corn Stover 2nd Stage Solids Cond 1	07-1319-003	3	0.102	0.029	28.3	0.080	0.135	0.055
Kink Index, 1/mm								
Corn Stover 2nd Stage Solids Cond 1	07-1319-003	3	1.8	0.1	6.4	1.7	1.9	0.2
Kink Angle, deg/mm								
Corn Stover 2nd Stage Solids Cond 1	07-1319-003	3	30	4	13.3	27	35	8
Kink Number, 1/mm								
Corn Stover 2nd Stage Solids Cond 1	07-1319-003	3	0.9	0.1	10.9	0.8	1.0	0.2

Note: Sample tested as received (no handsheets). Sample received as pulp. High COVs due to very short fibers.

The FQA results confirm that this is indeed a short fiber. For comparison, softwood fibers typically have a WWAFL of 2.5 – 3.0 mm, and fines are typically defined as any particle with a fiber length less than 0.20 mm. Thus, this material is essentially all fines. This implies that it would not be suited for paper making. It is comminuted to the point that it could be well suited, however, at least in terms of physical size, for subjecting to enzymatic hydrolysis for ethanol production. The moderate lignin content may inhibit hydrolysis somewhat, however.

Summary of Key Points

- The liquor fraction contains some sugars at low concentrations (5% total). They exist in oligomeric form.
- The lignin fractions, by contrast, are 95% pure. Heating values are consistent with typical lignin heating values. The IR spectra are comparable to hardwood lignins. The melting point/rheology of the lignin was not yet shown to be compatible with the needs of phenol-formaldehyde resin substitute.
- The fiber fraction has a moderate lignin content (10.7%) but is mechanically comminuted to an extreme that would make it well suited to enzymatic hydrolysis or further chemical processing.

8.5 PPG Industries Report



Compositional Analysis Report

R & D Analytical Services - Allison Park

PPG INDUSTRIES, INC.

JOB: COMPETITOR.4220
competitor4220lia.doc

REPORT:

TO: David Fenn
Park

LOCATION: Allison

FROM: Sue Campbell
2007

DATE: January 10,

SUBJECT: Characterization of Pure Vision Lignin 050206 (AZ)

Summary of Analysis

This report is written to summarize the results from the analysis of a Pure Vision Lignin product. Lignin is a complex natural product that is being evaluated for use as a raw material in several different C&R products. Analytical work was done to characterize this material. This information will be used to help understand the reactivity of this product and develop methods that can be used to compare different sources/lots of Lignin. A summary of the analytical results is given below. The Discussion section of this report gives a more detailed description of the analyses done.

Initial results from the analysis of the Pure Vision are summarized in Table 1.

Table 1 LIGNIN ANALYSIS OF LIGNIN – SUMMARY OF TEST RESULTS	
TECHNIQUE	RESULTS
WET LAB TEST	SOLIDS-110 13.2% ASH 1582 ppm Meq Acid 0.934 Phenolic OH, titration result – 1.082 meq. However, all literature indicates that phenolic content by titration is not a accurate method for use on Lignin materials.
GC/Solvnets	0.18% Ethanol
GPC	Mw 2410 Mn 1074 Polydispersity 2.2
DCP	S 300 ppm

	Ca 250 ppm Na 170 ppm Fe 130 ppm Al, K, Mg <20 ppm
NMR	C-13 NMR data shows expected phenolic polymer with a ratio of 1 to 11.5 of -OCH ₃ methoxy to aromatic groups, respectively. The data also shows strong signal for acetate (CH ₃ -C(=O)-OR) groups.
Pyrolysis GC/MS	Pyrolysis gc/ms analyses show expect lignin degradation products, such as phenols, cresol, methoxy phenols and guaiacol type components. Further work could be done to use pyrolysis gc/ms as a quantitative tool to compare different lots/suppliers of lignin if this becomes necessary.

Of particular interest was to develop a method to determine the amount and type of hydroxyl groups in Lignin. Based on a review of the literature, a method to used P-31 NMR on derivatized lignin was identified and developed for use at PPG. Initial work was done on a series of model systems to ensure the accuracy and precision of the method. Analyses were then done on the Pure Vision lignin. The method uses an internal standard that allow us to calculate the meq/g of phenolic and aliphatic hydroxyls as described below in Table 2.

TABLE 2 HYDROXYL/PHENOLIC CONTENT: PURE VISION LIGNIN P-31 NMR METHOD				
	ALIPHATIC -OH	SYRINGYL PHENOLIC UNITS	GUAIACYL/DEMETHYLATED PHENOLIC UNITS	ACID/ESTER
Value/meq/g	0.289	0.191	0.175	0.171

Discussion of Analysis

Wet Lab Tests: The sample was analyzed for total solids, ash, phenolic by wet lab techniques and the results are attached. The phenolic value determine by titration is suspect. The problems of using titration methods for the determination of phenolic content in Lignin type products has been referred to in several publications on Lignin. Because of this, further work was done using a P-31 NMR method for the analysis of this product. This work is described in Attachment A in the NMR section.



competitor4220wet1
.doc

GC: *A gc solvent test was done and the only volatile component identified was ethanol at 0.18% as shown in Attachment B.*



4220gc.xls

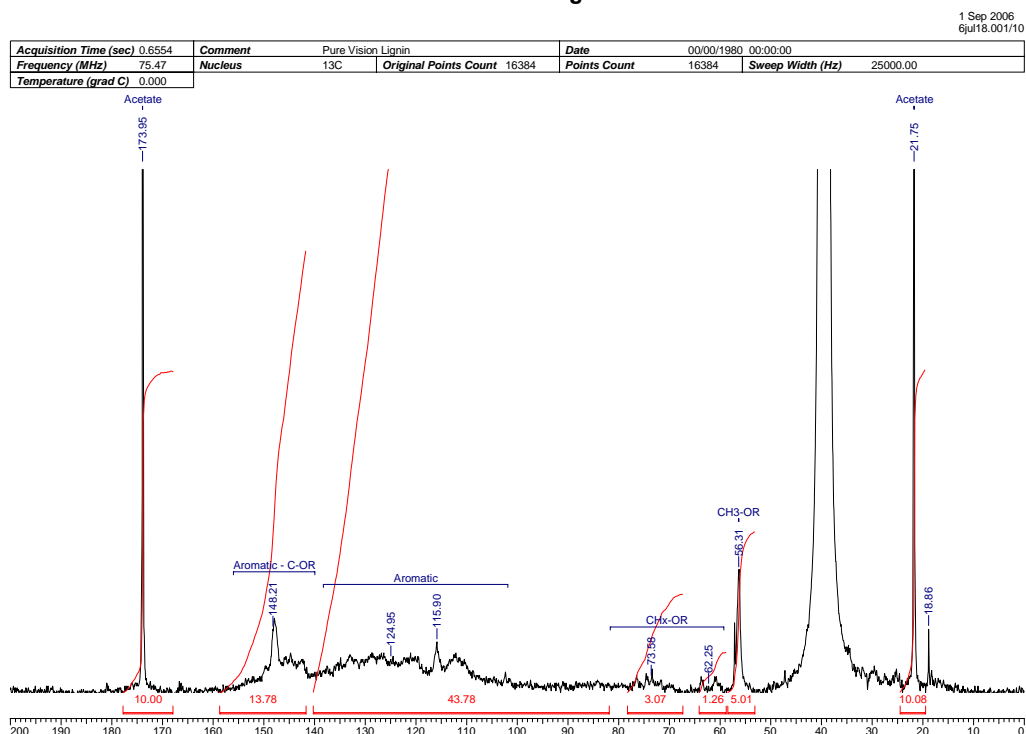
Pyrolysis GC/MS: The whole sample was ballistically heated to 560 °C, which causes fragmentation of the original polymer into smaller monomeric units. The smaller monomeric units were then separated and analyzed by GC/MS. Note that due to the high temperature used to pyrolyze the sample, some components detected can be due to fragmentation and rearrangement. This technique provides qualitative information and has been optimized for the identification of acrylate components. The full report is attached. This method has been used in the analysis of lignin type products. The components detected are the expected Lignin aromatic species. If needed, this may be a method that would be useful in the comparison of Lignin products from different sources, as documented in Attachment C.



competitor4220pyr.doc

C-13 NMR: Analyses were performed on air-dried sample of the PureVision Lignin. The sample for C-13 NMR was prepared with Cr (acac)₃ added as a relaxation agent and the data was obtained under quantitative conditions. The data shows expected phenolic polymeric structure with significant level of –OCH₃ methoxy groups indicated by the resonance at 56.3 ppm. The peaks at 174 and 21.8 ppm indicate the presence of an acetate groups. The ratio of methoxy to aromatic groups calculated from the C-13 NMR data is 1 to 11.5. The data is given below:

Pure Vision Lignin



P-31 NMR: Work was done to evaluate a P-31 NMR method on derivatized Lignin for determination of Hydroxyl/phenolic content of lignin. The derivatization reagent is 2-chloro-4,4,5,5-tetramethyl-1,3,2-dioxaphospholane.¹² The literature reports results that can be used to quantify not only total phenolic content, but the amount of aliphatic hydroxyl, Syringyl, Guaiacyl/Demethylated phenols, and carboxylic acids. This information is important because the amount of phenol along with the types of phenolic groups present will determine the reactivity of a given Lignin material.

Initial work was done on several standards to evaluate the precision and accuracy of the method. The standards were chosen as models for the three main phenolic groups found in Lignin. The sample preparation and P-31 NMR analyses were based on the experimental procedures outlined in the literature references. All samples were prepared in duplicate and cyclohexanol was used as the internal standard. The results, given below in Table 3, showed very good agreement between the two runs and with calculated versus theoretical phenolic content.

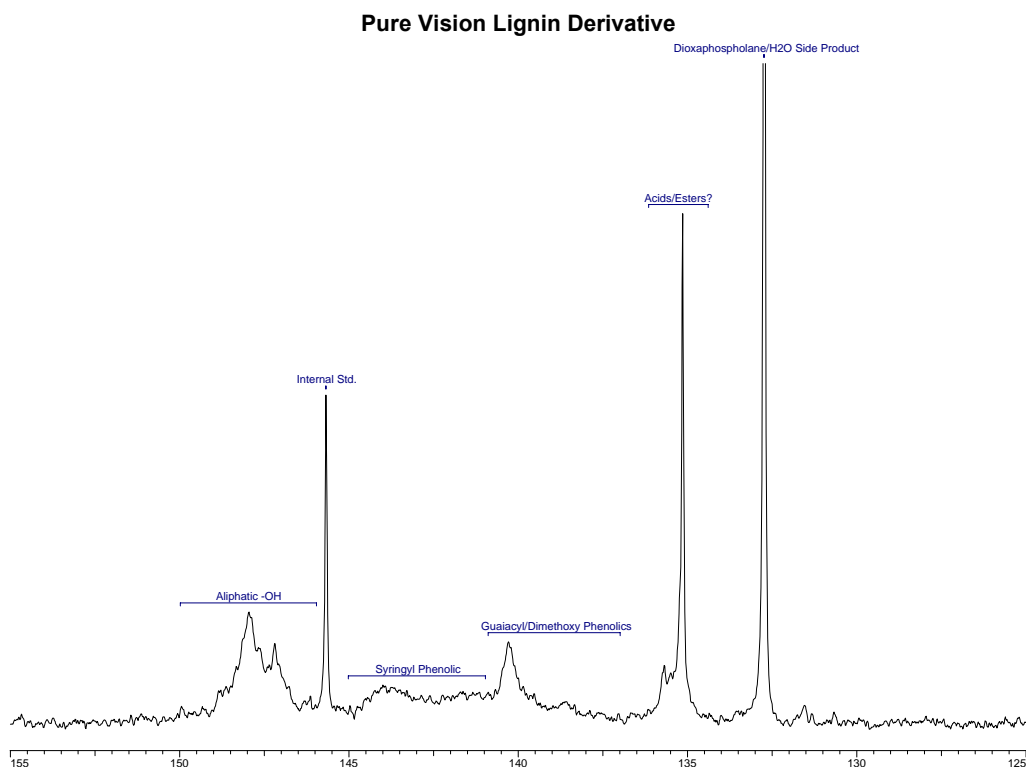
TABLE 3					
PHENOLIC CONTENT: P-31 NMR METHOD					
Compound	Theoretical phenolic content – meq/g	Experimental result- #1 meq/g	Experimental result- Run #2 meq/g	Experimental results - Avg. Value meq/g	Accuracy: % diff between theoretical vs. Experimental

¹ Argyropoulos, D. Bolker, H., Heitner, C., Archipov, Y., *J. Wood Chem Tech.*, 13(2), 187-212 (1993)

² Granata, A., Argyropoulos., *J. Agric. Food Chem*, 43, 6, 1995

Guaiacol	8.06	7.73	7.64	7.69	4.7%
2,4 dimethoxy phenol	6.49	6.33	6.47	6.50	1.4%
BPA	8.66	8.92	8.84	8.88	1.3%

The same procedure was then used to analyze the PureVision Lignin material. The assignment of the chemical shifts of the different lignin species were based on assignments reported in the literature. A P-31 NMR spectrum of derivatized Lignin with assignment of the different species is given below. The literature assigns the resonances in the 134-137 ppm region to derivatized carboxylic acids groups. Based on P-31 NMR studies done on the Pure Vision Lignin, I am not certain that this assignment is correct. I suspect that during the derivatization reaction, some ester groups are hydrolyzing and then reacting with the dioxaphospholane reagent. Based on these concerns, these peaks have been assigned as carboxylic acid/ester groups.



The derivatization was done on dried lignin material. This was necessary because of the sensitivity of the derivatization reagent to water. The values calculated from the P-13 NMR data are reported in Table 4 and these values have been corrected for the % solids of this product.

TABLE 4 HYDROXYL/PHENOLIC CONTENT: PURE VISION LIGNIN P-31 NMR METHOD				
	ALIPHATIC -OH	SYRINGYL PHENOLIC UNITS	GUAIACYL/DIMETHOXY PHENOLIC UNITS	ACID/ESTER
Run #1	0.309	0.205	0.186	0.177
Run #2	0.268	0.182	0.163	0.164
Average Value	0.289	0.191	0.175	0.171

A more detailed discussion of the experimental procedure for this method is given in Attachment D.



lignin.doc

GPC: Gel Permeation Chromatography (GPC) was conducted to determine the molecular weight distribution of the sample. The sample was analyzed by GPC in THF against polystyrene standards. The resulting chromatogram and distribution results are presented in Attachment E and below.



Pure Vision Lignin
050505(AZ).pdf

DCP: The samples were analyzed by DCP-AES (direct current plasma atomic emission spectroscopy) that is a quantitative elemental technique that is capable of simultaneous analysis of 33 different elements. Approximately 0.5 grams of each sample was digested with acid in sealed microwave digestion vessels, diluted to 50 ml volume in deionized water, and analyzed by DCP. The results are reported in the table below in parts per million (ppm) based on total sample weight and volume analyzed. Elemental results reported as “<” in Attachment F indicates the element was not detected and the amount reported is the detection limit for the specific element based on the sample weight and volume analyzed.



competitor4220ion.d
oc

PPG Industries Attachments

Attachment A



ION Lab Analysis
Allison Park

Analytical Report

[Visit the Analytical Web Page](#)

TO: George Sabulsky

FROM: Mitch Schneider

DATE: July 18, 2006

JOB: COMPETITOR.4220

SUBJECT: Pure Vision Lignin 050206 (AZ)

Pure Vision Lignin WET-06-04355

050206(AZ); Pure Vision

Lignin 050206(AZ)

Meq Acid

Recheck - Theory Too Low

Phenolic OH meq

1.096 meq

Meq Acid

0.934

Phenolic OH meq

1.083 meq

Pure Vision Lignin WET-06-05029

050206(AZ); Pure Vision

Lignin 050206(AZ)

SOLIDS-110

13.2

Ash

1582 ppm

Attachment B

COMPETITOR.4220

To: Sabulsky, George

From: Dave Remo

Date Received: 13-JUL-2006

Date Reported: 14-JUL-2006

Report # reports\competitor\2006\4220\4220gc.xls

Subject: Pure Vision Lignin 050206 (AZ)

Notebook ID Pure Vision Lignin 050206(AZ)

Description Pure Vision Lignin 050206(AZ)

LIMS ID GC-06-02246

ETOH 0.18

Results - w/w % Based on Total Sample



Analytical Report

GC Lab Analysis
Allison Park

[Visit the Analytical Web Page](#)

JOB: COMPETITOR.4220

competitor4220pyr.doc

TO: Sue Campbell

FROM: Sibylle Ingold

REPORT:

LOCATION: Allison Park

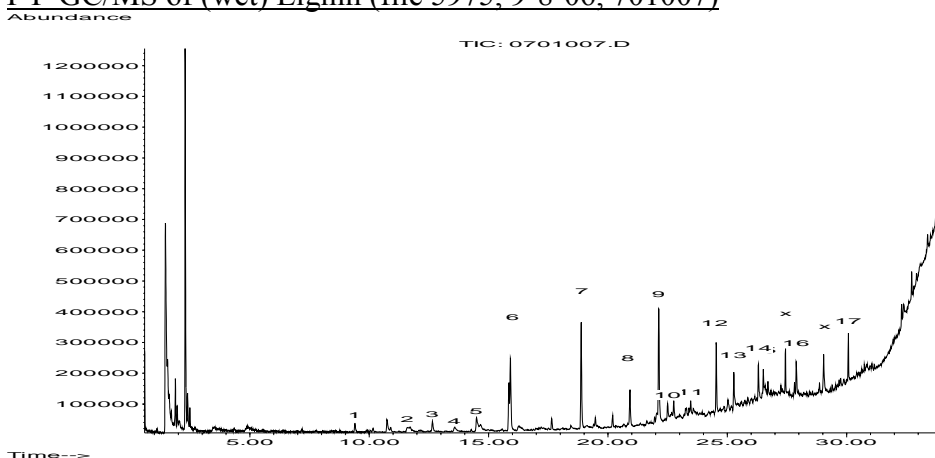
DATE: November 15, 2006

SUBJECT: Pyrolysis and THM of Vision Lignin 050206 (AZ)

1. Pyrolysis-GC/MS

Samples were pyrolyzed on the Frontier/GC/MS system using an RTX200 column to separate generated pyrolysis products.

PY-GC/MS of (wet) Lignin (file 5975, 9-8-06, 701007)



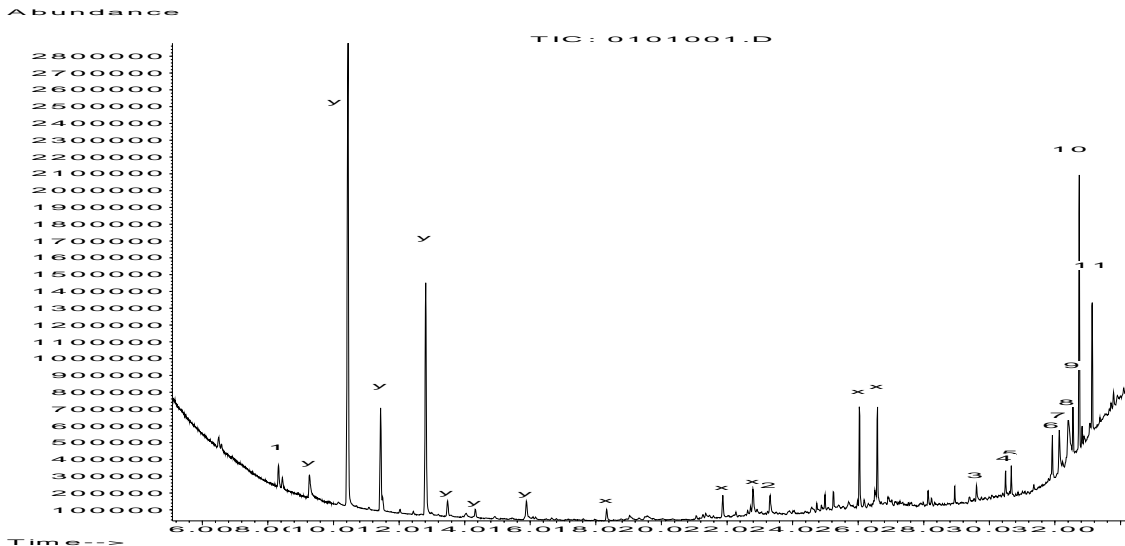
Peak Identification Key:

Peak #	Component	Peak #	Component
1	Furfural	9	4-Vinyl-2-methoxy-phenol
2	Phenol	10	Eugenol
3	Amine type component	11,12	Isoeugenol
4	2-Cresol	13	Vanillin
5	2,4-Imidazolidinedione	14	5-Propylguaiacol
6	2-Methoxyphenol	15	Acetovanillone
7	p- Creosol	16	Homovanillic acid
8	p-Ethylguaiacol	17	Dibutylphthalate

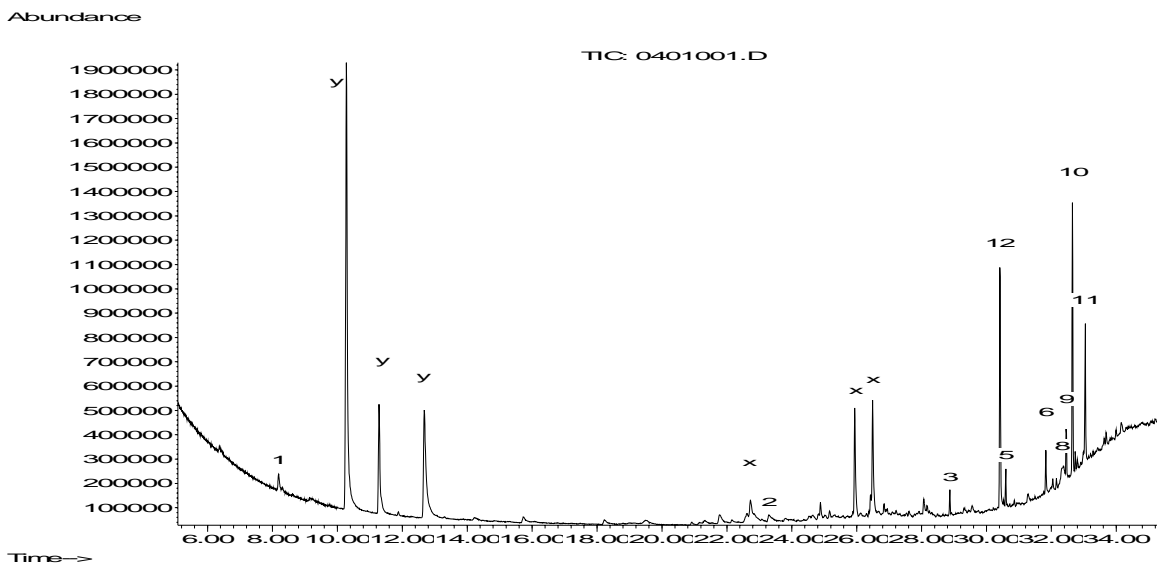
2. THM of Wet and Dry Lignin Samples

Thermal hydrolysis and methylation was done at 340C to analyze for organic acids components. Methyl esters and other components were separated using an RTX200 column. One additional component, 1,1'-(1-methylethylidene) bis-4-methoxy-benzene, was detected in the dry sample only.

a) THM, Wet sample (5975, 9-07a-06)



b) THM, Dried Sample (5975, 9-18b-06)



Peak Identification Key:

Peak #	Component	Peak #	Component
1	2-Methyl-3-octyl-2-undecenoic acid, ME	8	Bisphenol A
2	1-Dodecanol	9	Methylisopimerate
3	Hexadecanoic acid, ME	10	Dehydroabietic acid
4	9-Octadecenoic acid, ME	11	Methyl abietate
5	Octadecanoic acid, ME	12	1,1'-(1-methylethylidene) bis-4-methoxy-benzene
6	7-Ethenyl-dodecahydro-trimethyl phenanthrenecarboxylic acid, ME	X	Unknowns
7	4,4'-Methylenebis-benzeneamine	y	Methylation Rgt.

Attachment D

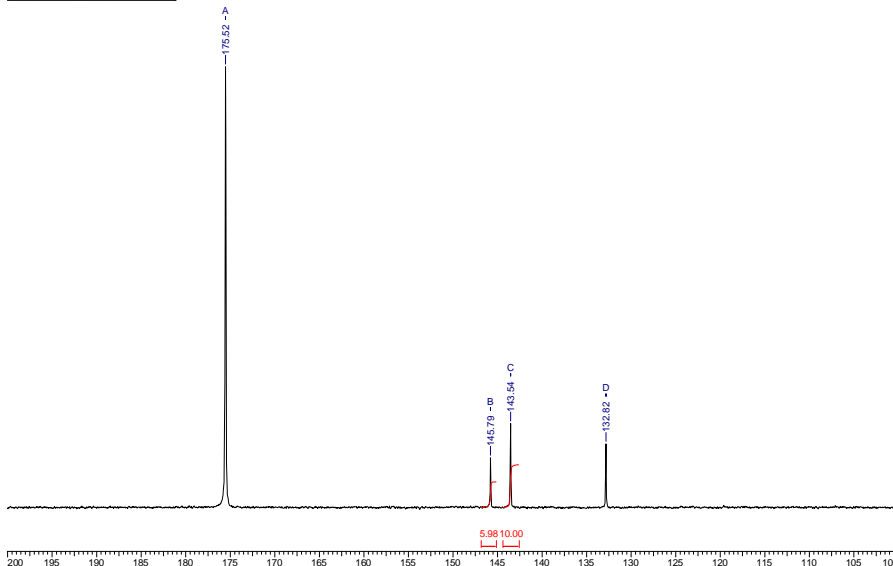
P-31 NMR DATA – 2-CHLORO-4,4,5,5,-TGETRAMEHTYL 1,3,2-DIOXAPHOSPHOLANE DERIVATIVES

1. 2,4 DIMETHOXY PHENOL

2,4 Dimethoxyl Phenol Derivative #1

28 Nov 2006
6NOV21.002/10

Acquisition Time (sec)	0.5243	Comment	2,4 Dimethoxy Phenol Deriv #1	Date	00/00/1980 00:00:00
Frequency (MHz)	121.49	Nucleus	31P	Original Points Count	32768
Temperature (grad C)	0.000			Points Count	32768
				Sweep Width (Hz)	62500.00



ASSIGNMENTS:

A – Unreacted dioxaphospholane

B – Cyclohexanol/Dioxaphospholane Derivative

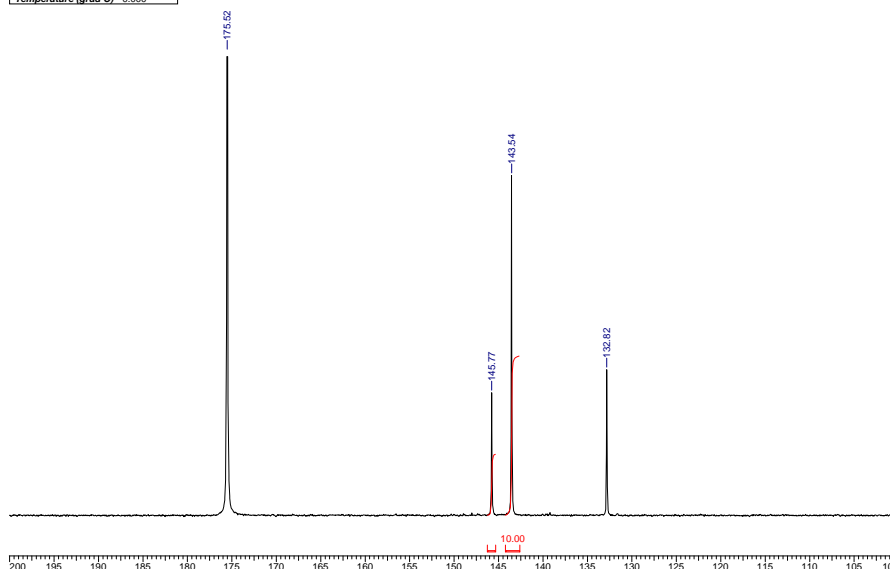
C – 2,4 Dimethoxy phenol/Dioxaphospholane Derivative

D – Unreacted Dioxaphospholane/H₂O Side product (present in dioxaphospholane starting material)

2,4 Dimethoxyl Phenol Derivative #2

29 Nov 2006
6NOV21.002/50

Acquisition Time (sec)	0.5243	Comment	2,4 Dimethoxy Phenol Deriv #2	Date	00/00/1980 00:00:00
Frequency (MHz)	121.49	Nucleus	31P	Original Points Count	32768
Temperature (grad C)	0.000			Points Count	32768
				Sweep Width (Hz)	62500.00

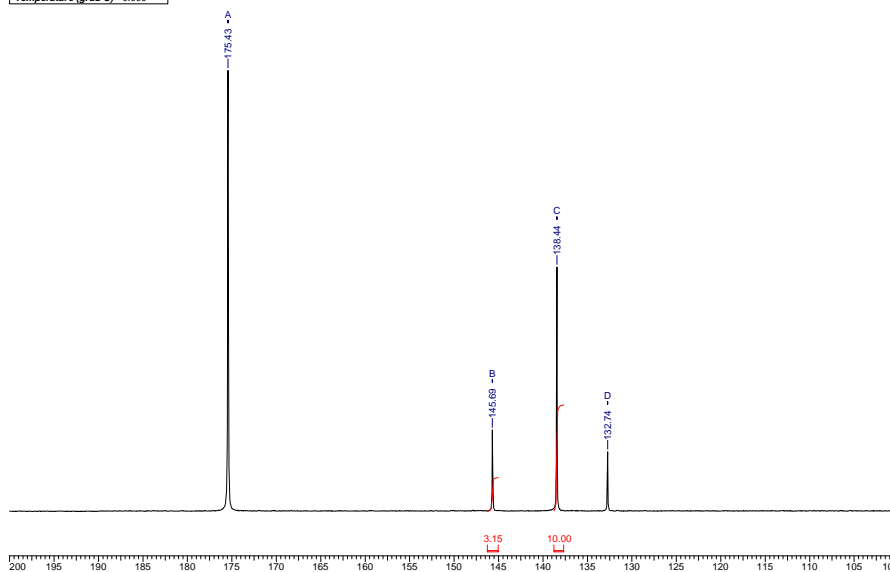


2. BPA

BPA Derivative #1

29 Nov 2006
6NOV21.002/20

Acquisition Time (sec)	0.5243	Comment	BPA Deriv #1	Date	00/00/1980 00:00:00
Frequency (MHz)	121.49	Nucleus	31P	Original Points Count	32768
Temperature (grad C)	0.000			Points Count	32768
				Sweep Width (Hz)	62500.00



ASSIGNMENTS:

A – Unreacted dioxaphospholane

B – Cyclohexanol/Dioxaphospholane Derivative

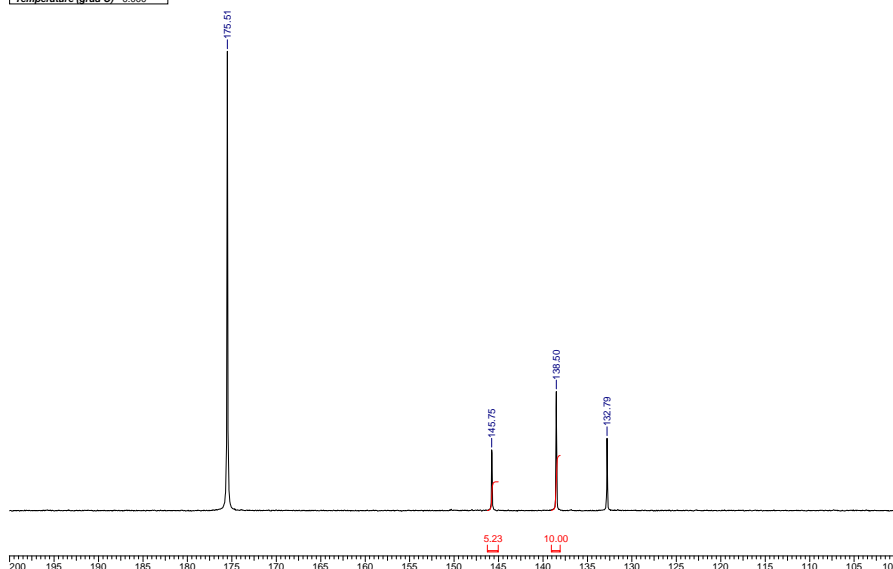
C – BPA/Dioxaphospholane Derivative

D – Unreacted Dioxaphospholane/H₂O Side product (present in dioxaphospholane starting material)

BPA Derivative #2

29 Nov 2006
6NOV21.002/30

Acquisition Time (sec)	0.5243	Comment	BPA Deriv #2	Date	00/00/1980 00:00:00
Frequency (MHz)	121.49	Nucleus	31P	Original Points Count	32768
Temperature (grad C)	0.000			Points Count	32768
				Sweep Width (Hz)	62500.00

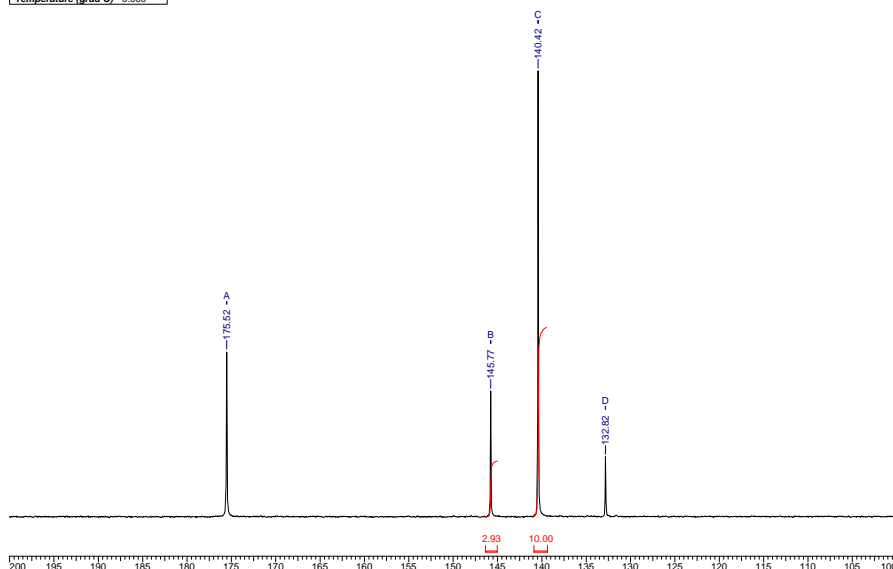


3. GUAIACOL

GUAIACOL DERV. #1

29 Nov 2006
6NOV21.002/71

Acquisition Time (sec)	0.5243	Comment	Guaiacol #1	Date	00/00/1980 00:00:00
Frequency (MHz)	121.49	Nucleus	31P	Original Points Count	32768
Temperature (grad C)	0.000			Points Count	32768
				Sweep Width (Hz)	62500.00



ASSIGNMENTS:

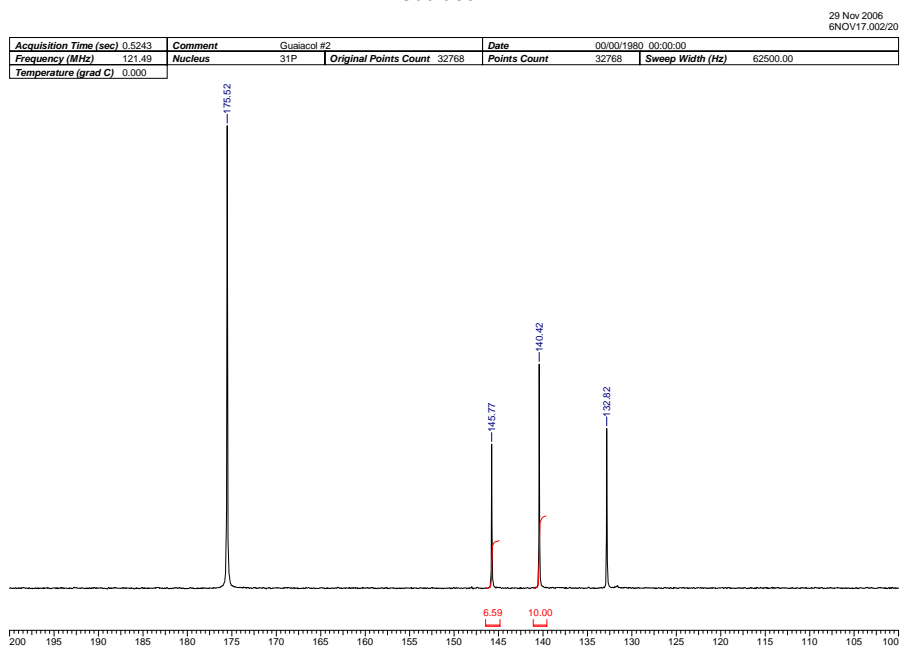
A – Unreacted dioxaphospholane

B – Cyclohexanol/Dioxaphospholane Derivative

C – 2,4 Dimethoxy phenol/Dioxaphospholane Derivative

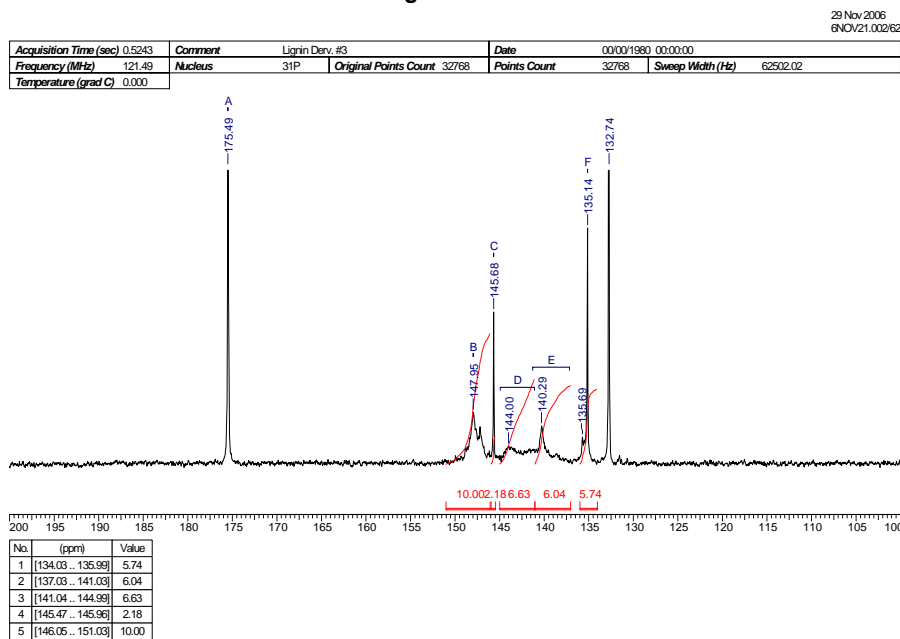
D – Unreacted Dioxaphospholane/H₂O Side product (present in dioxaphospholane starting material)

Guaiacol #2



4. LIGNIN

Lignin Derv #3



ASSIGNMENTS:

A – Unreacted dioxaphospholane.

B - Aliphatic OH/Dioxaphospholane Derivative.

C – Cyclohexanol/Dioxaphospholane Derivative.

D – Syringyl Phenolic/Dioxaphospholane Derivative.

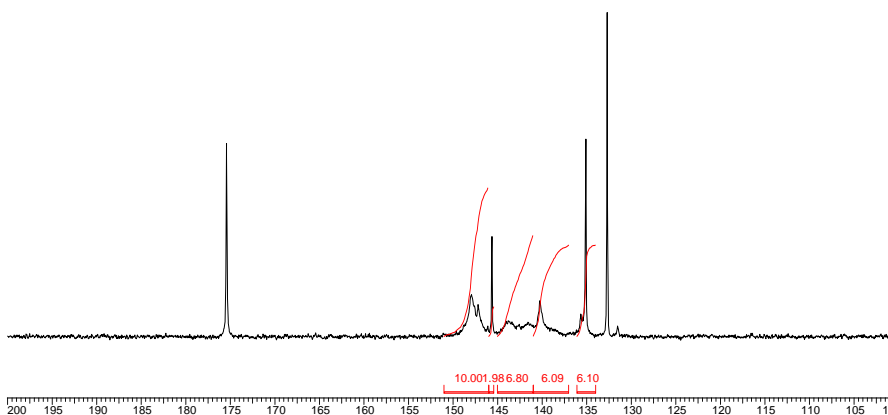
E – Guaiacyl and Dimethylated Phenolic/Dioxaphospholane Derivative.

F - Unreacted Dioxaphospholane/H₂O Side product (present in dioxaphospholane starting material)

Lignin Derv #4

29 Nov 2006
6NOV21.002/71

Acquisition Time (sec)	0.5243	Comment	Lignin Derv #4	Date	00/00/1980 00:00:00
Frequency (MHz)	121.49	Nucleus	31P	Original Points Count	32768
Temperature (grad C)	0.000			Points Count	32768
				Sweep Width (Hz)	62502.02



No.	(ppm)	Value
1	[134.00 .. 136.11]	6.10
2	[137.04 .. 141.00]	6.09
3	[141.01 .. 145.02]	6.80
4	[145.43 .. 145.99]	1.98
5	[146.01 .. 151.05]	10.00

Attachment E.

Allison Park GPC Data

SampleName: Pure Vision Lignin 050206(AZ) Submitter: David Fenn

Resin Code: NA LotNumber: NA Processing Method: B061406cal Sample Set Name: B061406

Project: JUNE2006LIMS Number: 3198

COMPETITOR.4220 **SABULSKY**

Not completely in soln

Instrument ID: B Vial: 15 Column: 2

PLgel mixed C

Column Serial No: 113-4/113-53

Solvent: THF

GPC Results

Peak Molecular Weight		Retention Time	% Area	Weight Average	Number Average	Z Average	Mw/Mn Polydispersity	%Polymer < 1000 MW(PS)	%Polymer < 500 MW(PS)
1	1205	16.8	84.79	2410	1074	7735	2.2	35.1	11.1
2	234	18.1	15.21						

6.00 8.00 10.00 12.00 14.00 16.00 18.00 20.00 22.00
Minutes

SampleName Pure Vision Lignin 050206(AZ); Date Acquired 6/14/2006 7:24:24 PM

Injection

Volume: 30.00 ul

Date printed: 6/15/2006 4:48:26 PM Result Id 3644



TO: George Sabulsky

FROM: Curt Radcliffe

DATE: June 16, 2006

JOB ID: COMPETITOR.4220

DESCRIPTION: Pure Vision Lignin 050206 (AZ)

Pure Vision Lignin 050206(AZ)

ION-06-0575

Pure Vision Lignin 050206(AZ)

Total S	300	ppm
Total Ca	250	ppm
Total Na	170	ppm
Total Fe	130	ppm
Total Al	15	ppm
Total K	11	ppm
Total Mg	5.8	ppm
Total Se	< 50	ppm
Total Bi	< 45	ppm
Total P	< 45	ppm
Total As	< 40	ppm
Total Sb	< 25	ppm
Total V	< 25	ppm
Total Ce	< 15	ppm
Total In	< 10	ppm
Total W	< 10	ppm
Total Sn	< 10	ppm
Total Pb	< 5.0	ppm
Total Si	< 5.0	ppm
Total Zn	< 5.0	ppm
Total B	< 4.0	ppm
Total Cr	< 3.5	ppm
Total Ni	< 3.0	ppm
Total Cd	< 2.5	ppm
Total Co	< 2.5	ppm
Total Ag	< 2.0	ppm
Total Zr	< 2.0	ppm
Total Mo	< 2.0	ppm
Total Mn	< 1.5	ppm
Total Ti	< 1.5	ppm
Total Cu	< 1.0	ppm
Total Li	< 1.0	ppm
Total Y	< 1.0	ppm
Total Ba	< 0.15	ppm
Total Sr	< 0.15	ppm

8.6 MAST Report

Fractionation of pre-hydrolysis products from lignocellulosic biomass by an ultrafiltration ceramic tubular membrane

Kendra R. Colyar

Department of Civil, Environmental, and Architectural Engineering, University of Colorado
Boulder, CO

John Pellegrino*

Department of Civil, Environmental, and Architectural Engineering, University of Colorado
Boulder, CO

Kiran Kadam

PureVision Technology, Inc.
Fort Lupton, CO

Abstract:

Development of the lignocellulosic-biomass-based biorefinery for making transportation fuels requires the production of valuable byproducts, minimizing the chemical consumables, and efficient water recovery and reuse. Our focus is on a liquid stream containing a variety of soluble lignin species and alkalinity that is produced by a novel extrusion reactor that was used to break down corn stover to cellulose, sugar acids, and lignin. We report on the ambient temperature fractionation of this byproduct stream with a γ -alumina ceramic tubular membrane. There are four primary figures-of-merit investigated in this study: permeance decline, total organic carbon recovery (TOC) and sodium recovery, and the average molecular mass of organic compounds rejected and permeated. These fractionation results are compared relative to differing feed compositions, recovery, and flux. There was definite fractionation between organic (mostly soluble lignin) compounds. The average molar mass of the organic compounds in the permeate remained around 1000 g/mol; however, they ranged from 1500 - 4000 g/mol in the retentate. In contrast to the TOC, there was no rejection of sodium ions by the membrane (a desirable objective.) With respect to flux decline, the primary form of resistance (>99%), causing significant permeance decline, was a gel/deposition layer formed on the membrane surface. However, this could be flushed away with periodic rinses using water and/or 0.1 M NaOH. After operation at a cumulative filtration load of $\sim 4.9 \text{ Mg/m}^2$ with various soluble lignin containing streams, 70% of the membrane's virgin pure water permeance could be recovered by a more vigorous cleaning with 0.1 M NaOH including soaking and permeation. Our results seem very consistent with those previously observed for membrane applications within the pulp and paper industry.

Keywords: γ -alumina, biorefinery, pre-hydrolysis, lignin, lignocellulose, ultrafiltration, ceramic tubular membrane, sodium, ultraviolet spectrophotometry, total organic carbon, molar absorptivity

*Address correspondence: John Pellegrino, CEAE Department, ECOT 441, University of Colorado, Boulder, CO, 80309-0428, Tel.: 303 735 2631, Fax: 303 492 7317, E-mail: john.pellegrino@colorado.edu

INTRODUCTION

The most sustainable feedstocks for bioethanol production are lignocellulosic biomass, such as low-cost residues and wastes from agricultural processes like corn stover [1]—of which 60-80 million dry tons per year are available for ethanol production in the United States [2]. Corn stover is predominantly composed of cellulose, hemicellulose, and lignin. Hemicellulose and lignin provide a protective sheath around cellulose, which must be chemically or biologically removed before cellulose-hydrolysis can occur to provide sugars for bioethanol production [3]. Each type of feedstock used to make ethanol requires some form of pre-treatment to minimize the degradation of the substrate and maximize the sugar yield [3]. The pre-treatment for the corn stover feedstock in this study was a novel extrusion reactor design [4], which involves sequential additions of a strong acid, such as sulfuric acid, and a strong alkaline agent, such as sodium hydroxide. The effluent from the latter stage contains a variety of lignin species, excess alkalinity, and dissolved carbohydrates—somewhat similar to the black liquor produced in the pulp and paper industry (PPI) (see Table 1). To make a lignocellulosic-biorefinery more economical and ecologically balanced, we are studying cost-effective processes to recover potentially valuable byproducts, minimize chemical consumables, and recycle water.

The filtration work we performed had two goals. One was to ascertain the fractionation that would be obtained by an inorganic membrane that might be useful for both the elevated temperature basic (the current focus) and acidic (future work) streams produced by the developing pre-treatment process. The second goal was to operate the ultrafiltration process in a small-scale production fashion in order to produce permeate useful for subsequent studies. This latter aspect has allowed us to benchmark how robust the membrane's separation characteristics were to "imperfect" cleaning protocols.

There are four primary figures-of-merit investigated in this study: permeance decline, total organic carbon (TOC) fractionation, Na^+ recovery in the permeate, and the average molar mass of organic compounds retained and permeated through the membrane. The permeance decline was monitored to determine the degree of reversible (concentration polarization and surface, or gel, layer) and irreversible fouling (pore and surface adsorption) that occurred due to prolonged filtration and changing feed compositions. The TOC fractionation corresponded to the amount of relatively large molar mass organic species retained by the membrane, and the Na^+ recovery represented the amount of it in the initial feed not sequestered in the retentate (for example, as Na^+ salts of organic acids). The average molar mass of organic compounds retained and permeated by the membrane was determined by using their ultraviolet (UV) absorbance and molar absorptivity at 274 nm.

Background

There have been many recent studies [5-16] conducted on membrane separation processes to recover chemicals and water in the PPI, much like what is desired in a lignocellulosic-biorefinery. In addition, early PPI application research and commercial installations stretch back to the late 1960's and are quite comprehensively enumerated by Wallberg, Jönsson and co-workers, in ref. [10]. More recently, new membrane materials, both polymeric and inorganic, have become available that have a broader range of pH, solvent, and temperature stability and have been evaluated at higher temperatures for hemicellulose and lignin [12-14] recovery from alkaline liquors.

An early study conducted by Hill and Fricke [5] examined the efficacy of using polymeric ultrafiltration (UF) membranes to fractionate lignin from softwood kraft black liquor (KBL). They investigated the molar mass of fractions retained and permeated (using the ultraviolet absorbance and molar absorptivity, similar to this work) versus the nominal molar mass cutoff (MWCO) of the membrane. A nanofiltration-like membrane ($\text{MWCO} \leq 500 \text{ g/mol}$) was apparently required to retain all the phenolic components. A similar fractionation study with polysulfone polymeric membranes with cutoffs ranging between 4 and 20 kg/mol was also performed by Wallberg et al. [10]. They reported 80% retention of lignin with the 4 kg/mol UF membranes and insignificant retention of sodium and sulfur (an objective), and were able to regenerate the membranes with alkaline cleaning.

In a variety of separations applications, the use of inorganic membranes is increasing, and so to in the pulp and paper industry due to their resistance to high temperatures and acidic and alkaline solutions, and potentially longer life spans. Liu et al. [8] investigated the applicability of inorganic membranes for major constituent fractionation and high flux operations in the treatment of black liquor from a straw-based pulp and paper mill. They determined that inorganic microfiltration (MF) membranes could efficiently reject most lignin and silica in the black liquor. This is of particular interest for wheat straw feed stocks that have high silica content, which can cause difficulties in alkaline recovery systems. The composition of the black liquor used in Liu et al.'s [8] experiments is summarized in Table 1 for a comparison with the solutions of interest in this study.

Wallberg et al. [9] conducted studies on the UF of softwood KBL by using an alumina-titania ceramic tubular membrane (CTM). Their work investigated the effect of temperature on the permeate flux and the percent retention of lignin and inorganic compounds. Wallberg et al. [9] found that at higher operating temperatures the permeate flux increased and the lignin retention decreased, which is likely due to the increased solubility of lignin at elevated temperatures. The increased volumetric flux at higher temperatures is extremely advantageous for the pulp and paper industry because KBL effluent is generally above boiling. Wallberg and Jönsson and co-workers have continued studying inorganic membranes for a variety of KBL and PPI applications [11, 12, 15]. These investigators noted that over a wide variety of membranes the retention of lignin compounds decreased at elevated temperatures and they also suggest that trace multivalent ions aid formation of lignin colloids that facilitate the overall lignin retention.

Many researchers have noted that the optimal membrane geometry (e.g. MWCO) for lignin fractionation targets is not always obvious due, in part, to the heterogeneity of the lignin from different sources and the “cooking” process variables. In addition, the membrane process conditions, including the mass transfer boundary layer will make a difference (for example, 10, 11, 13, 16). Among the differences between previous studies on CTM KBL filtration and this work is that our measurements were made at room temperature and the liquor is derived from corn stover. Agricultural residues such as corn stover contain lower lignin content than softwoods (see Table 2) and other typical pulping feed stocks, such that less pretreatment is necessary to prepare the material for enzymatic hydrolysis in bioethanol production. In this work, we perform initial studies to compare results obtained with a biomass-to-fuel liquor to those from prior PPI applications in order to assess how well prior PPI benchmarks for

membrane unit operations can extrapolate into the emerging biofuels/biorefinery industry applications.

EXPERIMENTAL

Materials

The pre-hydrolysis liquors used in this study were obtained from PureVision Technology, Inc. located in Fort Lupton, CO. PureVision has developed an extrusion reactor design [4] that breaks down woody biomass, such as corn stover, into a cellulosic fraction (as a dense plug) and two aqueous streams, one acidic and the other basic, containing various valuable byproducts. Two batches of the latter (basic) effluent were used as the main feedstocks for this work, referred to as liquors 1 and 2. Their compositions are summarized in Table 1, along with that of an initial batch, referred to as liquor 0, which we used for preliminary studies. The pre-treatment hydrolysis process is still being optimized so the liquor composition changes depending on process modifications, such as varying the ratio of sodium hydroxide to biomass (corn stover) and the method of solids separation. For example, liquor 0 and liquor 1 were centrifuged at 40 rpm and liquor 2 was pressure filtered through a 100 μm filter. Due to the different suspended solids removal techniques, the total suspended solids (TSS) and total organic carbon (TOC) content are considerably different between these liquors (see Table 1).

Filtration apparatus

A UF γ -alumina CTM with a nominal pore size of 5 nm and effective membrane area of $\sim 10.8 \text{ cm}^2$ was obtained from CeraMem Corporation for these experiments. It is a single tubular membrane (circular cross-section) with an $\sim 0.65 \text{ cm}$ inside diameter and $\sim 5.3 \text{ cm}$ length. The pure water permeance (PWP) through the CTM, prior to any filtrations with liquors, was approximately $2.77 \times 10^{-7} \text{ m}^3 \cdot \text{m}^{-2} \cdot \text{s}^{-1} \cdot \text{kPa}^{-1}$. The filtration experiments were lumen fed and conducted in a batch mode, thus the retentate was recycled to the feed container throughout the experiment. The feed was delivered through high-pressure tubing (Masterflex PharMed L/S 18) into a Cole-Palmer (Masterflex) console pump. The average feed flow rates supplied by the pump during tests 1 and 2 were $8.7 \times 10^{-7} \text{ m}^3/\text{s}$ and $9.4 \times 10^{-7} \text{ m}^3/\text{s}$, which corresponded to average crossflow velocities through the CTM during tests 1 and 2 of 0.10 and 0.12 m/s, respectively. A back-pressure regulator, located between the membrane and retentate line, established the transmembrane pressure gradient to generate permeate. Figure 1 shows a schematic of the different components in the filtration apparatus.

Experimental approach

For clarity, a schematic flowsheet of the experimental steps is presented in Figure 2. Determination of the clean membrane's pure water permeance before any testing is labeled PWP 1. Prior to test 1 the effect of transmembrane pressure on the volumetric flux was determined for liquors 0 and 1 to see if a gel layer formed (Figure 3). Following the liquor 0 filtrations, the membrane was flushed with filtered, deionized, 18 M Ω resistance water (aka MQ water) and 0.1 M NaOH, and the new pure water permeance (PWP 2) was determined as a baseline for work with liquor 1. Following tests 1 and 2, the membrane was cleaned and the new pure water permeances (Figure 4) of the membrane (PWP 3 and PWP 4) were measured to calculate the degree of irreversible fouling that occurred during the liquor filtration tests 1 and 2.

During test 1 six separate batches of ~400-700 g of liquor 1 feed were filtered at a transmembrane pressure of 552 kPa (80 psi). After approximately 50 to 70% recovery of feed as permeate (aka permeate recovery) for each batch, the test was stopped and a new batch of ~400-700 g of liquor 1 was added to the feed container and the test was resumed. Permeate was collected into pre-weighed vials, which were weighed and replaced when full to obtain the permeance decline trend. The retentate samples, collected after each permeate vial replacement, were obtained from the retentate line (for batches 1-4 only). The retentate flow rate was measured during each sampling time to monitor any change in crossflow velocity and to calculate the hydrodynamic boundary layer mass transfer coefficient. Following batches 1, 2, and 4 the membrane was flushed with MQ water.

During test 2, one large batch of ~4000 g of liquor 2 feed was permeated at a transmembrane pressure of 278 kPa (40 psi). Permeate was continuously weighed on an analytical mass balance (Sartorius L810) and the retentate samples were collected periodically from the retentate recycle line to monitor the same effects as described for test 1. Following 16% permeate recovery (approximately 75 h) the membrane was flushed with 0.1 M NaOH, due to a 40% drop in permeance. Following the sodium hydroxide flush, test 2 resumed and run to a total of 80% permeate recovery.

TOC and sodium recovery

The total organic carbon and sodium recovery were determined for batches 1-4 of test 1 and all of test 2. Total organic carbon was measured using a Sievers 800 TOC Analyzer following the method outlined in Standard Methods 5310 C [17]. Potassium hydrogen phthalate (KHP) standards were used that ranged from 0 to 10 mg KHP/kg MQ water. The TOC recovery (TOC_{rec}) was determined by the mass of TOC in permeate at time t ($TOC_{p,t}$, g) divided by the mass of TOC in the feed at time 0 ($TOC_{f,0}$, g). The TOC recovery was calculated by the following equation:

$$TOC_{rec} = \frac{TOC_{p,t}}{TOC_{f,0}}. \quad (1)$$

The sodium concentration was determined using a Dionex Ion Chromatography analyzer with an IonPac CS12 (10-32) cation analytical column. Sodium chloride (NaCl) standards from Sigma-Aldrich were prepared at concentrations of 5, 10, 20, 30, 40, and 50 mg NaCl/kg MQ water. Similar to TOC, the sodium recovery was calculated by the following equation:

$$Na^+_{rec} = \frac{Na^+_{p,t}}{Na^+_{f,0}} \quad (2)$$

where the subscripts have a similar interpretation as above.

Molecular mass of fractionated organic species

An ultraviolet (UV) spectrophotometer, HACH DR/4000U, was used to determine the approximate compositional change of the lignin in the various streams. Five-hundred-fold dilutions were performed on the feed, retentate, and permeate after 30 min of test 1, and on the feed, retentate and permeate after 80 min of test 2 to compare the UV spectra as shown in Figure 5. Five-hundred fold dilutions were also done on all samples throughout tests 1 and 2 for UV analysis in order to compare the compositional change in the feed, retentate, and permeate by differing peak absorbances at 274 nm. This wavelength was chosen because π - π^* electron

transitions occur between 270 and 280 nm on the UV spectrum range for phenolic substances (such as lignin), benzoic acids, and polycyclic aromatic hydrocarbons [18, 19]. The decomposition products of lignin contain fractions of humic acid, which exhibit a featureless increase in absorbance with decreasing wavelength [20], which is also displayed in Figure 5. Chin et al. [20] acknowledged that since many of these lignin products are precursors of humic substances, molar absorptivities may yield important clues regarding the degree of aromaticity, extent of "humification", and molecular mass of compounds that absorb UV light between 270-280 nm. In response to this relationship, Chin and coworkers [20] developed a useful correlation between the molar absorptivity of humic substances in this UV range and the high-pressure size exclusion chromatography (HPSEC) mass averaged molecular mass. A regression analysis of their data resulted in the following equation for characterizing the relationship between the molar absorptivity at 280 nm and molecular mass [20]:

$$M_M = 3.99\varepsilon + 490 \quad (3)$$

where, M_M is the average molecular mass (g/mol) and ε the molar absorptivity ($\text{L}\cdot\text{mol}^{-1}\cdot\text{cm}^{-1}$) at 280 nm. This correlation has been successful for humic substances with $M_M > 490$ g/mol in the absence of interfering chemical substances, such as metal oxides [20].

Total suspended solids and total solids

The total suspended solids (TSS) and total solids (TS) content were not monitored continuously during these experiments; however, the initial TSS and TS content of liquor 1 and 2 were determined for comparison between feeds used in other studies [5-9], for example, Lui et al. [8], is shown in Table 1. The TSS content was determined for duplicate samples by centrifugation in 12 cm radius device at 3370 rpm for 10 min. The percent total suspended solids were calculated by the following:

$$\% TSS = \frac{M_s - M_{\text{sup}}}{M_s} * 100\% \quad (4)$$

where, % TSS is the percent total suspended solids, M_s is the mass of sample (g), and M_{sup} is the mass of supernatant liquid (g). The total solids (TS) content of the initial liquor was determined for duplicate samples by evaporation of the liquid phase at approximately 95°C in a vacuum oven at an absolute pressure of ~20 kPa until no visible liquid remained. The percent total solids are given by the following:

$$\% TS = \frac{M_{\text{solid}}}{M_s} * 100\% \quad (5)$$

where, % TS is the percent total solids, M_s is the mass of sample (g), and M_{solid} is the mass of solid (g) that remained after evaporation of the liquid.

RESULTS AND DISCUSSION

Permeance decline

The γ -alumina CTM had been used for preliminary experiments prior to the main tests, and had been cleaned. These experiments were conducted to determine the effect of transmembrane pressure on the volumetric flux of liquors 0 and 1 through the CTM (Figure 3). (A similar experiment was conducted with liquor 2 after test 2.) As the transmembrane pressure increased, the higher volumetric flux caused compression of accumulated lignin particles on the membrane surface. The membranes's PWP was determined after the initial experiment with liquor 0 as 1.28

$\times 10^{-7} \text{ m}^3 \cdot \text{m}^{-2} \cdot \text{s}^{-1} \cdot \text{kPa}^{-1}$, which was ~46% of its "virgin" pure water permeance. At this point experiments with liquor 1 began.

The permeance of liquor 1 (at $\Delta P_{\text{tm}} = 552 \text{ kPa}$) during the flux versus ΔP_{tm} experiment (described above), and the permeance decline of liquor 1 (test 1) at $\Delta P_{\text{tm}} = 552 \text{ kPa}$ is shown in Figure 6 for all six batches individually run to 50-70% permeate recovery. The permeance of liquor 1 never approached a steady-state, either overall, or within any individual batch. It dropped from ~2.1 to $0.65 (\times 10^{-8} \text{ m}^3 \cdot \text{m}^{-2} \cdot \text{s}^{-1} \cdot \text{kPa}^{-1})$ over the entire course of permeating ~1952 g—this corresponded to ~1802 L/m² of membrane in the six batches. Following batches 1 and 2 the membrane was flushed with MQ water. The initial solution permeance in batch 2 was approximately the same as the initial solution permeance of batch 1; however, a subsequent MQ flush following batch 2 did not regenerate the membrane permeance as shown in Figure 6. After batch 4 the membrane was flushed with MQ water and 0.1 M NaOH and the membrane permeance increased ~1.4x higher than at the end of batch 4. Since our experimental protocol was a batch recycle, the lack of steady state is consistent with continuous accumulation of macromolecules from an increasingly more concentrated feed stream.

The permeance decline of liquor 2 (test 2) at $\Delta P_{\text{tm}} = 278 \text{ kPa}$ is shown in Figure 7.

As before, loss of permeance was continuous with accumulation of unpermeated species, only punctuated by cleaning and operating perturbations, as follows. Following 16% permeate recovery (and a 40% drop in permeance) the membrane was cleaned with 0.1 M NaOH. The cleaning procedure entailed a 45 min flush with MQ with roughly 85 mL of permeation at 278 kPa, followed by 2.5 h of a 0.1 M NaOH flush with no permeation. As seen in Figure 7, Figure 7. the membrane permeance was not fully regenerated by this cleaning procedure. After determining a new pure water permeance ($1.23 \times 10^{-7} \text{ m}^3 \cdot \text{m}^{-2} \cdot \text{s}^{-1} \cdot \text{kPa}^{-1}$), the filtration of liquor 2 was resumed and carried out to an overall 80% permeate recovery.

When varying total feed masses are used, as was done in this study, the relationship between permeance decline and the total mass permeated is a more meaningful basis of comparison than using filtration time or % recovery. Figure 8 shows the effects on flux decline from feed composition—the starting composition is "reset" to the initial value with the different batches of liquor 1 test (not so with liquor 2 test), as well as the composition of test 2 being different overall—and the total mass permeated. Following each batch of the liquor 1 test the permeance was not fully generated and the same observation was made for the liquor 2 test. Although the permeance of the first three batches of test 1 are considerably different from test 2, the fifth batch has a very similar permeance decline trend and magnitude as the beginning (the first 400 g of liquor 2 permeated) of test 2 despite the differing feed compositions and pressures used.

We will see that these results are somewhat consistent with the occurrence of adsorption in and on pores, insofar as the irreversible part increases as the total mass permeated increases, due to more adsorbed/aggregated species accumulating in hard-to-clean inner spaces. The overall decrease in permeance is also representative of the increasing mass of a deposition (or gel) layer from successful filtration. The presence of a surface gel/deposition layer is supported by Figure 3 which shows that with increasing transmembrane pressure the volumetric flux of liquor 0, 1, and 2 slowly approaches a constant, maximum value. This maximum flux decreases respectively with liquor 0, 1, and 2 due to irreversible fouling that has occurred inside the membrane prior to

and during tests 1 and 2 (Figure 3). It is important to note that a constant value was *not* reached, thus we cannot insist that a gel-layer was formed during these experiments, but the form of the flux versus pressure data is consistent with the “weak form” of critical flux [21, 22].

Vela et al. [23] conducted membrane characterization tests with a ZrO₂-TiO₂ CTM with a nominal pore size of 4 nm and a surface area of 35.5 cm² using solutions of 35 kg/mol polyethylene glycol (PEG). Their experiments were conducted at a transmembrane pressure of 300 kPa and several crossflow velocities (1-3 m/s.) The steady-state permeance obtained by Vela et al. [23] at 300 kPa and 1 m/s crossflow velocity was $3.7 \times 10^{-8} \text{ m}^3 \cdot \text{m}^{-2} \cdot \text{s}^{-1} \cdot \text{kPa}^{-1}$, which is ~ 2.5 x higher than the permeance obtained during batch 1 of test 1 and 8x higher than the permeance obtained during the early stages of test 2. Test 2 and Vela et al.’s [23] experiments were run at similar pressures (278 kPa and 300 kPa), however, the early stage permeance obtained during test 2 was drastically lower than Vela et al [23]. They concluded that their flux decline was primarily due to gel-layer formation; this is not strictly the case in the lignin filtration process, but we can conclude that the intrinsic resistance per unit mass of the lignin surface deposition is significantly greater than that for the PEG.

Fouling mechanisms and resistance

During UF experiments there are three primary flux reduction mechanisms (which are all exacerbated by concentration polarization): osmotic pressure, gel-layer formation, and adsorption of solutes on the membrane surface and in the membrane pores [23, 24]. However, during the UF of macromolecular solutions, the osmotic pressure can often be considered negligible [25]. The flux decline viewpoint used in this study was a combination of the osmotic-pressure-adsorption model used by Ko et al. [24] and the gel-polarization model developed by Porter [25]. Although a classic gel-layer may not have formed during these experiments, a deposit-layer and pseudo-gel-layer have similar growth mechanisms and effects on mass transfer. Thus, the gel-layer resistance term was added to the equation used by Ko et al. [24] as an additional layer of resistance that contributes to the flux decline from the solutions used in this study.

It is important to note that what we calculate as the R_g (resistance of a gel layer) is everything that can be washed away by the MQ water (and/or NaOH) flush made prior to measurements of pure water permeance. Thus it may incorporate several types of aggregated material.

Concentration polarization is the increase in concentration of colloidal and macromolecular material in a layer adjacent to the membrane surface. This can then increase surface and pore mouth adsorption processes, as well as, lead to a phase change, or gel formation. UF membranes are exceptionally prone to this latter form of fouling, especially when they are used to separate macromolecular solutions that can self-associate, during which flux decline can occur in seconds. This avenue of fouling is considered to be reversible and can be mitigated by the crossflow velocity across the membrane surface, regular cleaning, and the use of hydrophilic or charged membranes to minimize adhesion to the membrane surface [26]. All other sources of flux decline are considered irreversible, even though rigorous chemical and physical cleaning regimes may be able to remove some of the fouling material and lower the resistance afterward.

From the initial pure water permeance, the membrane’s “virgin” intrinsic resistance was determined as $3.61 \times 10^{12} \text{ m}^{-1}$.

$$R_{m,1} = \frac{1}{\eta_w PWP_1} \quad (6)$$

where, $R_{m,1}$ is the membrane's intrinsic resistance (m^{-1}), PWP_1 is the pure water permeance ($m^3 \cdot m^{-2} \cdot s^{-1} \cdot kPa^{-1}$), and η_w is the dynamic viscosity of MQ water ($kPa \cdot s$). The membrane resistance obtained experimentally by Vela et al. [23] for a ZrO_2 - TiO_2 membrane was $8.9 \times 10^{12} m^{-1}$, which is on the same order of magnitude as the γ -alumina membrane used in this study, but somewhat higher, due to the different separation layer and larger nominal pore size of the γ -alumina CTM.

Following filtrations with MQ-water and liquor 0, and a flush with MQ water and 0.1N NaOH, the membrane's pure water permeance irreversibly decreased to $1.28 \times 10^{-7} m^3 \cdot m^{-2} \cdot s^{-1} \cdot kPa^{-1}$. Using this as the pure water permeance (PWP_2) of the used membrane, the total resistance due to the membrane and an adsorbed layer ($R_{m,2}$) was determined as $7.81 \times 10^{12} m^{-1}$ using the same relationship as Eq. (6), but with the new values. Thus, the resistance due to adsorption within the pores (and pore plugging) was the difference between these two values $\sim 3.57 \times 10^{12} m^{-1}$, equivalent to another γ -alumina membrane in series.

Similarly, following test 1, the membrane was flushed with MQ water but, however, it was *not* flushed with NaOH solution, and therefore the individual contribution of irreversible fouling (adsorption) was not determined prior to test 2. However, following 16% recovery of test 2, the membrane was fully cleaned by flushing with MQ water, followed by 0.1 M NaOH. Then the pure water permeance (PWP_3) was determined as $1.23 \times 10^{-7} m^3 \cdot m^{-2} \cdot s^{-1} \cdot kPa^{-1}$. With this, the total resistance due to the membrane and the accumulated adsorbed layer on the membrane ($R_{m,3}$) was determined as $8.13 \times 10^{12} m^{-1}$ following Eq. (6).

Following test 2, the membrane was thoroughly cleaned by flushing with MQ water and 0.1M NaOH, and soaked in the same NaOH solution for ~ 20 h. The new pure water permeance (PWP_4) *increased* to $1.96 \times 10^{-7} m^3 \cdot m^{-2} \cdot s^{-1} \cdot kPa^{-1}$. This 37% increase in the pure water permeance was most likely due to the more thorough cleaning in which all surfaces of the membrane were in contact with the NaOH solution for an extended time. With this, the total resistance due to the membrane and the accumulated adsorbed layer on the membrane ($R_{m,4}$) was determined as $5.1 \times 10^{12} m^{-1}$ (again using the form of Eq. (6)).

As we performed all the filtrations the total resistance due to the formation of a "gel" layer on the membrane surface, and the unremoved adsorbed foulants (in, on, and/or plugging pores) was calculated as a function of the flux of the liquors through the membrane using the following [24]:

$$R_{T,i} = \frac{1}{\eta_{l,i} P_{l,i}(t)} \quad (7)$$

where, $R_{T,i}$ is the gel-layer resistance (m^{-1}) formed during test i , $P_{l,i}$ is the permeance of liquor i through the membrane ($m^3 \cdot m^{-2} \cdot s^{-1} \cdot kPa^{-1}$) as a function of time, and $\eta_{l,i}$ is the dynamic viscosity of liquor i determined with a Cannon-Fenske routine viscometer. For liquors 1 and 2 the viscosities were $1.16 \times 10^{-6} kPa \cdot s$ and $1.06 \times 10^{-6} kPa \cdot s$ (at $20^\circ C$), respectively.

The total resistances and the various membrane filtration resistances are plotted in Figure 9. $R_{m,1}$ is the virgin membrane's resistance and $R_{m,2}$ is the first value of a dirty membrane's resistance

after flushing away the reversible fouling. These numbers were obtained with pure water filtration. Over the ensuing period of filtering $\sim 2.4 \text{ Mg/m}^2$ of both liquor 1 and 2 there were several water flushes performed (see Figure 2) and the total filtration resistance maintained at a level over an order of magnitude higher than the both $R_{m,1}$ and $R_{m,2}$. At this point (after the 2.4 Mg/m^2 of permeate) a flush with both DI water and 0.1 M NaOH was followed by a PWP measurement, yielding $R_{m,3}$, which was only slightly greater than the previous "dirty membrane" value, $R_{m,2}$. Thus, we infer that the overwhelming majority ($>99\%$) of the filtration resistance is due to a "flushable" surface layer (aka a "gel" layer).

The filtration of liquor 2 was continued, without any further flushes, until an accumulated total of $\sim 4.9 \text{ Mg/m}^2$ had been permeated. For most of that period (up to $\sim 4 \text{ Mg/m}^2$ of permeate) the total filtration resistance stayed in the range of 10-20x the dirty membrane's value ($R_{m,3}$). Between 4 and 4.9 Mg/m^2 of permeate the total resistance increased over another order of magnitude. Nonetheless, most of this resistance was reversible upon flushing and soaking with MQ H_2O and 0.1 M NaOH , and there was indication that some of the previously "irreversibly" attached foulants had been successfully removed because the dirty membrane's resistance was now \sim halfway between the virgin value and the previous dirty membrane's one ($R_{m,3}$).

In general, it appears that the intrinsic resistance the membrane provides is $0.36 \times 10^{13} \text{ m}^{-1}$; irreversibly adsorbed material contributes additional resistance between ~ 0.15 and $0.45 \times 10^{13} \text{ m}^{-1}$; and reversible gel deposition provides the majority of the total resistance, on the order of $4 - 20 \times 10^{13} \text{ m}^{-1}$ (during lower recoveries), and up to $>600 \times 10^{13} \text{ m}^{-1}$ at very high recovery of feed as permeate.

Interestingly, high gel/deposition-layer resistance agrees with the observation made by Vela et al. [23] that ceramic membrane experiments run at lower crossflow velocities yield a surface gel layer that is the primary resistance mechanism. Lui et al.'s [8] experiments with a α -alumina ceramic tubular membranes and black liquor also concur. They observed that the gel-layer contributes approximately 80% of the total filtration resistance. (N.B. It's not clear that a gel-layer is actually formed, since its signature—flux independent of increasing transmembrane pressure—was not really determined by ourselves or the other investigators. We refer to it as a gel even though it is more likely a reversible build-up of agglomerated lignin fragments.)

Concentration polarization

Membrane fouling due to adsorption of molecules and gel/deposition-layer formation on the membrane surface can lead to irreversible decline in membrane permeance [27]. Concentration polarization is considered to be easily reversible and can be mitigated by crossflow velocity across the membrane surface to minimize the thickness of the boundary layer for mass transfer. The Reynolds number for the flow of the liquor through the lumen of the tubular membrane was calculated by the following [28]:

$$\text{Re} = \frac{d_h U \rho_l}{\eta_l} \quad (8)$$

where, d_h is the hydraulic diameter (m), U is the average cross flow velocity (m/s), ρ_l is the density of liquor 1 or 2 (g/m^3) at 20°C , and η_l is the dynamic viscosity ($\text{g}\cdot\text{m}^{-1}\cdot\text{s}^{-1}$) of liquor 1 or 2 at 20°C . The average Reynold's numbers during tests 1 and 2 were 602 and 781, which corresponded to laminar flow ($\text{Re} < 2300$). The Schmidt number (Sc), the ratio of the shear

component for diffusivity to the diffusivity for mass transfer, was calculated by the following [28]:

$$Sc = \frac{\eta_l}{\rho_l D} \quad (9)$$

where, D is the diffusivity of the macromolecules (calculated as 0.92 and $1.01 \times 10^{-10} \text{ m}^2/\text{s}$ for liquor 1 and 2, respectively, using the Stokes-Einstein relationship the radii of gyration calculated in a later section), and the other variables were as previously defined.

Both the Sc and Re could change with time as the feed becomes more concentrated (both viscosity and density will change since these experiments were run in batch mode.) However, these changes were ignored in the calculations herein because the viscosity of the retentate did not change considerably for our liquors, but that is a source of uncertainty for further consideration. Finally, the Sherwood number (Sh) was calculated by the Graetz-Leveque equation [29-31]:

$$Sh = 1.86 Re^{0.33} Sc^{0.33} \left(\frac{d_h}{L} \right)^{0.33} \quad (10)$$

where, L is the filtration length of membrane (m) and other variables were previously defined. The boundary layer mass transfer coefficient is calculated by the following [31]:

$$k_{BL} = \frac{ShD}{d_h} \quad (11)$$

where, k_{BL} is the boundary layer mass transfer coefficient (m/s), and the other variables were previously defined. The average k_{BL} during tests 1 and 2 was $1.1 \times 10^{-5} \text{ m/s}$ and $1.42 \times 10^{-5} \text{ m/s}$, respectively.

We use the classical definition of the concentration polarization coefficient for 100% retained species [31]:

$$M = \frac{c_{wall}}{c_b} = \exp \left(\frac{J_{vl}}{k_{BL}} \right) \quad (12)$$

where, M is the concentration polarization coefficient, c_{wall} is the concentration of the retained species at the wall of membrane (mol/L), c_b is their concentration in the bulk solution (mol/L), J_{vl} is the volumetric flux of liquor 1 or 2 through the membrane ($\text{m}^3 \cdot \text{m}^{-2} \cdot \text{s}^{-1}$), and k_{BL} is as defined above. The average concentration polarization coefficient during tests 1 and 2 was 1.99 and 1.09, respectively. These values vary over a range of 16% and 21% for tests 1 and 2, respectively, during the full course of the filtrations. Thus, conditions exist for development of a gel/deposition layer, especially during the earliest stages of the filtration when the flux is the highest.

TOC and sodium recovery

TOC analysis was used as the measure of rejection of all organic species during these experiments. The dashed (45°) line displayed in Figure 10 depicts zero selectivity or separation factor of a particular species through the membrane, i.e. no rejection or enhanced transport. The TOC data points are below this line so the some organic compounds were rejected by the membrane. Wallberg et al. [9] obtained similar results with an alumina-titania CTM during KBL batch filtrations with respect to the retention of lignin compounds and the sodium ions in the retentate. (N.B. Ref. 9 is not the only study conducted on these figures-of-merit, we are just

using it as a convenient recent benchmark for our current work.) The TOC retention (aka “recovery” in [9]) was calculated by the following:

$$TOC_{ret} = \frac{(1 - VR)c_{r,VR}}{c_{f,0}} \quad (13)$$

where, TOC_{ret} is the TOC retention in the retentate, VR is the volume reduction or permeate recovery, c_r is the concentration of TOC in the retentate at VR (g/L), and $c_{f,0}$ is the initial concentration of TOC in the feed (g/L). The TOC retention and permeate recovery for tests 1 and 2 are presented in Figure 11. The TOC retention results is more similar between test 2 and [9], due to the similar permeate recoveries.

The lignin concentration in [9] was determined by Beer’s law using the UV absorption at 280 nm and the molar absorption constant of 24.8 L/g/cm. The TOC content and UV absorbance was also used in our study to determine the molar absorptivity, thus it is rational to compare the TOC concentration rejected in our study with the lignin rejected in [9]. As shown in Figure 12, the trend of TOC and lignin concentration in the retentate in our study increases similarly as [9], especially during test 2, but the concentration of lignin in the retentate [9] is generally ten times higher than the concentration of TOC in the retentate in our study due to the different initial concentrations.

The other objective of our study was to recover the sodium, which would be recycled back to the lignocellulose pre-hydrolysis step as sodium hydroxide following another concentration process. As seen in Figure 10, the general trend of sodium recovery in the permeate samples shows almost complete permeation. Thus, sodium ions appear not to be associated with the higher molecular mass lignin fractions retained by this membrane, and are *not convincingly* (due to the uncertainty in the Na^+ analysis) permeated selectively. To achieve 100% sodium recovery with any membrane system, a full recycle, feed and bleed process would be required.

Molecular mass of fractionated organic species

The molecular size and quantity of organic species retained by the membrane was determined by UV spectroscopy and literature correlations between the molar absorptivity and average molecular mass. The representative range of lignin precursors appears within the UV wavelength range of 270-280 nm. A wavelength of 274 nm was used in this study because the major peak for liquor 1 and 2 appears at this wavelength (see Figure 5). The molar absorptivity at 274 nm was determined by the following:

$$\varepsilon = \frac{UVA_{274}}{TOC_{500} \cdot 12000 \frac{mg}{mol}} \quad (14)$$

where, ε is the molar absorptivity at 274 nm ($L \cdot mol^{-1} \cdot cm^{-1}$), UVA_{274} is the ultraviolet absorbance at 274 nm at 500-fold dilution divided by the quartz cell length of 1 cm, TOC_{500} is the concentration of total organic carbon in mg/L at 500-fold dilution, and 12000 mg/mol is the molecular mass of carbon. The molar absorptivity at 274 nm for liquor 1 was 285 $L \cdot mol^{-1} \cdot cm^{-1}$ (24 $L \cdot g^{-1} \cdot cm^{-1}$) and 420 $L \cdot mol^{-1} \cdot cm^{-1}$ (35 $L \cdot g^{-1} \cdot cm^{-1}$) for liquor 2, respectively, as seen in Figure 13. The molar absorptivity of liquor 1 at 274 nm agrees with the value used in [9] of 24.8 $L \cdot g^{-1} \cdot cm^{-1}$ at 280 nm for chlorine-free bleached softwood liquor, which was developed by Fengel et al. [32]. The permeate molar absorptivity was approximately one quarter to one half the retentate

molar absorptivity for tests 1 and 2, which demonstrates that there was fractionation of organic species that absorb light at 274 nm (Figure 13).

Using Eq. (3), developed by Chin et al. [20], the average molecular mass of organic compounds rejected and permeated by the membrane was estimated. The average molecular masses of the retentate and permeate during test 1 was 2100 and 1040 g/mol, respectively, and 1700 g/mol (retentate) and 1080 g/mol (permeate) for test 2. The different average molecular masses between the two liquors are likely due to the different initial feed compositions and the uncertainties inherent in this approach. Liu et al. [8] observed that the molecular mass distribution of KBL favored smaller molecules in more alkaline solutions, which is consistent with the smaller average molecular mass of liquor 2 (pH 12.2) in this study. During both tests the average retentate molecular mass increased considerably after 40% permeate recovery, which may be due to agglomeration of particles. The trends with permeate recovery are presented in Figure 14.

The molecular mass of compounds in the retentate and permeate was used to estimate their radius of gyration in order to check for consistency with the nominal pore size of the CTM (5 nm). We used the following correlation from literature data [26]:

$$R_G = 15.452 * (M_M \times 10^{-3})^{0.7675} \quad (15)$$

where, R_G is the radius of gyration (angstroms) and M_M is the molecular mass (g/mol). The average radius of gyration of compounds that absorb light at 274 nm in the feed, retentate and permeate of test 1 are 1.8, 2.0, and 1.5 nm, and 2.0, 1.8, and 1.8 nm in test 2. The similar small size of the particles in the three streams is somewhat questionable since there was notable rejection observed and the nominal pore size of the CTM was 5 nm, so we consider these values rough approximations.

Despite the uncertainty in these values, the radius of gyration for the liquor 1 and 2 agrees with the study conducted by Vainio et al. [33] on dissolved KBL particles. They determined the radius of gyration of dissolved kraft lignin particles by X-ray scattering as a function of the solvent. In alkaline solutions, the phenolic hydroxyls in the lignin particles acquire a negative charge, which causes a strong electrostatic repulsion between lignin particles and only small particles form. The radius of gyration of kraft lignin in a 0.1 M NaOH solution (pH of 12.8) was approximately 1.8 nm [33], which is very similar to what we estimated for the soluble lignin in liquors 1 and 2.

γ -alumina membrane integrity

As mentioned in the Introduction, we are working in consort with a pre-treatment reaction process whose operating conditions have not been predetermined, and may, in fact, be influenced by the efficiency of the subsequent separation processes. This led us to begin our investigations with a commercial membrane material that promised to have robustness and desirable separation characteristics (based on the nominal pore size) for the overall application. Notwithstanding this, it is important to note that other researchers [34-36] have reported that γ -alumina forms are not completely stable in the higher pHs of liquor 2 and the 0.1 M NaOH cleaning solution.

Schaep et al. observed that γ -alumina showed corrosion at pH < 2 [34], as indicated by leaching of Al, and increases in both PWP, and nominal MWCO determined in polyethylene glycol (PEG) transport tests. Also, Van Gestel et al. created multilayer, combinations of alumina and titania

NF-sized ceramic membranes, and observed that those containing weakly-crystallized $\gamma\text{-Al}_2\text{O}_3$ (and $\gamma\text{-AlOOH}$) should be restricted to $3 \leq \text{pH} \leq 11$ because relatively greater amounts of Al leaching was observed in their static corrosion tests [35], and the low pH effects were confirmed in dynamic tests [36] that included PEG rejection and PWP measurements.

Therefore, we performed several additional high pH exposure and nominal characterization tests, after the liquor filtration work reported herein, to assess whether membrane deterioration may have influenced our results and the conclusions drawn from them.

After the final experiment shown in Figure 2, the CTM was flushed with 2L of MQ water, flushed with 0.5 L of 0.1 M NaOH ($\sim\text{pH } 12.6$) for 10 min, and then permeated with the NaOH for 5 min at 276 kPa. The membrane was then stored for 2 months in MQ water at 277 K. The sequence of measurements conducted after storage and corresponding results are indicated in Table 3. First, we obtained the pure water permeance of the membrane, then a challenge test was done with a solution of bovine serum albumin (BSA) (at its isoelectric pH in MQ water) at the indicated concentration. Since BSA has a nominal diameter of 7 nm [37] we reasoned it be a good indicator of catastrophic damage to the nominal 5 nm pores of the γ -alumina separating layer.

The BSA solution filtrations were performed for 20 min in batch mode (retentate recycled to the feed and permeate collected) so that the BSA was being concentrated. The ΔP_{TM} was kept constant at ~ 260 kPa and the average flux was $2 - 3 \times 10^{-5}$ m/s. The reported BSA rejections (defined in the classical sense $= 1 - c_{\text{feed}}/c_{\text{permeate}}$) are the average of two samplings of the feed and permeate at 10 and 20 min, whose concentration was determined by UV absorbance at 280 nm. The results of these measurements indicated that the PWP remained lower than that for the "virgin" membrane and exhibited similar partial recovery from fouling after treatment with strong base as we observed during the liquor filtrations. The BSA rejection stayed nominally complete ($>99.4\%$) which is consistent with the 5 nm separating layer remaining functionally intact. Therefore, while the long-term corrosion of this commercial γ -alumina CTM versus $\text{pH} > 11$ may remain problematic, the filtration figures-of-merit we have reported are likely representative of the membrane's characteristics without any significant deterioration.

CONCLUSIONS

The primary form of resistance, which caused the most permeance decline during both tests, was a gel (or deposition) layer formation on the surface of the membrane. This layer's resistance was 10-20x times greater than the membrane and the persistently-adsorbed layer's resistance, and accounted for $>99\%$ of the total resistance, but could be removed with a simple flush of water and/or 0.1 M NaOH. It was found that a more rigorous cleaning protocol with NaOH, included soaking and permeation, could regenerate the membrane's pure water permeance to within 70% of its virgin value even after permeating $\sim 4.9 \text{ Mg/m}^2$ of lignin-containing solution and 3 water flushes and 3 water + 0.1 M NaOH solution flushes administered on a periodic basis.

There was fractionation between lignin species in the feed. The comparison between this study and prior work shows that batch experiments run to higher permeate recovery yield lower TOC retention. This implies that lignin fractionation with membranes that have 4-5 nm pores is not strictly based on steric or size considerations. Perhaps, the gel/deposition layer is acting as a dynamic membrane layer. This remains for further study. In contrast to the TOC, the

concentration of sodium ions in the retentate and permeate were equal; thus there was no notable retention of sodium ions by the membrane.

The size of lignin compounds in the permeate remained fairly constant in both liquors and test modes. The average molecular mass of organic compounds in the retentate appeared to change with recovery but, interestingly, increased 24% for liquor 1 and decreased 23% for liquor 2. This may be due to the different initial viscosities of liquors 1 and 2 (higher for liquor 1), which may imply ‘larger’ organic compounds to start with, and subsequently “seed” the further colloidal agglomeration during the batch experiments.

The average molecular mass was used to determine an approximate radius of gyration for lignin compounds in the feed, retentate, and permeate solutions; however, lower molecular mass particles, such as these, are underrepresented by the R_G - M_M model used in this study. Although this model is not a perfect correlation for this size of particles, the average radius of gyration was notably similar to the size of lignin particles in alkaline solutions determined with X-ray scattering [33].

The key differences in the results obtained in test 1 and 2 were the average size of lignin fragments fractionated, otherwise the CTM was found to provide very consistent performance figures-of-merit. The results obtained in this study provide initial design metrics for the use of ceramic tubular membranes in lignocellulosic biorefineries for the recovery of caustic chemicals which may be recycled within the process and the fractionation of lignin compounds which are valuable byproducts. The results seem very consistent with the extensive knowledge base developed by previous research for PPI applications.

Acknowledgements

This research was undertaken with support from the NSF/IURC for Membrane Applied Science and Technology at the University of Colorado. We also are grateful to Dr. Richard Higgins of CeraMem Inc. for supplying membrane samples and helpful discussions.

NOMENCLATURE

A_{tube}	inner cross-sectional area of membrane (m^2)
c_b	bulk solution concentration (mol/L)
c_p	permeate concentration (mol/L)
$c_{r,VR}$	retentate concentration at a certain volume reduction (permeate recovery) (mol/L)
c_{wall}	membrane wall concentration on feed side (mol/L)
D	diffusivity of humic substance (cm^2/s)
d_h	hydraulic diameter (m)
J_{vi}	volumetric flux of liquor 1 or 2 ($\text{m}^3 \cdot \text{m}^{-2} \cdot \text{s}^{-1}$)
k_{BL}	mass transfer coefficient (m/s)
L	active length of membrane (m)
M	concentration polarization coefficient (-)
M_M	molecular mass (g/mol)
M_s	mass of sample (g)
M_{solid}	mass of solid (g)
M_{sup}	mass of supernatant (g)

$\text{Na}^+_{f,0}$	sodium concentration in feed at time 0 (g Na^+ /L)
$\text{Na}^+_{p,t}$	sodium concentration in permeate at time t (g Na^+ /L)
Na^+_{rec}	sodium recovery in permeate (-)
$P_{l,i}(t)$	solution permeance of liquor 1 or 2 ($\text{m}^3 \cdot \text{m}^{-2} \cdot \text{s}^{-1} \cdot \text{kPa}^{-1}$)
PWP_j	pure water permeance of MQ water for membrane at different stages, $j = 1$ was the virgin membrane (see below for other j 's) ($\text{m}^3 \cdot \text{m}^{-2} \cdot \text{s}^{-1} \cdot \text{kPa}^{-1}$)
r	inner radius of ceramic tubular membrane (m)
R_a	resistance due to adsorption in and on pores 1 (m^{-1})
R'_a	fraction of total resistance due to adsorbed layer (m^{-1})
Re	Reynolds number (-)
R_G	radius of gyration (\AA)
R_g	resistance due to gel/deposition layer on the membrane surface (m^{-1})
R'_g	fraction of total resistance due to gel layer (m^{-1})
R_m	intrinsic resistance of clean membrane (m^{-1})
R'_m	fraction of total resistance due to membrane (m^{-1})
Sc	Schmidt number (-)
Sh	Sherwood number (-)
$\text{TOC}_{f,0}$	total organic carbon concentration in feed at time 0 (g TOC/L)
$\text{TOC}_{p,t}$	total organic carbon concentration in permeate at time t (g TOC/L)
TOC_{rec}	total organic carbon recovery in permeate (-)
TOC_{ret}	total organic carbon retention in retentate (-)
TOC_{500}	total organic carbon concentration in the stream at 500 fold dilution (g TOC/L)
TS	total solids (g TS/g sample)
TSS	total suspended solids (g TSS/g sample)
$\%TS$	percent total solids (%)
$\%TSS$	percent total suspended solids (%)
U	average cross flow velocity across membrane surface (m/s)
UVA_{274}	ultraviolet absorbance at 274 nm (-)
VR	volume reduction (also referred to as permeate recovery)
Greek	
ΔP_{tm}	transmembrane pressure (kPa)
ε	molar absorptivity ($\text{L} \cdot \text{mol}^{-1} \cdot \text{cm}^{-1}$)
η	dynamic viscosity ($\text{kPa} \cdot \text{s}$ or $\text{g} \cdot \text{m}^{-1} \cdot \text{s}^{-1}$)
ρ	density (g/m^3)
Subscripts	
a	adsorbed layer
b	bulk
BL	boundary layer
f	feed
f,r	retentate
$f,0$	feed at time 0
g	gel/deposition layer
$l,1$	liquor 1
$l,2$	liquor 2
m	membrane

m_j j = 1, new membrane; j = 2, membrane before test 1; j = 3, membrane after test 1 and 16% recovery of test 2; j = 4, membrane after test 2
p permeate
p,t permeate at time t
ret retentate
rec recovery
r,VR retentate at a certain volume recovery

REFERENCES

1. Glassner, D. and Hettenhaus, J. (1997) Enzyme hydrolysis of cellulose: Short-term commercialization prospects for conversion of lignocellulosics to ethanol. Report to the Biofuels Program, National Renewable Energy Laboratory, Golden, CO.
2. Kadam, K.L. and McMillan, J.D. (2003) Availability of corn stover as a sustainable feedstock for bioethanol production. *Bioresource Technol.*, 88: 17-25.
3. Hamelinck, C.N., Van Hooijdonk, G., and Faaij, A. (2005) Ethanol from lignocellulosic biomass: techno-economic performance in short-, middle- and long-term. *Biomass and Bioenergy*, 28: 384-410.
4. Wingerson, R.C. Apparatus for the separation and treatment of solid biomass. U.S. Patent application 20060283995, December 21, 2006.
5. Hill, M. and Fricke, A.L. (1984) Ultrafiltration studies on a kraft black liquor. *Tappi J.*, 67: 100-103.
6. Poddar T.K., Singh, R.P., and Bhattacharya, P.K. (1989) Ultrafiltration flux and rejection characteristics of black liquor and polyethylene glycol. *Chem. Eng. Comm.*, 75: 39-56.
7. Bhattacharjee, C. and Bhattacharya, P.K. (1993) Flux decline analysis in ultrafiltration of kraft black liquor. *J. Membr. Sci.*, 82: 1-14.
8. Liu, G., Liu, Y., Ni, J., Shi, H., and Qian, Y. (2004) Treatability of kraft spent liquor by microfiltration and ultrafiltration. *Desalination*, 160: 131-141.
9. Wallberg, O., Jönsson, A.-S., and Wimmerstedt, R. (2003) Ultrafiltration of kraft black liquor with a ceramic tubular membrane. *Desalination*, 156: 145-153.
10. Wallberg, O., Jönsson, A.-S., and Wimmerstedt, R. (2003) Fractionation and concentration of kraft black liquor lignin with ultrafiltration. *Desalination*, 154: 187-199.
11. Wallberg, O., Jönsson, A.-S. (2003) Influence of the membrane cut-off during ultrafiltration of kraft black liquor with ceramic membranes. *Trans. IChemE*, 81: 1379-1384.
12. Wallberg, O., Linde, M., Jönsson, A.-S. (2006) Extraction of lignin and hemicelluloses from kraft black liquor. *Desalination*, 199: 413-414.
13. Dafinov, A., Font, J. and Garcia-Valls, R. (2005) Processing of black liquors by UF/NF ceramic membranes. *Desalination*, 173, pp. 83-90.
14. Schlesinger, R., Gotzinger, G., Sixta, H., Friedl, A., and Harasek, M. (2006) Evaluation of alkali resistant nanofiltration membranes for the separation of hemicellulose from concentrated alkaline process liquors. *Desalination*, 192, pp. 303-314.
15. Wallberg, O., Jönsson, A.-S. (2006) Separation of lignin in kraft cooking liquor from a continuous digester by ultrafiltration at temperatures above 100° C. *Desalination*, 195, pp. 187-300.
16. Satyanarayana, S.V., Bhattacharya, P.K. and De, S. (2000) Flux decline during ultrafiltration of kraft black liquor using different flow modules: a comparative study. *Sep. Pur. Technol.*, 20: 155-167.

17. APHA, AWWA and WEF (1998) *Standard Methods of Water and Wastewater 20th Edition*, Washington, D.C.
18. Traina, S.J., Novak, J., and Smeck, N.E. (1990) An ultraviolet absorbance method of estimating the percent aromatic content in humic acids. *J. Environ. Qual.* 19: 151-153.
19. Braun, D.W., Floyd, A.J., and Sainsbury, M. (1988) *Organic Spectroscopy*. John Wiley: New York, pp. 3-23.
20. Chin, Y., Alken, G., and O'Loughlin, E. (1994) Molecular weight, polydispersivity, and spectroscopic properties of aquatic humic substances. *Environ. Sci. Technol.*, 28: 1853-1858.
21. Field, R.W., Wu, D., Howell, J.A., and Gupta, B.B. (1995) Critical flux concept for microfiltration fouling. *J. Membr. Sci.*, 100: 259-272.
22. Bacchin, P., Aimar, P., Field, R.W. (2006) Critical and sustainable fluxes: Theory, experiments and applications. *J. Membr. Sci.*, 281: 42-69.
23. Vela, M., Vincent, C., Blanco, S.A., Garcia, J.L., Gozálvez-Zafrilla, J.M., and Rodríguez, E.B. (2007) Modelling flux decline in crossflow ultrafiltration of macromolecules: comparison between predicted and experimental results. *Desalination*, 204: 328-334.
24. Ko, M.K. and Pellegrino, J.J. (1992) Determination of osmotic pressure and fouling resistances and their effects on performance of ultrafiltration membranes. *J. Membr. Sci.*, 74: 141-157.
25. Porter, M.C. (1972) Concentration polarization with membrane ultrafiltration. *Ind. Eng. Chem. Prod. Res. Dev.*, 11 (3): 234-248.
26. Baker, R.W. (2004) *Membrane Technology and Applications*, 2nd Ed.; John Wiley & Sons Ltd: Chichester, England.
27. Sablani, S.S., Goosen, M.F.A., Al-Belushi, R., and Wilf, M. (2001) Concentration polarization in ultrafiltration and reverse osmosis: a critical review. *Desalination*, 141: 269-289.
28. Henderson, S.M, Perry, R.L., and Young, J.H. (1997) *Principles of Process Engineering*, 4th Ed.; American Society of Agriculture Engineers: St. Joseph, MI.
29. Lee, S., Amy, G., and Cho, J. (2004) Applicability of Sherwood correlations for natural organic matter (NOM) transport in nanofiltration (NF) membranes. *J. Membr. Sci.*, 240: 49-65.
30. Sherwood, T.K., Brian, P.L.T., and Fisher, R.E. (1967) Desalination by reverse osmosis. *Ind. Eng. Chem. Fund.*, 6: 2.
31. Blatt, W.F., Dravid, A., Michaels, A.S., and Nelson, L.M. (1970) Solute polarization and cake formation in membrane ultrafiltration: causes, consequences, and control techniques. In: J. E. Flinn (Ed.). *Membrane Science and Technology*, Plenum Press: New York, NY. pp. 47-97.
32. Fengel, D., Wegener, G., and Feckel, J. (1981) Beitrag zur Charakterisierung analytischer and technischer Lignine, *Holzforschung*, 35: 51-57.
33. Vainio, U., Maximova, N., Hortling, B., Laine, J., Stenius, P., Simola, L.K., Gravitis, J., and Serimaa, R. (2004) Morphology of dry lignins and size and shape of dissolved kraft lignin particles by x-ray scattering. *Langmuir*, 20: 9736-9744.
34. Schaep, J., Vandecasteele, C., Peeters, B., Luyten, J., Dotremont, C., and Roels, D. (1999) Characteristics and retention properties of a mesoporous γ -Al₂O₃ membrane for nanofiltration. *J. Membr. Sci.*, 163: 229-237.

35. Van Gestel, T., Vandecasteele, C., Buekenhoudt, A., Dotremont, C., Luyten, J., Leysen, R., Van der Bruggen, B., and Maes, G. (2002) Alumina and titania multilayer membranes for nanofiltration: preparation, characterization and chemical stability, *J. Membr. Sci.*, 207: 73-89.
36. Van Gestel, T., Vandecasteele, C., Buekenhoudt, A., Dotremont, C., Luyten, J., Van der Bruggen, B., and Maes, G. (2003) Corrosion properties of alumina and titania NF membranes. *J. Membr. Sci.*, 214: 21-29.
37. Sigma-Aldrich BSA data sheet.

Table 1. Composition of liquors in this study (liquor 0, 1 and 2) and raw black liquor (8).

	liquor 0	liquor 1	liquor 2	raw black liquor (8)
feedstock	corn stover	corn stover	corn stover	straw
pre-treatment by biorefinery or mill	centrifugation	centrifugation	pressure filtration	200 mesh filtration
dynamic viscosity (Pa·s) x 10 ⁻³	n.a.	1.16	1.06	n.r.
conductivity (μS/cm)	13390	13180	14340	n.r.
pH	7.9	7.7	12.2	11
total suspended solids content (g TSS/L)	21	7.4	1.5	n.r.
total solids (g TS/L)	47	31	18.9	82-92
lignin content (g/L)	n.a.	n.a.	n.a.	28
TOC content (g TOC/L)	10.2	11.1	5.76	n.r.
sodium content (g Na ⁺ /L) (from IC)	n.a.	4.8	5.2	4.7
molar absorptivity at 274 nm (L/g/cm)	25.5	24	35	n.r.
average molecular mass (g/mol)	1700	1800	2200	30000-80000

n.a. = not determined; n.r. = not reported

Table 2. Chemical composition of main components in spruce wood (soft wood) and corn stover.

main components	spruce wood (8)	corn stover (9)
cellulose (% dry weight)	41.9	38
lignin (% dry weight)	27.1	18.8
xylan (% dry weight)	8.1	18

Table 3: Summary of BSA filtrations for γ -alumina integrity test

run	PWP $\times 10^7$ ($\text{m}^3 \cdot \text{m}^{-2} \cdot \text{s}^{-1} \cdot \text{kPa}^{-1}$)	BSA feed concentration (mg/L)	BSA rejection (%)	post run cleaning step
a	2.37	1	99.4 ± 0.1	30 min MQ H ₂ O flush 30 min 0.1N NaOH flush 15 min MQ H ₂ O flush
b	2.06	1	99.6 ± 0.2	30 min MQ H ₂ O flush 30 min 0.1N NaOH flush 15 min MQ H ₂ O flush
c	2.36	0.5	99.4 ± 0.1	not applicable

Figure Captions

Figure 1. Filtration apparatus schematic used with γ -alumina, 5 nm, CTM.

Figure 2. Schematic flowsheet of the experimental steps and protocols including cleanings and determination of filtration resistances

Figure 3. Effect of transmembrane pressure on the volumetric flux of liquor 0, 1 and 2 through the CTM.

Figure 4. Effect of transmembrane pressure on the volumetric flux of pure water through the CTM; the slope of the line is the pure water permeance (PWP). PWP₁ = PWP of new membrane; PWP₂ = PWP of membrane before test 1; PWP₃ = PWP of membrane after 16% recovery of test 2; PWP₄ = PWP of membrane after test 2.

Figure 5. Ultraviolet absorbance spectra for the liquor 1 and 2 feed, retentate, and permeate at 500-fold dilution. Test 1: feed = open triangles, retentate after 30 min = open squares, permeate after 30 min = open diamonds. Test 2: feed = filled triangles, retentate after 80 min = filled squares, permeate after 80 min = filled diamonds.

Figure 6. Permeance decline for batches 1 - 6 for test 1. The membrane was flushed with MQ water following batches 1, 2, 4, and 6. The permeance with liquor 1 at 552 kPa during the flux versus ΔP_{tm} test (Figure 3) = large open circles and the data for batches 1-6 are labeled and use filled circles of decreasing size.

Figure 7Figure 7.

. Permeance decline for test 2. The membrane was cleaned following approximately 16% recovery of permeate to regenerate the membrane. The first 16% recovery = larger open diamonds and 16-80% recovery = smaller open diamonds.

Figure 8. Permeance decline versus mass permeated for tests 1 and 2. For test 1 the batches are identified as follows: data from flux versus ΔP_{tm} test with liquor 1 at 552 kPa = larger open circles; batches 1-6 are labeled and use filled circles of decreasing size. For test 2, the first 16% recovery = larger open diamonds and 16-80% recovery = smaller open diamonds.

Figure 9. Total filtration resistance versus the accumulated mass per unit area permeated. The horizontal straight lines indicate new membrane's resistance ($R_{\text{m},1}$) and the various "dirty" membrane resistances ($R_{\text{m},1}$, $R_{\text{m},3}$, $R_{\text{m},4}$) measured at the points indicated by the vertical arrows.

Figure 10. TOC and sodium ion recovery in permeate for tests 1 (batches 1-4) and 2. TOC for test 1 = filled squares, TOC for test 2 = filled circles, sodium ion for test 1 = open squares, sodium ion for test 2 = open circles, non-selective transference (no fractionation) = dashed line.

Figure 11. TOC retention and permeate recovery comparison for tests 1 (batch 1) and 2, and ref. [9]. Only batch 1 from test 1 shown for clarity. Black bars = TOC rejection, crosshatched = permeate recovery.

Figure 12. Retentate TOC concentration for tests 1 and 2 versus retentate lignin concentration in ref. [9]. Only batch 1 from test 1 shown for clarity. Filled symbols (left-hand axis) and light symbols (right-hand axis). Test 1 (batch 1) = filled circles, test 2 = filled diamonds, ref. [9] = open squares.

Figure 13. Molar absorptivity of organic compounds at 274 nm at 500-fold dilution of retentate and permeate for tests 1 and 2. Only batch 1 for test 1 shown for clarity. Retentate for test 1 = filled squares, permeate for test 1 = open squares, retentate for test 2 = filled circles, permeate for test 2 = open circles.

Figure 14. Average molecular mass of organic compounds of retentate and permeate for tests 1 and 2. Only batch 1 for test 1 shown for clarity. Retentate for test 1 = filled squares, permeate for test 1 = open squares, retentate for test 2 = filled circles, permeate for test 2 = open circles.

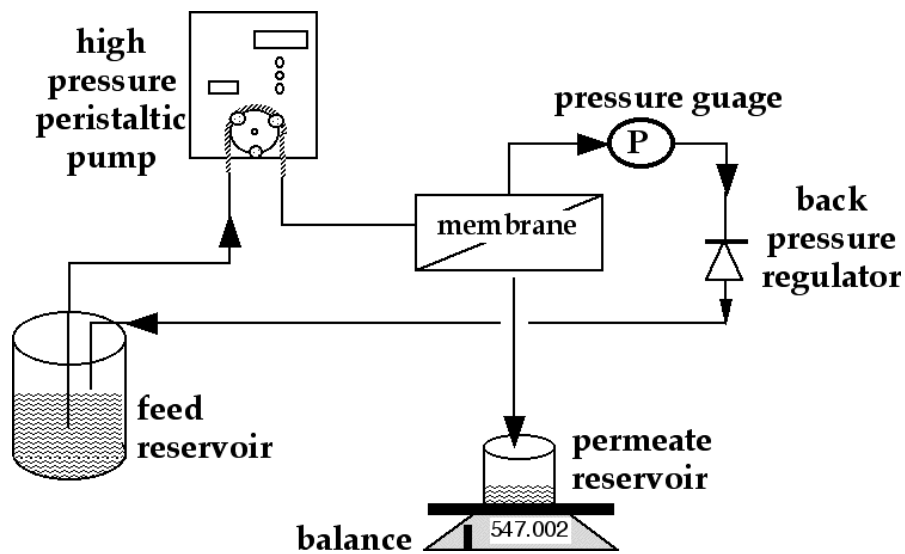
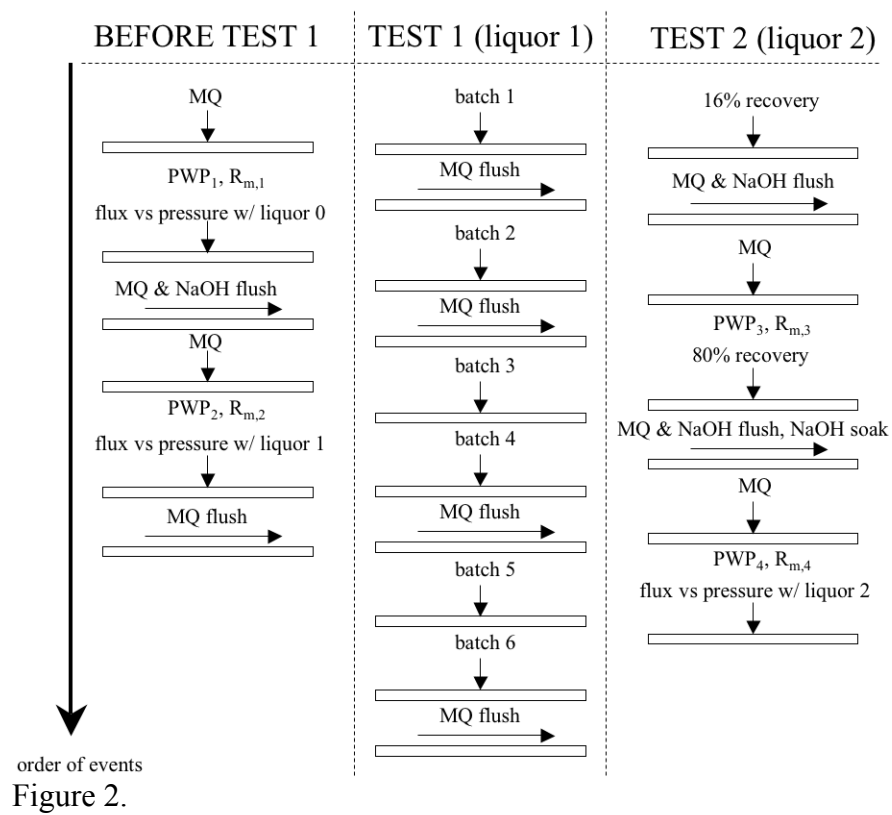


Figure 1.



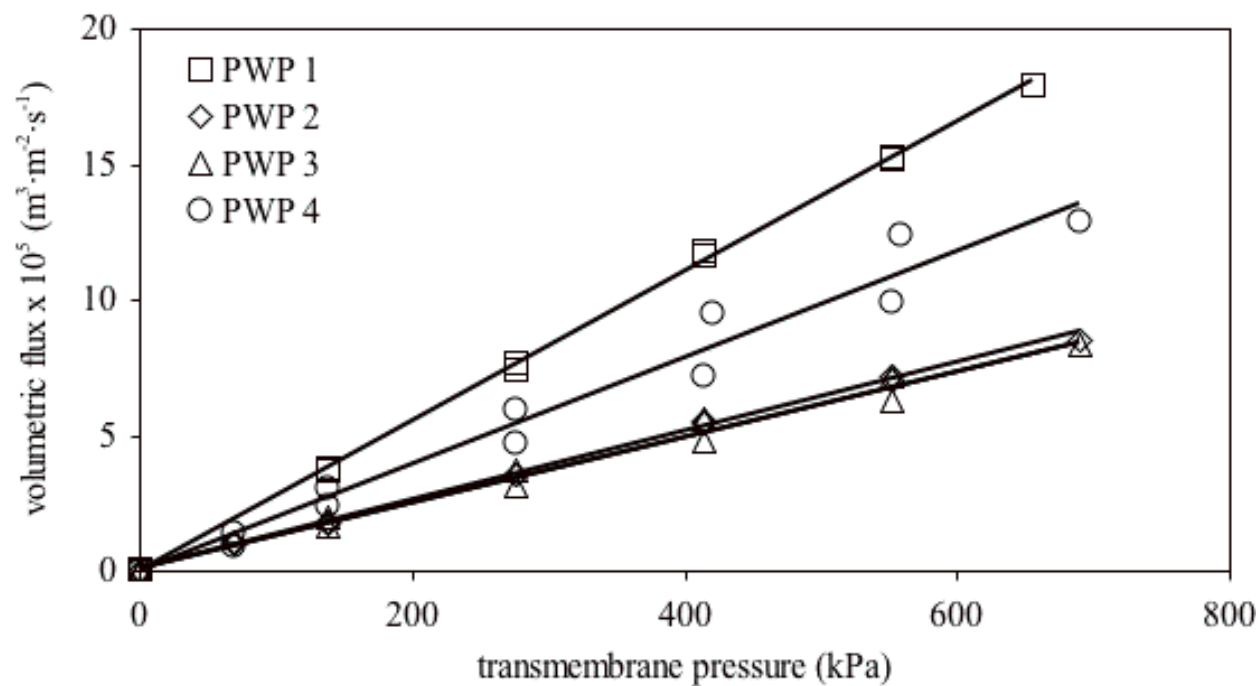


Figure 3.

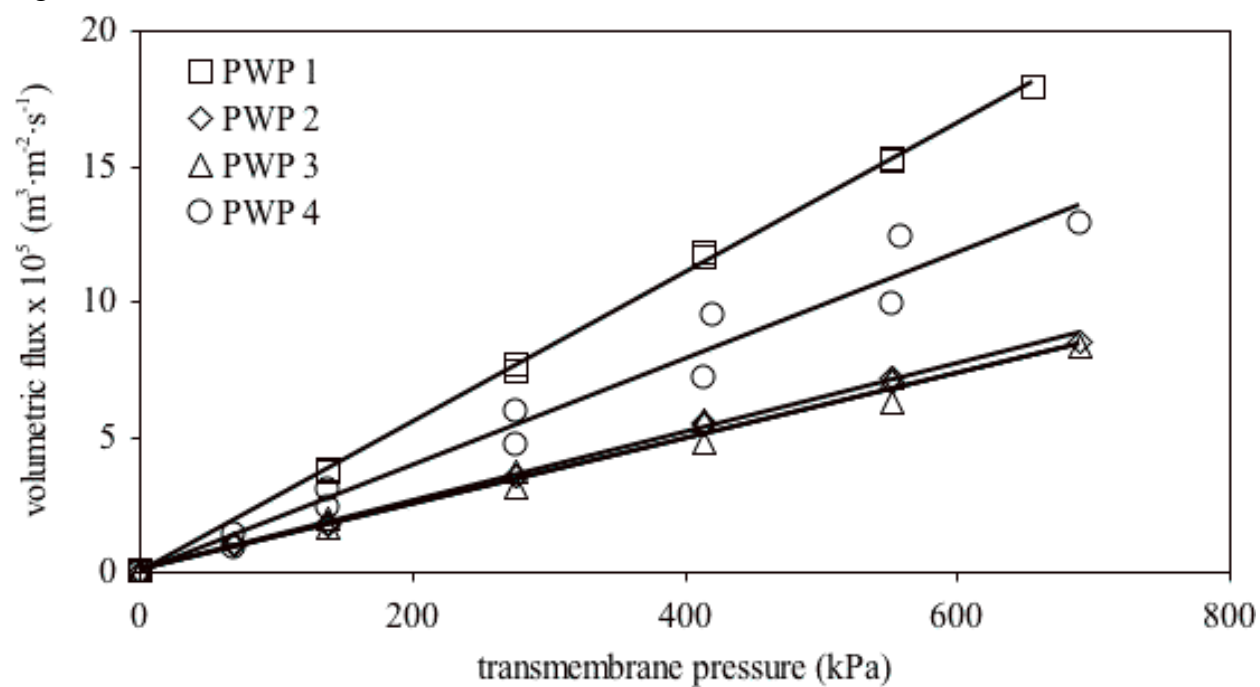


Figure 4.

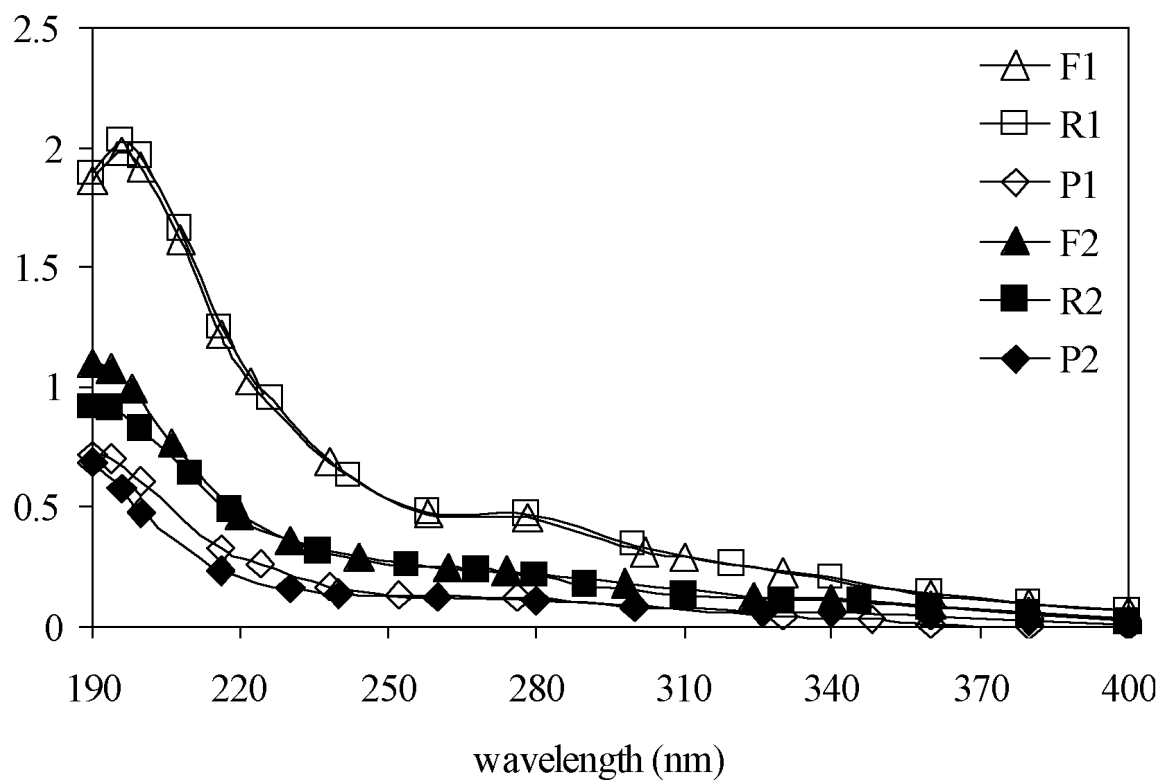


Figure 5.

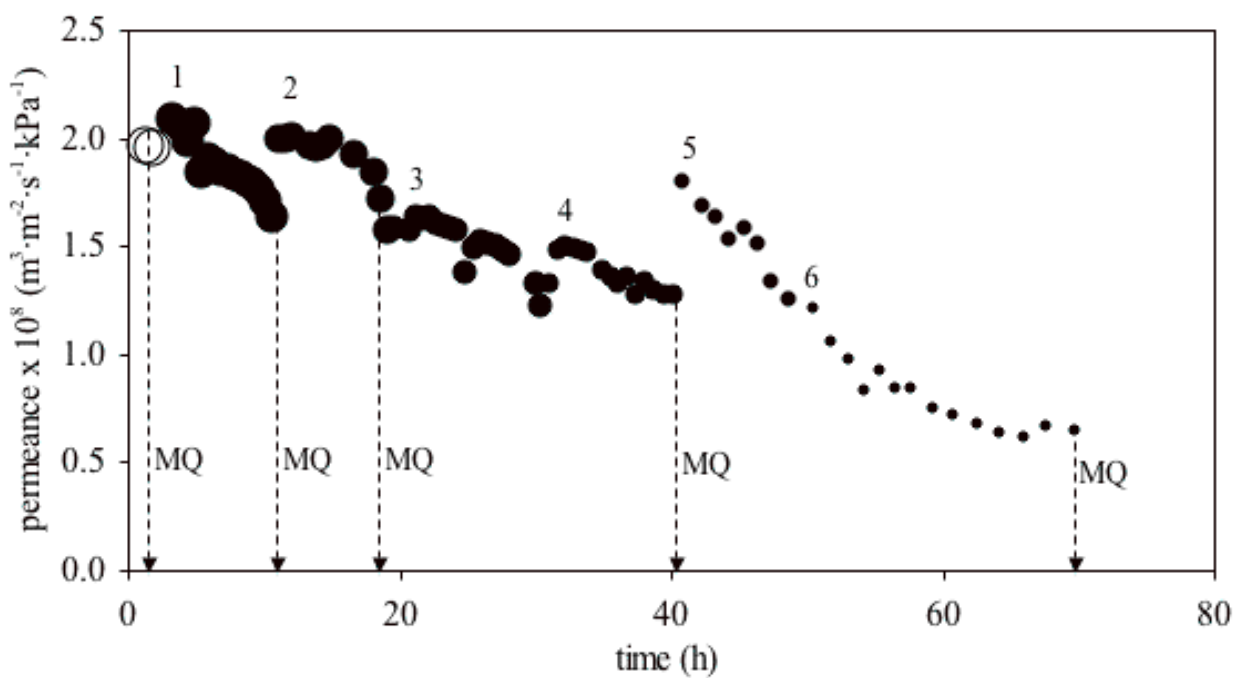


Figure 6.

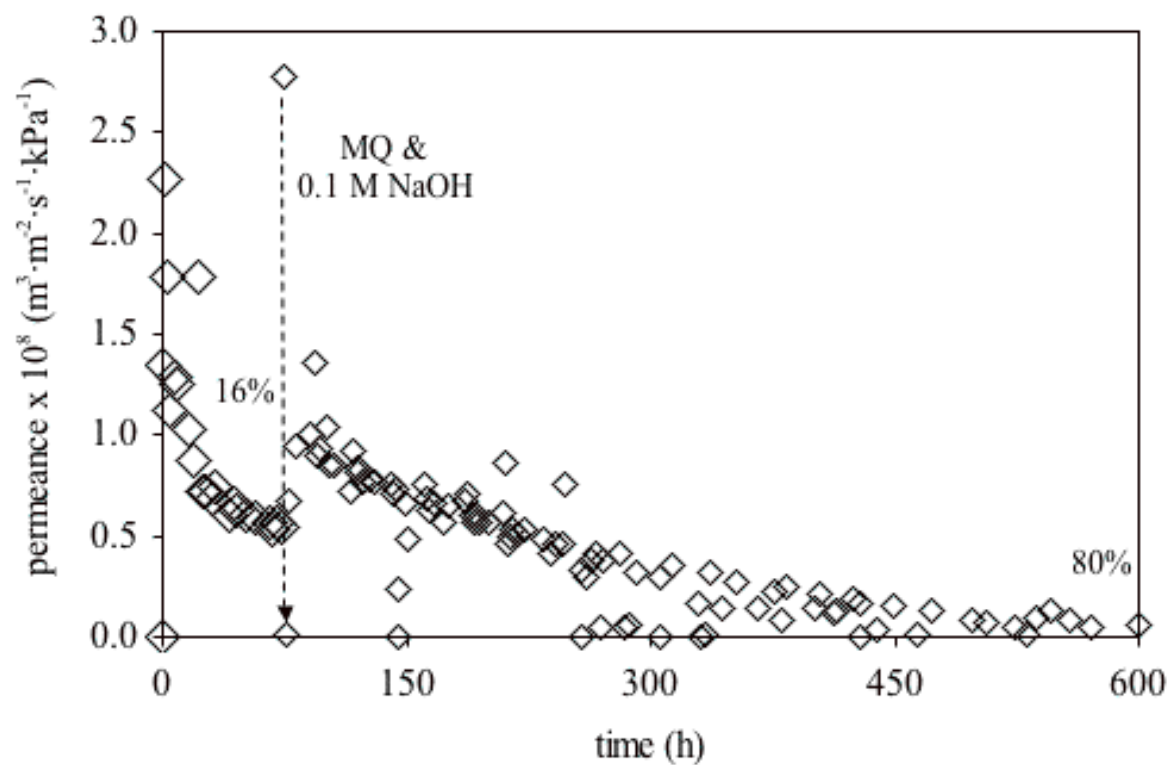


Figure 7.

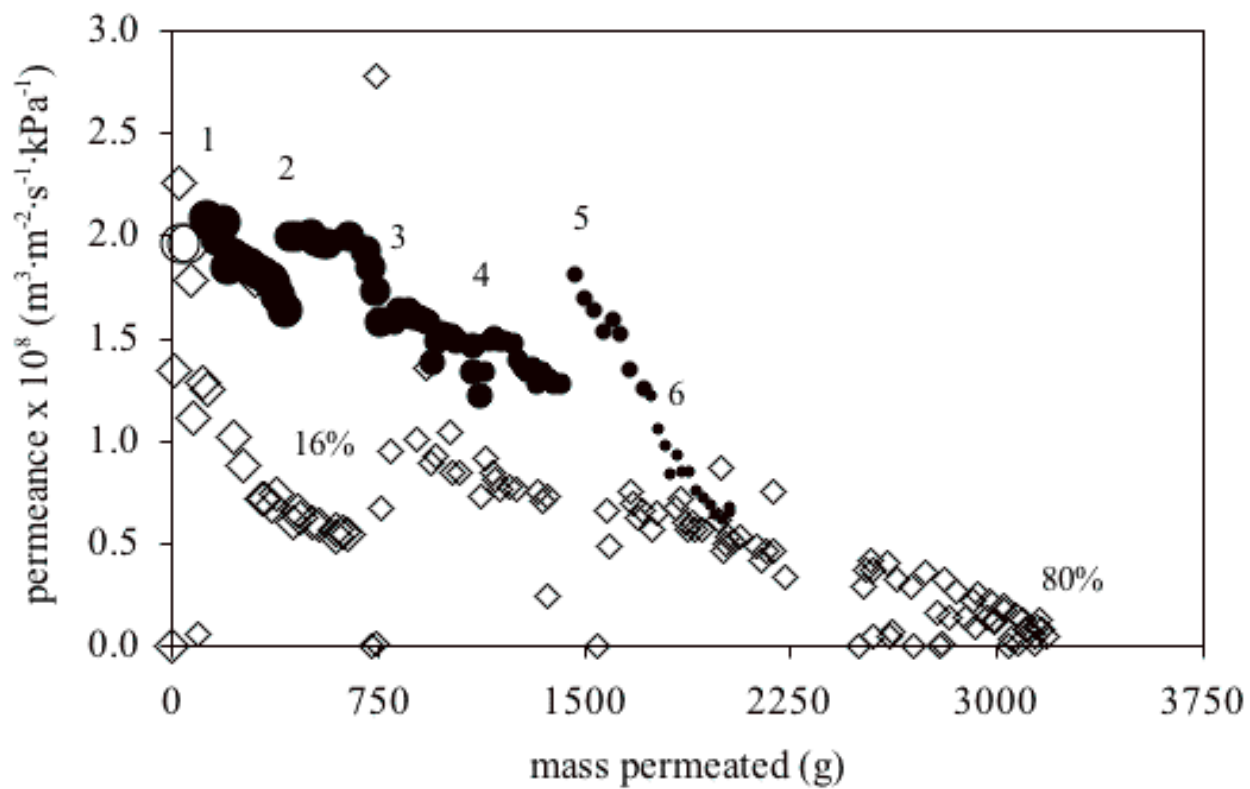


Figure 8.

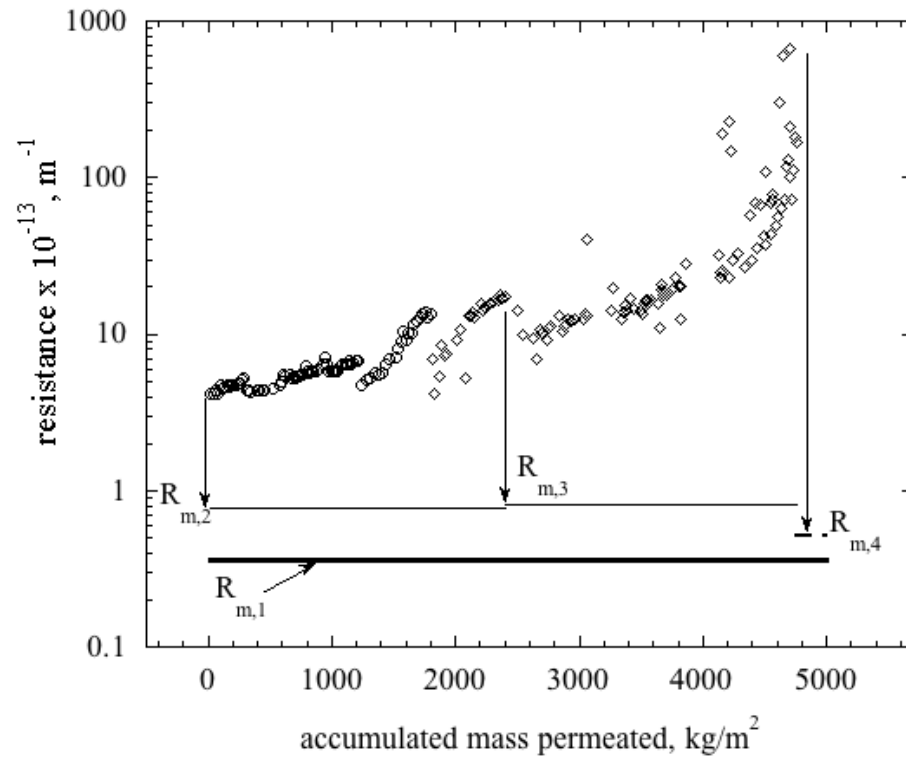


Figure 9.

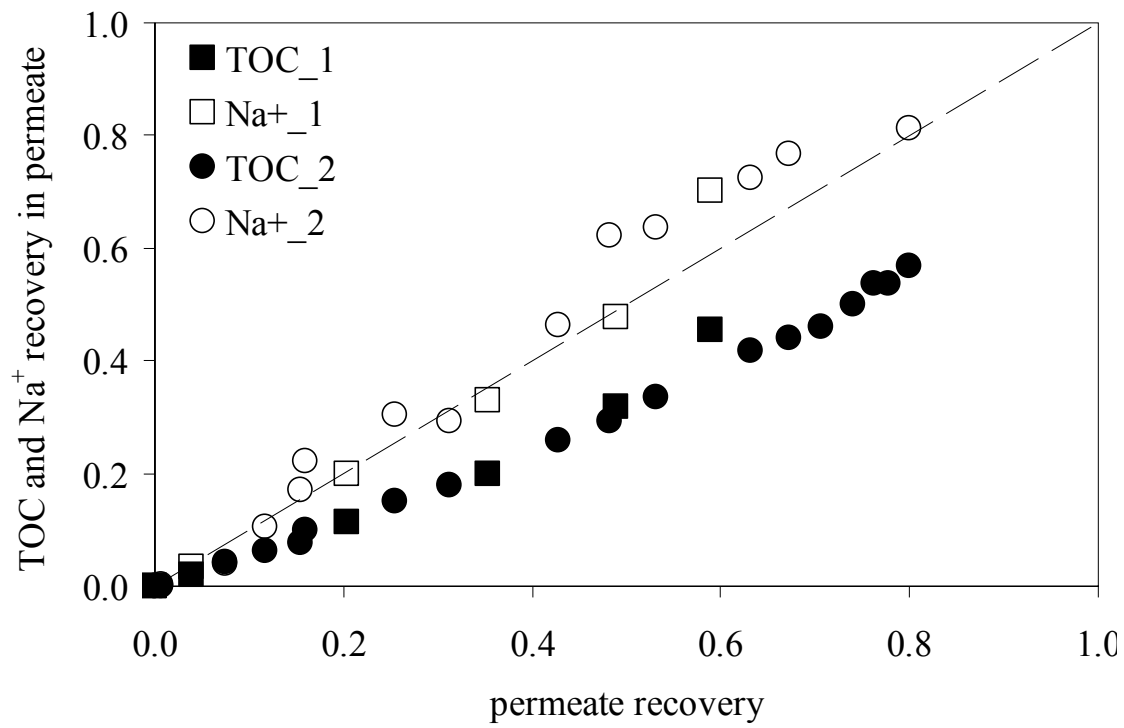


Figure 10.

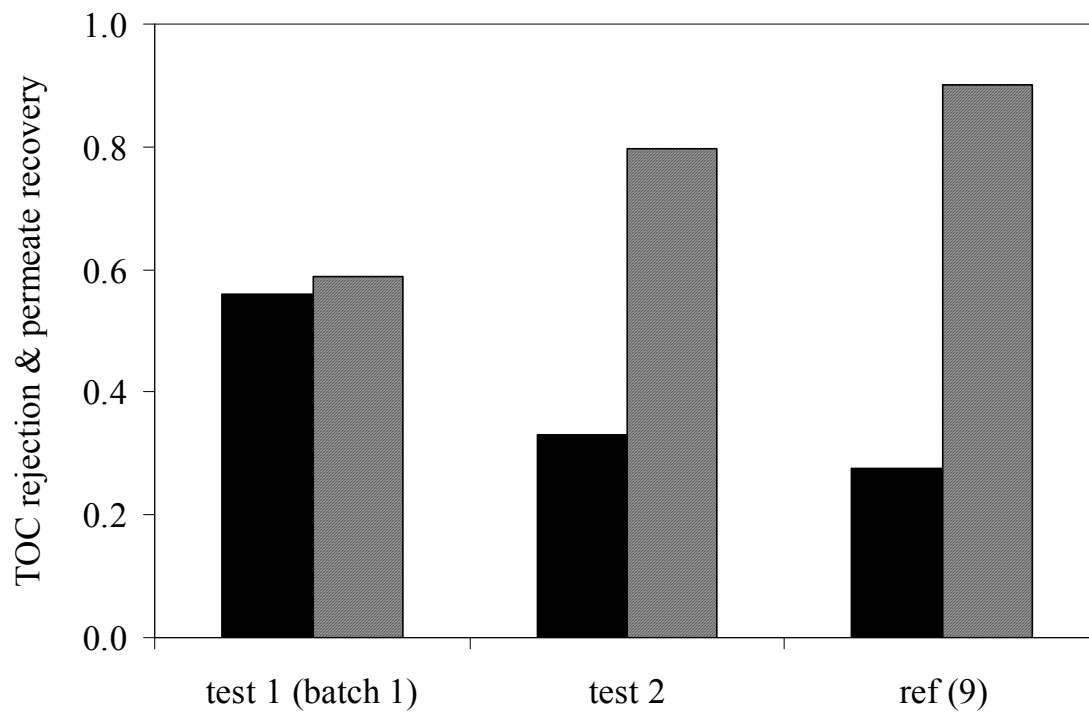


Figure 11.

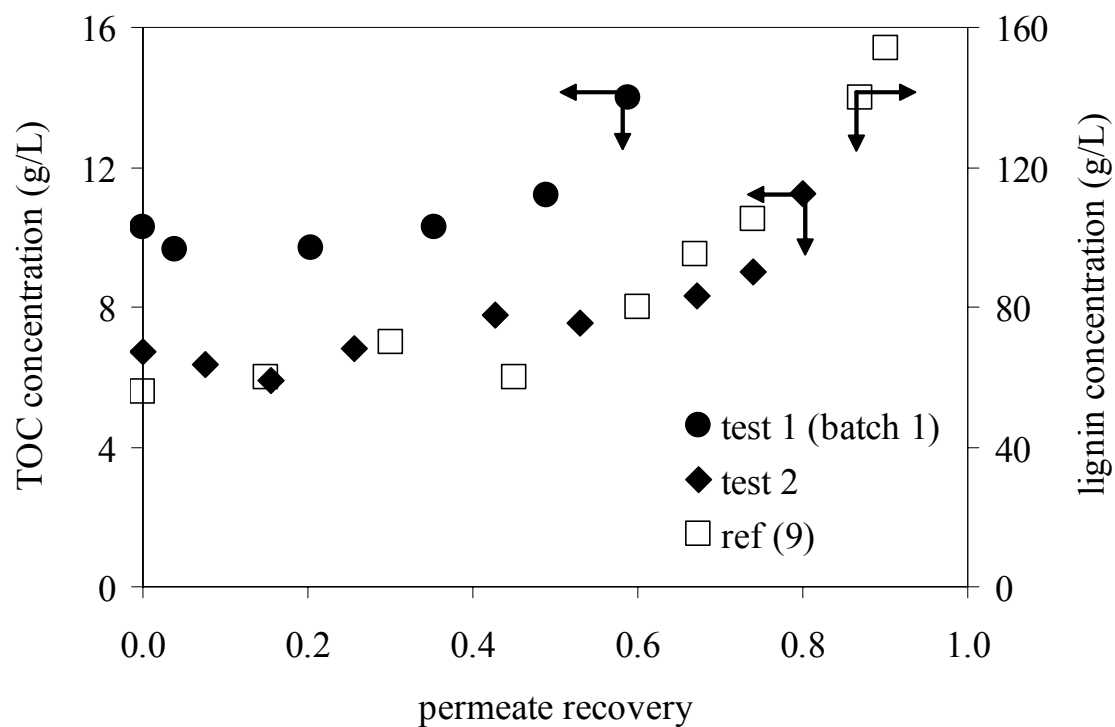


Figure 12.

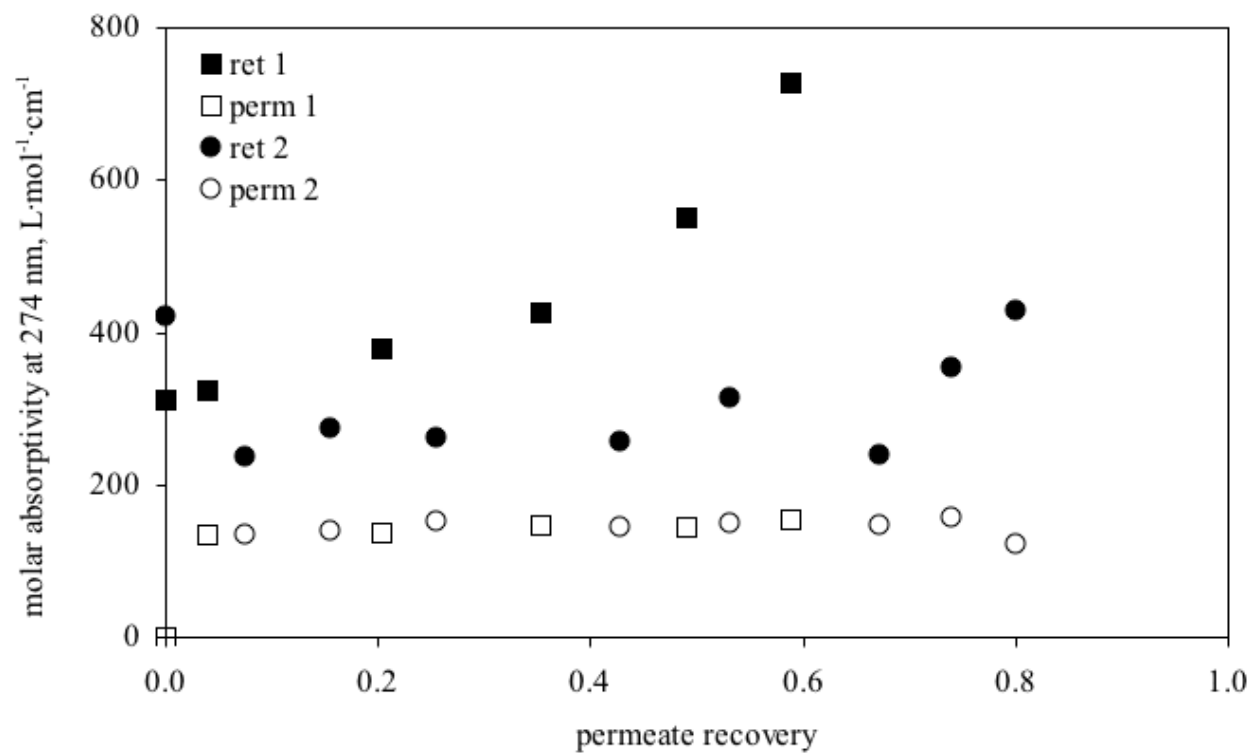


Figure 13.

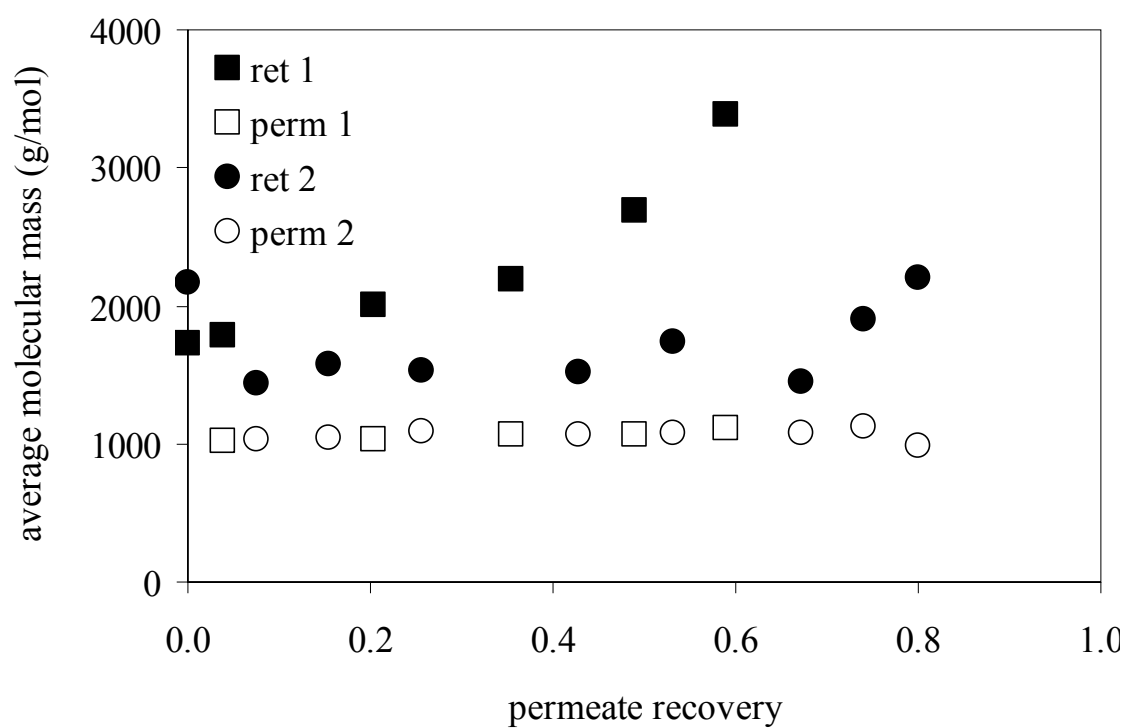


Figure 14.